



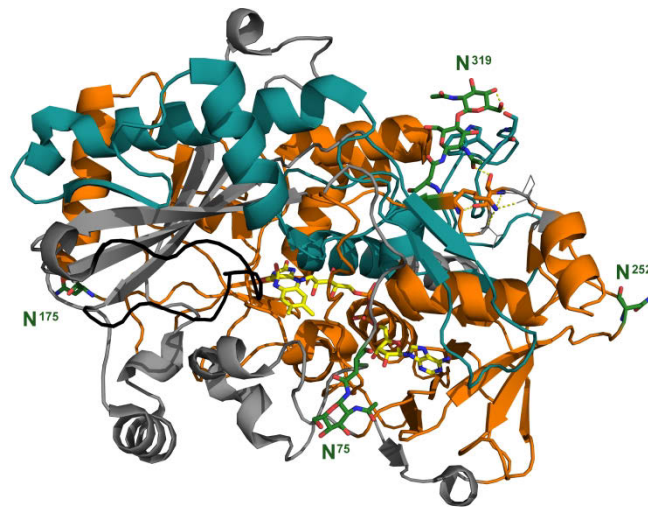
**VIBT**  
Vienna Institute  
of BioTechnology

**BioTOP**  
Biomolecular  
Technology of Proteins

**FWF**

**University of Natural Resources and Applied Life Sciences, Vienna**  
Department of Food Science and Technology, Division of Food Biotechnology

# Rational engineering of Pyranose Dehydrogenase for application to enzymatic bio-fuel cells



**PhD Thesis**

DI Christoph Gonaus

**Supervisors**

Assoc. Prof. Dr. Clemens Karl Peterbauer  
Univ.Prof. Dipl.-Ing. Dr.techn. Dietmar Haltrich

**Vienna, October 2016**



Dieses Werk widme ich meinen Eltern, die mich immer auf meinem Weg unterstützt haben.



## Danksagung

Ich danke meinen Betreuern Prof. Clemens Peterbauer und Prof. Dietmar Haltrich, dass sie mir diese Arbeit ermöglichten. Ihre Tür stand immer offen und sie standen mir mit Rat und Tat und mit ihren Anregungen zur Seite.

Prof. Lo Gorton und seine damalige Doktoratsstudentin Maria Yakovleva waren maßgebliche Kooperationspartner und gaben ganz wesentlichen Input. Aber nicht nur dafür will ich mich bedanken, sondern auch für die Gelegenheit die mir Prof. Gorton gab, bei einem 3 monatigen Auslandsaufenthalt in Lund, in seiner Gruppe elektrochemische Messungen durchzuführen. Tack så mycket också för språkkursen på svenska.

I also want to thank Prof. Christina Divne for giving me the opportunity of staying at Karolinska Institutet in Stockholm, where I could venture into the field of X-ray crystallography.

Special thanks to my great colleagues during my research stays abroad, especially to Tan Tien Chye and Rosaria Gandini in Stockholm and Christopher Schulz and Kamrul Hasan in Lund.

Ich möchte diese Gelegenheit auch nutzen Katharina Schropp und Sara Groiss zu danken, deren Master- bzw. Bachelorarbeit ich das Glück hatte betreuen zu dürfen. Sie lieferten wertvolle Beiträge zu dieser Arbeit, im Rahmen ihrer Master- bzw. Bachelorarbeit.

Weiters danke ich Dr. Christa Jakopitsch für die unglaublich engagierte Koordination des PhD Programms BioToP. Die von ihr organisierten Annual Retreats schafften Zusammenhalt zwischen den Studenten, gewährten Einblicke jenseits des eigenen Tellerrands und wertvolles Feedback zur eigenen Arbeit und schafften die Möglichkeit Betreuer und Studenten in entspannter Atmosphäre besser kennen zu lernen. Mein externer BioToP Betreuer Prof. Christian Obinger wiederum gab mir wertvolle Rückmeldung bei den jährlichen Progress Reports.

Besonders will ich auch allen Mitgliedern und ehemaligen Mitgliedern der Arbeitsgruppe Lebensmittelbiotechnologie danken: Cindy Lorenz als gute Seele und Technikerin des Labors, Dr. Roman Kittl der mich bei der Masterarbeit betreute aber mir auch danach immer wieder weiterhalf, meinen Kollegen Daniel Kracher, Hoang-Minh Nguyen, Michael Graf, Iris Krondorfer und Dagmar Brugger und allen anderen die ich während meiner Arbeit hier kennen lernen und mit denen ich das Labor und das Büro teilen durfte. Sie waren es die eine freundschaftliche und konstruktive Atmosphäre schafften.

Dem Fonds zur Förderung der wissenschaftlichen Forschung (FWF) danke ich für dessen Finanzierung und dem PhD-Programm BioToP für den großartigen akademischen Rahmen dieser Arbeit.

Nicht zuletzt ein großer Dank an alle anderen die ich während meiner Zeit als Doktorand kennenlernen durfte, in der Uni aber auch abseits, speziell auch meiner Familie, die mich auch aufmunterte wenn es mal nicht so weiterging wie erhofft.

# Content

---

<b>Abstract .....</b>	<b>1</b>
<b>Zusammenfassung .....</b>	<b>2</b>
<b>Aim and scope .....</b>	<b>4</b>
<b>Introduction .....</b>	<b>5</b>
Pyranose dehydrogenase: An oxidoreductase of the GMC structural family.....	5
Potential applications of pyranose dehydrogenase .....	9
N-glycosylation: Function and engineering potential.....	16
<b>Chapter I: _____</b>	<b>30</b>
<b>Transcription analysis of pyranose dehydrogenase from the basidiomycete     <i>Agaricus bisporus</i> and characterization of the recombinantly expressed enzyme</b>	
<b>Chapter II: _____</b>	<b>50</b>
<b>Engineering of pyranose dehydrogenase for application to enzymatic anodes in     biofuel cells</b>	
<b>Chapter III: _____</b>	<b>67</b>
<b>Comprehensive analysis of <i>Agaricus meleagris</i> pyranose dehydrogenase N-     glycosylation sites and the performance of partially non-glycosylated enzymes</b>	
<b>Discussion .....</b>	<b>89</b>



## Abstract

Enzymatic bio-fuel cells transform chemical into electrical energy, with the help of enzyme modified anode and cathode. Unlike traditional metal based fuel cells, they can employ sugars as fuel and can be designed without anode and cathode separating membranes, which enables much simpler designs and strong downscaling potential. They have therefore been suggested for powering transportable micro devices and implantable sensors, where sugar and O<sub>2</sub> are supplied by the host body. One of the major remaining challenges is the achievable maximum power output of these systems, which in turn depends on the specifications of anode and cathode.

Here, rational enzyme engineering of a promising oxidoreductase for anode modification, pyranose dehydrogenase, was employed to increase achievable maximum current densities. The flavoenzyme pyranose dehydrogenase from litter degrading basidiomycetes is an interesting candidate due to its broad substrate specificity, capability of dioxidation, and inability of reducing O<sub>2</sub> to H<sub>2</sub>O<sub>2</sub>. These characteristics enable the use of fuels other than D-glucose and are potentially beneficial for bio-fuel cell performance.

Pyranose dehydrogenase from *Agaricus bisporus* was heterologously expressed in this work and compared to the three other reported recombinant pyranose dehydrogenases, to select the most promising target for enzyme engineering. *Agaricus meleagris* pyranose dehydrogenase I was chosen due to its generally moderately better catalytic efficiency and enzyme stability.

The posttranslational modification of protein N-glycosylation has been previously shown to be disadvantageous for enzyme modified electrodes. Therefore, the rational engineering strategy was based on reducing N-glycosylation by selectively knocking-out the N-glycosylation sites. A systematic set of partially N-glycosylated *Agaricus meleagris* pyranose dehydrogenase I variants was tested on Os-polymer modified graphite electrodes. Interestingly, knocking out the only apparently overglycosylated site, the peripheral N<sup>252</sup>, did not create a variant with improved performance on Os-polymer modified electrodes. The site N<sup>319</sup>, on the other side, could not be knocked out without preventing functional recombinant expression in *Pichia pastoris*. However, electrodes based on the variant N75G/N175Q yielded an approximately 10-fold increased maximum current density (290 μA cm<sup>-2</sup>) compared to the equivalent electrodes with recombinant wild type enzyme. *Agaricus meleagris* pyranose dehydrogenase I N75G/N175Q is therefore a promising candidate for application to future enzymatic bio-fuel cell anodes. The reason for the improved current density was thought to be interference of N-glycans at N<sup>75</sup> and N<sup>175</sup> with the electron transfer from the active site to the Os-redox centres, as both sites are located near to the active site entrance.

## Zusammenfassung

Enzymatische Biobrennstoffzellen wandeln chemische Energie in elektrischer Energie um, mithilfe von Enzym modifizierter Anode und Kathode. Anders als traditionelle Metallkatalysten basierte Brennstoffzellen, können sie Zucker als Brennstoff verwenden und ohne Anode und Kathode trennende semipermeable Membranen konstruiert werden, wodurch einfachere und stark miniaturisierte Konstruktionen ermöglicht werden. Aus diesem Grund wurden sie für die Energieversorgung von mobilen Miniaturgeräten und von implantierbaren Sensoren, wo Zucker und Sauerstoff vom umgebenden Körper zur Verfügung gestellt werden, vorgeschlagen. Eine der größten verbleibenden Herausforderungen betrifft die erreichbare maximale elektrische Leistung dieser Systeme, welche wiederum von den Spezifikationen der Anode und Kathode abhängt.

Rationales Proteindesign wurde in diesem Werk an einer vielversprechenden Oxidoreduktase, Pyranose Dehydrogenase, angewandt, um eine Erhöhung der maximalen Stromdichte zu erreichen. Das Flavoenzym Pyranose Dehydrogenase, von Laub zersetzenden Basidiomyceten, ist ein interessanter Kandidat aufgrund des breiten Substratspektrums, der Fähigkeit zur Dioxidation und da es die Reduktion von  $O_2$  zu  $H_2O_2$  nicht katalysiert. Diese Charakteristika ermöglichen die Verwendung von alternativen Brennstoffen, abseits von D-Glucose und sind potentiell förderlich für die Leistungsfähigkeit von Biobrennstoffzellen.

Pyranose Dehydrogenase von *Agaricus bisporus* wurde in dieser Arbeit rekombinant exprimiert und mit den anderen 3 publizierten rekombinanten Varianten verglichen um die vielversprechendste Basis für rationales Proteindesign zu identifizieren. *Agaricus meleagris* Pyranose Dehydrogenase I wurde dafür, aufgrund der generell moderat höheren katalytischen Effizienz und Enzymstabilität, schlussendlich ausgewählt.

Vorige Berichte zeigten bereits einen nachteiligen Einfluss von N-Glykosylierung, einer posttranslationalen Proteinmodifizierung, auf Enzym modifizierte Elektroden. Deshalb wurde eine rationale Proteindesignstrategie gewählt die auf der Reduzierung der N-Glykosylierung abzielte. Dies wurde durch gezieltes eliminieren von N-Glykosylierungsstellen erreicht und ein systematisches Set an partiell N-glykosylierten *Agaricus meleagris* Pyranose Dehydrogenase I Varianten wurde auf Os-Polymer modifizierten Graphitelektroden getestet. Interessanterweise führte die Eliminierung der einzigen überglykosylierten Stelle, N<sup>252</sup>, nicht zu einer Enzymvariante die auf Os-Polymer modifizierten Elektroden höhere Stromflüsse erzeugte. Die Stelle N<sup>319</sup> wiederum konnte nicht eliminiert werden, ohne die funktionelle rekombinante Produktion des Enzyms in *Pichia pastoris* zu unterbinden. Elektroden basierend auf der Variante N75G/N175Q hingegen zeigten eine ca. 10-fache Steigerung der maximalen Stromflussdichte ( $290 \mu A cm^{-2}$ ) im Vergleich zu äquivalenten Elektroden mit dem rekombinanten wildtyp Enzym. *Agaricus meleagris* Pyranose Dehydrogenase I N75G/N175Q

ist somit ein vielversprechender Kandidat für Anwendung in zukünftigen enzymatischen Biobrennstoffzellenanoden. Die verbesserte elektrische Stromdichte könnte durch die wegfallende Behinderung des Elektronentransfers, zwischen aktivem Zentrum und Os-Redoxzentren, aufgrund der fehlenden N-Glykane bei N<sup>75</sup> und N<sup>175</sup>, begründet sein.

## Aim and scope

The oxidoreductase pyranose dehydrogenase was engineered for application to enzymatic bio-fuel cells by targeting its N-glycosylation, with the aim of increasing achievable maximum current densities with pyranose dehydrogenase/Os-polymer modified anodes.

In a first step, the most promising pyranose dehydrogenase variant was identified, as basis for rational engineering. **Chapter I** reports the heterologous expression of pyranose dehydrogenase from *Agaricus bisporus* and its comparison to the other three published recombinant pyranose dehydrogenases. As a result, *Agaricus meleagris* pyranose dehydrogenase I was chosen for rational engineering. The engineering strategy was based on parallel work by Yakovleva et al., where anodes modified with *in-vitro* deglycosylated enzyme showed 2-fold increased maximum current densities. However, *in-vitro* deglycosylation is an expensive additional step of enzyme preparation and affects all N-glycosylation sites indiscriminately. As enzyme production in the non-glycosylating production host *Escherichia coli* did not yield functional enzyme, knocking out N-glycosylation sites by site directed mutagenesis was investigated as alternative. This allowed the production of partially N-glycosylated enzyme and also the study of the role of the different glycosylation sites. In **Chapter II**, a set of variants with only partial N-glycosylation was tested on graphite anodes for improved maximum current densities. **Chapter III** was investigating the effect of the different N-glycosylation site knock outs in greater detail. Overglycosylated sites and essential sites for functional expression were identified and the impact of the knock out mutations on enzyme stability and catalytic efficiency was described.

## Introduction

### Pyranose dehydrogenase: An oxidoreductase of the GMC structural family

#### GMC structural family

The so called glucose-methanol-choline (GMC) structural family of oxidoreductases was first described by Cavener et al. [1]. It is a group of flavoenzymes, which usually oxidizes primary and secondary alcohols to corresponding aldehydes or ketones [2]. Enzymes of the GMC family which are oxidizing sugars are, among others, cellobiose dehydrogenase (CDH, EC 1.1.99.18), glucose 1-oxidase (GOx, EC 1.1.3.4), pyranose 2-oxidase (P2O, EC 1.1.3.10) and pyranose dehydrogenase (PDH, EC 1.1.99.29). Members with alternative substrates include alcohol oxidase (AOX, EC 1.1.3.13) and aryl-alcohol oxidase (AAO, EC 1.1.3.7) [3,4].

GMC oxidoreductases share a p-hydroxybenzoate hydroxylase (PHBH) like fold as common structural feature [4,5], where an FAD binding domain is closely linked to a substrate binding domain [2,6,7]. The majority contains dissociable, yet tightly bound, FAD cofactors. However, some integrate the FAD via a covalent  $\delta\alpha$ -N<sup>3</sup>-histidyl bond [2].

#### Pyranose dehydrogenase

Pyranose dehydrogenase (PDH, EC 1.1.99.29, Figure 1) is a secreted and N-glycosylated monomeric fungal GMC oxidoreductase of a mass of 67-75 kDa with an N-Glycan content of around 7%. It has been isolated from a number of basidiomycetes belonging to the family of *Agaricaceae* and *Lycoperdaceae*. Those have in common to grow on lignocellulose rich litter [8–10]. *Agaricus bisporus*, known as the button mushroom, was the first organism of which PDH was purified from (*Ab*PDH) [9]. Subsequently it also had been isolated from *Macrolepiota rhacodes* (*Mr*PDH) [10], *Agaricus xanthoderma* (*Ax*PDH) [11] and *Agaricus meleagris* (*Am*PDH) [8] supernatant.

#### Substrate range and biological function

A broad range of non-phosphorylated sugars can be oxidized by pyranose dehydrogenases. All major sugars contained in wood polysaccharides, among others D-glucose, D-galactose, D-xylose, L-arabinose, as well as the di-saccharide cellobiose with its 1-4  $\beta$ -glycosidic link, were catalysed at comparable turnover numbers. PDH oxidizes positions C1 to C4, depending on the substrate and the

enzyme variant. Also di-oxidation at C2 and C3, has been reported [12,13]. This sets it apart from related enzymes like glucose 1-oxidase with its narrow substrate selectivity [14]. Other GMC members, like CDH and P2O, which are more substrate promiscuous than glucose 1-oxidase, are still more regioselectively oxidizing the substrate, targeting C1 or preferentially C2, respectively [15,16].

Subsequent to the reduction of the cofactor FAD via oxidation of sugars, electrons can be transferred to quinones and metallo-complexes. These include 1,4-benzoquinone and some of its substituted forms, as well as ferrocenium ion ( $\text{Fc}^+$ ), 2,6-dichloroindophenol (DCIP) and 2,2'-azino-bis(3-ethylbenzothiazoline-6-sulfonic acid) cation radical ( $\text{ABTS}^+$ ). However, as a true dehydrogenase, pyranose dehydrogenase does not utilize molecular oxygen as electron acceptor [8,9,11,12,17].

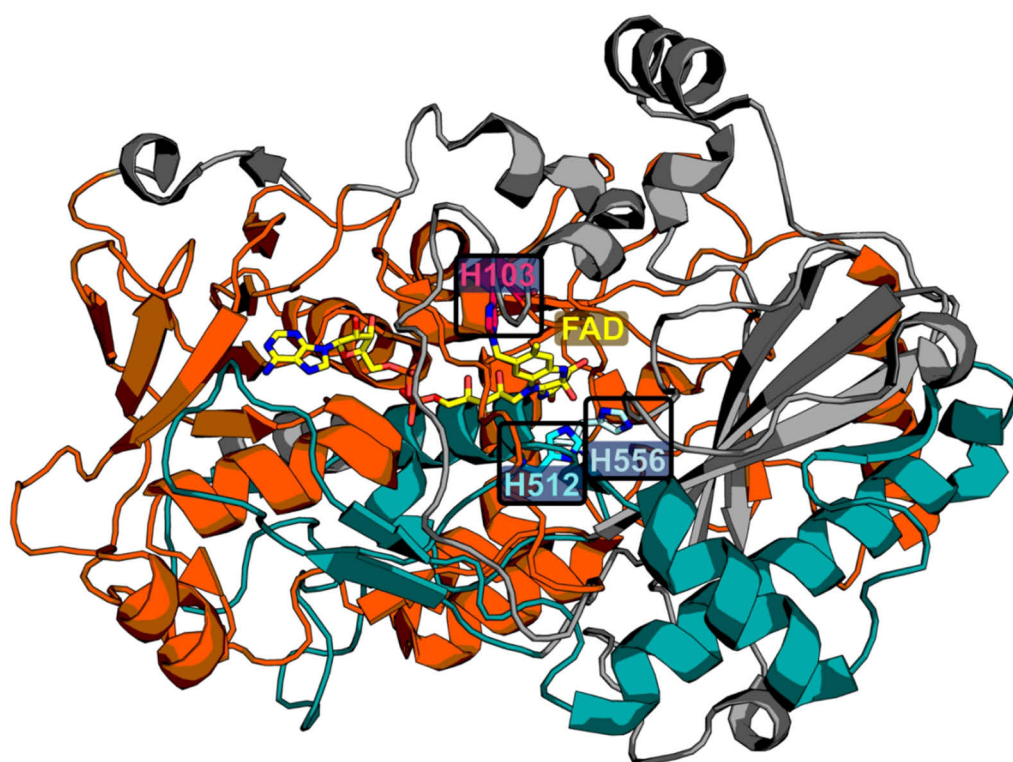


**Figure 1:** *AmPDH1* crystal structure (4H7U) with FAD binding domain (GMC\_oxred\_N, orange), substrate binding domain (GMC\_oxred\_C, turquoise), non-conserved parts (grey), co-factor FAD (yellow), the active site bases  $\text{H}^{512}$  and  $\text{His}^{556}$  (cyan), and FAD binding  $\text{His}^{103}$  (pink) [18,19].

The biological function of pyranose dehydrogenase, expressed by this group of litter-degrading basidiomycetes, is still not well understood. PDH cannot support lignin degradation via  $\text{H}_2\text{O}_2$  formation, as was proposed for the related P2O, due to its extremely low rates of  $\text{H}_2\text{O}_2$  formation [12,17]. A role in the reduction of quinones, key intermediates of lignin degradation, was suggested instead, analogue to the reduction by P2O [12]. This is thought to support degradation by preventing repolymerization [20,21]. A proposed alternative biological function, for PDH and P2O, is the neutralization of strongly antimicrobial quinones produced by plants. This could be achieved by

reduction of quinones to hydroquinones, and thereby create a growth advantage for saprophytes such as the native producers of PDH. An observed moderate stress-related induction of PDH expression in *Agaricus meleagris* was in line with this proposed function [12,3]. A further indication for that function is that Morin et al. found that known detoxification enzymes were overrepresented in general in the genome of the PDH producer *Agaricus bisporus*, compared to other fungi [22]. Interestingly, PDH and P2O, which have been suggested to serve these similar functions, appear to be mutually exclusively expressed as no organism has been identified to date with both genes [10,3].

### Structure

Unlike the related tetrameric P2O, of which many variants could be elucidated by X-ray crystallography, structural information on PDH is limited to date to a single variant, *Agaricus meleagris* PDH1 (*AmPDH1*). Tan et al. published its resolved structure (PDB: 4H7U, Figure 1) and the structurally most closely related enzyme was aryl-alcohol oxidase (PDB: 3FIM). As expected from a GMC structural family member it featured a PHBH-like fold with an FAD binding domain and a substrate binding domain. Unlike most flavoenzymes, however, but similar to the related P2O, the co-factor FAD was covalently bound to His<sup>103</sup> (8 $\alpha$ -N<sup>3</sup>-histidyl bond) [2,18].

### Reaction mechanism

In the absence of elucidated crystal structures of PDH-substrate complexes, the reaction mechanism of PDH was investigated by means of molecular dynamics simulation and study of active site variants. A reductive half-reaction was proposed analogous to the one of P2O. There, the initial reaction step is a proton abstraction from the substrate by a general base. The intermediate state is then stabilized by that protonated base and a subsequent hydride transfer from the substrate to the flavin N<sup>5</sup> is reducing the co-factor. His<sup>512</sup> and His<sup>556</sup> (Figure 1 and 2) were suggested as possible catalytic bases for this half-reaction [23,24]. Consequently, those two residues were investigated by site directed mutagenesis and His<sup>512</sup> was confirmed as the only catalytic base, as the variant H512A had a 10<sup>5</sup>-fold decreased catalytic efficiency with D-glucose. His<sup>556</sup> on the other side was central to substrate binding, with a 110-fold decreased affinity of the variant H556A to D-glucose. By testing additional active site variants of *AmPDH1*, nearby residues Val<sup>511</sup>, Tyr<sup>510</sup> and Gln<sup>392</sup> (Figure 2) were shown to play a role in substrate binding as well [25].

Less is known about the oxidative half reaction of *AmPDH1*. It is also not fully understood why PDH is a dehydrogenase, relying on alternative electron acceptors, while the related P2O utilizes dioxygen as well. More fundamentally, the factors deciding if flavoenzymes are oxidases or dehydrogenases, in general, remain unclear [17,26,27]. In the flavoenzyme family of vanillyl-alcohol oxidases (VAO), a gatekeeping residue in the active site, stabilizing the C(4a) FAD adduct, was postulated to determine if the enzyme is an oxidase [28]. A C(4a) adduct has been identified as reaction intermediate of P2O as

well [29], where it is used in the formation of  $H_2O_2$  [30]. Even though PDH is a dehydrogenase, its only available crystal structure also featured a C(4a) adduct, which appeared to be stabilized by His<sup>512</sup> and His<sup>556</sup> (Figure 2). This was thought to have been an artificial radiation fragment but showed, nonetheless, that the active site of PDH could accommodate this adduct [18]. One of the two active site residues of P2O, which were found to influence oxygen reactivity substantially, was Asn<sup>593</sup>, the analogue to *Am*PDH1 His<sup>556</sup>. The variant N593C had a 1700-fold reduced catalytic efficiency with dioxygen but also a 2 to 22-fold decreased catalytic efficiency with alternative electron acceptors. The other residue was Leu<sup>547</sup>, an analogue to *Am*PDH1 Val<sup>511</sup>. Replacing it by a positively charged arginine reduced oxygen reactivity 100-fold, without negatively affecting its dehydrogenase activity [27]. While P2O could be therefore shifted from its oxidase towards its dehydrogenase activity, the opposite approach with PDH proved more challenging. In a site saturation mutagenesis study of active site residues, only substitutions of His<sup>103</sup>, the residue covalently linking the cofactor FAD, could be identified as improving oxygen reactivity. The variant H103Y had a 5-fold increased reactivity with molecular oxygen compared to the wild type enzyme. This rate was still too poor to determine steady-state constants, however [17]. Other active site variants created by site directed mutagenesis (Q392A, V511F and H556A) were also shown to increase oxygen reactivity, but only by a factor of 2-4 [25].

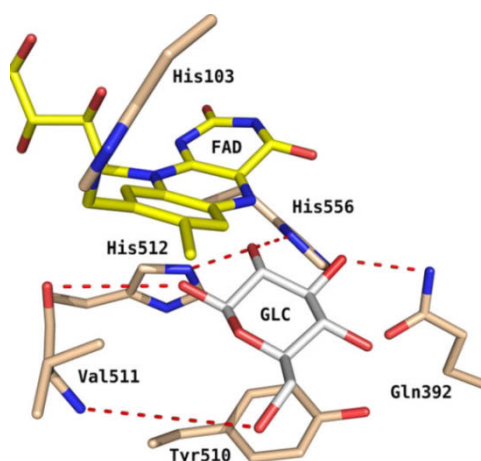


**Figure 2:** D-glucose crafted into the active site of *Am*PDH1 (4H7U) [18] for oxidation of C2. D-glucose coordinates were taken from structurally aligned *Trametes ochracea* P2O (PDB: 3PL8) with bound D-glucose. From Graf et al, 2015. [25,23]

### Expression of pyranose dehydrogenase

A broad range of *Agaricales* was successfully cultivated in static liquid cultures with detectable PDH activity in the supernatant [10]. Initial characterization studies of *Ab*PDH [9,31], *Ax*PDH [11] and *Am*PDH [8,32] relied on homologous expression in static cultures and subsequent purification of secreted PDH from the supernatant. Especially cultivation of *Agaricus xanthoderma* and *Agaricus*

*meleagris* for PDH production was slow and labour intensive (1.5-2 months). To improve volumetric time yields and scalability of PDH expression, heterologous expression strategies were implemented for PDH [33,34]. The first reported heterologous expression of a pyranose dehydrogenase was in a fungal expression system. The gene *pdh1* from *Agaricus meleagris* was expressed in a 2 L *Aspergillus niger* suspension culture at a space-time-yield of  $733 \text{ U L}^{-1} \text{ d}^{-1}$ . The specific activity of purified enzyme,  $56 \text{ U mg}^{-1}$ , and its mass and extent of N-glycosylation were in agreement with properties of the native enzyme [33]. Alternative recombinant expression systems based on bacteria or yeasts were also tested as they could enable easier genetic manipulation than fungal systems. The bacterial system *Escherichia coli* only yielded non-functional inclusion bodies but efficient expression could be established with the methylotrophic yeast *Pichia pastoris*. At a 50 L bioreactor scale a space-time-yield of  $1,330 \text{ U L}^{-1} \text{ d}^{-1}$  could be achieved with a total amount of 13.4 g recombinant *AmPDH1* after purification. It had 80% of the specific activity of native enzyme but was observed to be hyperglycosylated on SDS-page [34]. Another yeast expression system, *Saccharomyces cerevisiae*, is prone to even greater hyperglycosylation (see chapter 2.3: Maturation in the Golgi yields a broad variety of N-glycan structures), but enables further simplification of genetic manipulation compared to *Pichia pastoris*. Krondorfer et al. used it for high throughput expression screening of *AmPDH1* variants, whereas subsequent expression of selected *AmPDH1* variants for purification and characterization was then done in *Pichia pastoris* [17]. Other than *AmPDH1*, also *AcPDH* and *AxPDH* have been previously functionally expressed in *Pichia pastoris*, even though to substantially lower space time yields of  $4.5 \text{ U L}^{-1} \text{ d}^{-1}$  and  $55 \text{ U L}^{-1} \text{ d}^{-1}$  [35]. In this work, functional expression of an additional variant, *AbPDH*, was reported for the first time.

## Potential applications of pyranose dehydrogenase

### Bioconversion

Pyranose dehydrogenase was suggested as an alternative for P2O in bioconversion reactions of sugars. Oxidation of D-galactose to 2-dehydro-D-galactose, is the first of two steps towards redox-isomerization to D-tagatose, which is sold as low caloric and prebiotic sweetener [36]. This reaction is catalysed by P2O only at a poor catalytic efficiency [12,37]. For PDH however, D-galactose is among the preferred substrates. Bioconversion to 2-dehydro-D-galactose, at a 400 ml scale, was achieved within 3.5 h to quantitative yields and with no detectable side products. 110 U of *AmPDH1*, 1,4-benzoquinone as electron acceptor, and *Trametes pubescens* laccase for its enzymatic regeneration, were used in this system [8]. An alternative process that has been suggested is the conversion of D-lactose to lactobionolactone and 2-dehydro-lactose, via C1 and C2 oxidation, respectively. The substrate D-lactose is a major by-product of the dairy industry, and while other enzymes have been

reported to catalyse its C1 oxidation, PDH was the first reported enzyme to oxidize its C2 position, yielding 2-dehydro-lactose. This is an intermediate during further conversion to the higher value prebiotic sugar lactulose, which is used for treatment of constipation. None of the screened PDH variants showed exclusive selectivity for C2, however, and lactobionolactone was found as side product, which would need to be separated [12,38].

### **Enzymatic biosensors**

One of the challenges for PDH in bioconversion systems is its incapability of utilizing molecular oxygen, hence the need for an additional electron acceptor regeneration system. In electrochemical applications however, where PDH is used for catalyzing the anodic half-reaction, this feature is a valuable advantage. Almost no reactivity with molecular oxygen means little to no generation of enzyme damaging  $H_2O_2$  and also prevents that electrons are transferred to molecular oxygen instead of the electrode [12,17]. Therefore recent studies have focused on use of PDH in enzymatic bio-fuel cells and biosensors.

A biosensor is a device which selectively quantifies a specific substance in a matrix, like water or blood. It contains a biological recognition element which selectively senses the substrate in a quantifiable manner. Subsequently, an adjacent transduction element transforms for example the catalytic conversion event into a quantifiable physical signal [39], whereby the resulting signal needs to be proportional to the substrate concentration in the sample [40]. A large variety of different biosensor concepts exist, one of them is an amperometric biosensor where the sensing element is a catalytically active oxidoreductase immobilized on an electrode. In this case, the current of the electrode is measured, upon exposure to the sample liquid while a set potential is applied. Catalytic current is generated by the enzyme oxidizing the substrate and transferring the garnered electrons to the anode [41,42]. Three generations of biosensor designs are differentiated based on how this electron transfer is realized. In 1<sup>st</sup> generation biosensors a natural redox mediator of the enzymatic reaction, commonly  $O_2$  or  $H_2O_2$ , is sensed at the electrode surface. The downsides of this approach are disadvantageous working electrode potentials which are needed for oxidation of  $H_2O_2$ , or reduction of  $O_2$ , and a signal which is influenced by the concentration of available molecular oxygen. These issues were resolved in 2<sup>nd</sup> generation biosensors where artificial electron mediators, with an optimized redox potential, are employed, which are recycled as they transfer the electrons to the electrode surface. Initially those were also freely diffusing substances but modern designs often use redox polymers anchored to the electrode to prevent leaching and dilution of the mediator. 3<sup>rd</sup> generation biosensors are the latest concept. Unlike the former two designs they do not rely on mediated electron transfer (MET) but on direct electron transfer (DET) from the enzyme's cofactor to the electrode surface through electron tunneling. To achieve this, the cofactor has to be in very close proximity to the

electrode surface and only a limited number of enzymes are therefore capable of direct electron transfer [41,43–45].

The largest market for enzymatic biosensor today is rapid blood-glucose determination in diabetes treatment. These biosensors are commonly based on highly selective glucose oxidase [46]. With its substrate promiscuity [47], PDH is not suitable for measuring single specific sugars selectively, like those blood-glucose biosensors. Instead, in a recent PDH based biosensor, an *Am*PDH1 modified carbon paste electrode (Figure 3), with DCIP as electron mediator, was employed to measure cellulase activity and study activity loss over time. Previously reported CDH based sensors were challenged by the variability of cellulase products due to mutarotation of the product molecules. Those sensors could only detect product in the  $\beta$ -anomeric but not in the  $\alpha$ -anomeric form. As *Am*PDH1 was shown to be anomericly unspecific, it was not affected by this limitation and therefore commended for use in steady state kinetic measurements of cellulases [48,49].

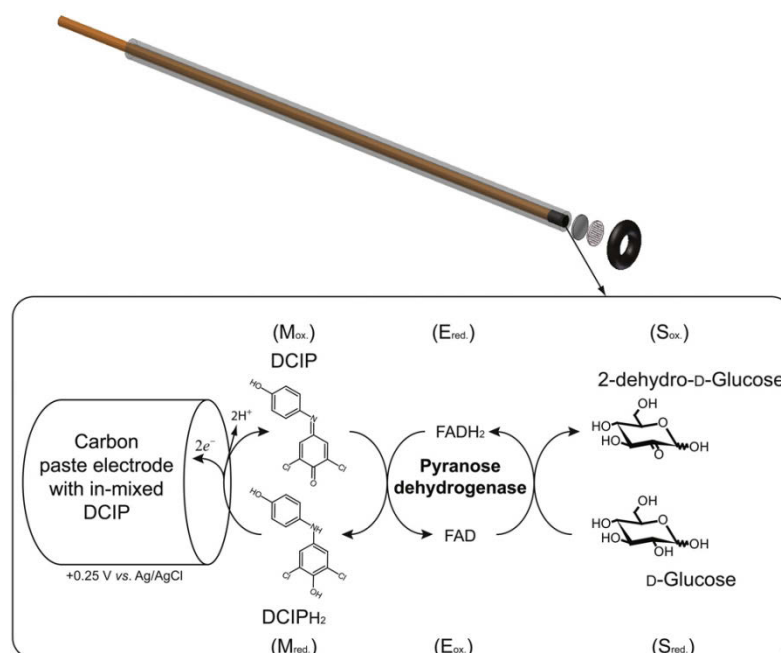


**Figure 3.** Schematic view of *Am*PDH1/DCIP biosensor for detection of cellulase reaction products, from Cruys-Bagger et al. (2014) [49].

### Enzymatic bio-fuel cells

Like enzymatic biosensors, also enzymatic bio-fuel cells employ electrodes with immobilized enzymes. The aim is however not to measure a substrate concentration but to transform chemical energy into electricity [41]. Akin to traditional fuel cells, enzymatic bio-fuel cells consist of a fuel oxidizing anode and an oxidant reducing cathode. These reactions are however not catalysed by non-

selective catalytic metals but by substrate selective biocatalysts in form of enzymes [50]. The concept of an enzymatic bio-fuel cell is illustrated by the example in Figure 4. Enzymes are immobilized on inert electrodes. Fuel, in this case D-glucose, is oxidized at the anode and molecular oxygen is reduced to water at the cathode. As in biosensors, electrons are transferred between cofactor and electrode surface either directly (DET) or mediated by redox mediators (MET) [50,51].

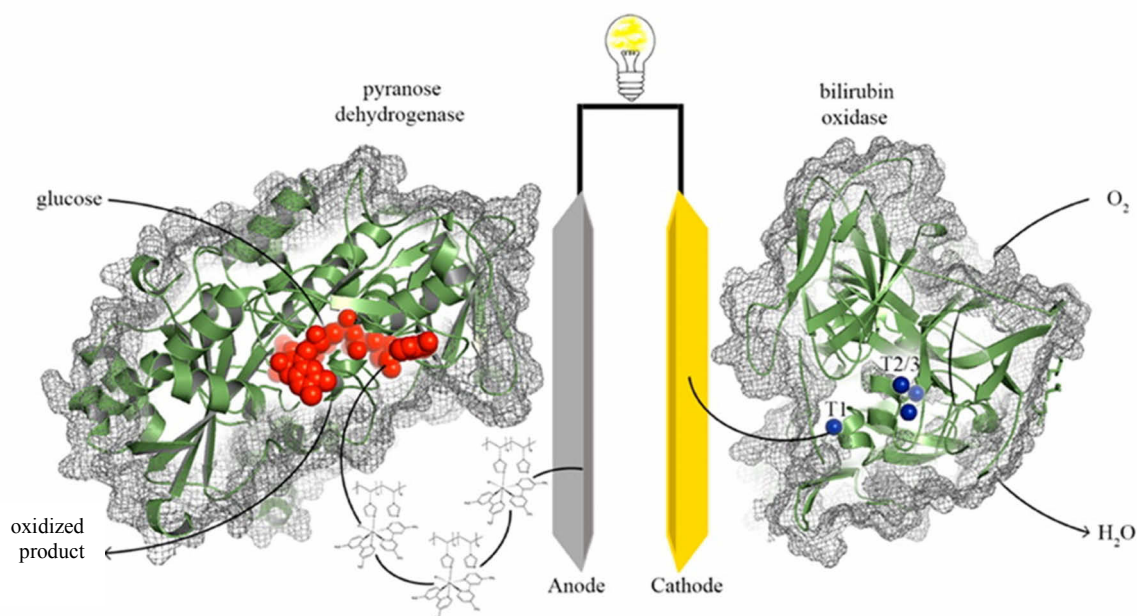


**Figure 4.** Schematic view of a glucose/ $O_2$  enzymatic bio-fuel of Ó Conghaile et al. (2016). A deglycosylated *AmPDH1*/Os-polymer/multiwalled carbon nanotube modified graphite electrode served as anode and a *Myrothecium verrucaria* bilirubin oxidase/gold nanoparticle modified gold electrode as cathode. Based on Ó Conghaile et al. (2016) [51].

Key parameters for the performance of such systems are open circuit voltage (OCV), maximum current density and maximum power density. The OCV is the highest possible cell potential, which is achieved in the absence of current. The highest theoretical OCV of a sugar based enzymatic bio-fuel cell is 1.18-1.24 V at 298 K. The real OCV is lower due to ohmic losses as well as limitation of mass-transfer and electron transfer rates, and rarely higher than 0.5 V [50,52]. In practice, the OCV depends on the difference between the midpoint potentials of the anodic and cathodic enzyme cofactors or redox mediators. Enzyme cofactors and redox mediators for the anodic half reaction should therefore feature a low, and those for the cathodic half reaction a high, midpoint potential. Bio-fuel cell performance can be visualized in form of polarization and power density curves as shown in Figure 5. Higher current densities lead to lower cell voltages (Figure 5A) but, up to a point, also to higher power densities (Figure 5B). The optimal conditions, which yield the maximum power density, are a compromise between cell voltage and current density [53].

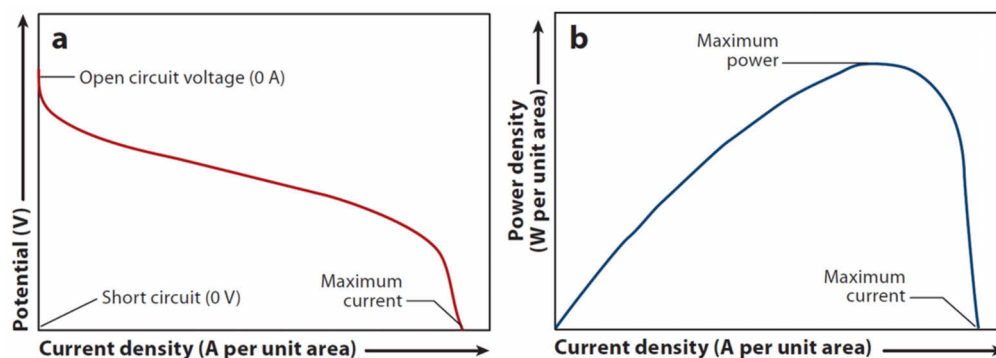


**Figure 5.** Schematic polarization curve (A) and power density curve (B). From Meridith and Minter (2012) [53].

Commonly used enzymes for enzymatic bio-fuel cells have been glucose oxidase and glucose dehydrogenase for the anodic, and bilirubin oxidase and laccase for the cathodic half reaction [54]. The choice of suitable enzymes depends on numerous characteristics, besides their midpoint potential. Substrate specificity, catalytic efficiency and oxidation pattern are central aspects [50,53,55], as they influence which fuels can be used efficiently. Equally important is the question how the enzyme can be “wired” to the electrode and if direct electron transfer is possible or mediated electron transfer strategies have to be chosen [54,56]. A feasible bio-fuel cell design furthermore needs enzymes with a high stability and low production costs. Enzymes also need to work efficiently at mild pH and ambient temperatures, which are regularly chosen operating conditions [53]. Moreover, they should not be inhibited by commonly present electrolytes such as chloride [56], and no disadvantageous side reactions should occur, such as production of enzyme damaging  $\text{H}_2\text{O}_2$  [34,57].

As mentioned before, enzymatic bio-fuel cells have the advantage of operating with sugars, or other organic compounds as fuel, at generally mild conditions. This commends them as an implantable energy source, as glucose and oxygen are widely available in the human body. Initially they were therefore considered for powering artificial hearts or cardiac pacemakers where they could, however, not compete with batteries. The main challenges were limited power densities, low cell voltage and operational stability [52,58,59]. More recent progress in nanobiotechnology, however, revived research for implantable applications. With novel strategies of “wiring” enzymes to electrodes, mediated electron transfer could be established without freely diffusing redox mediators. Consequently no semipermeable separator was necessary anymore, to prevent interference between anode and cathode [60]. Thus, membraneless enzymatic bio-fuel cell designs became possible, setting them apart from separator dependent metal catalyst based fuel cells and batteries, and enabling simplified designs and strong miniaturization potential [50,59,61,62]. Numerous methods of “wiring” enzymes to electrodes have been developed. These include immobilizing the catalytically active enzyme in hydrogel forming redox-polymers (Figure 6A), and adsorbing enzyme to carbon nanotubes or other inert but conducting nanomaterials (Figure 6B) [56]. Hydrogels with high electron diffusion

rates were developed based on Os-polymers. There, Os-complexes with tailored redox potentials were covalently linked via a long spacer to the polymer backbone to act as mobile, yet anchored, electron mediator [59,63]. Carbon nanotubes on the other side have become popular electrode surface modifications for both, mediated and direct electron transfer, in current enzymatic bio-fuel cell research due to their large surface area, high conductivity and formation of porous layers [64].

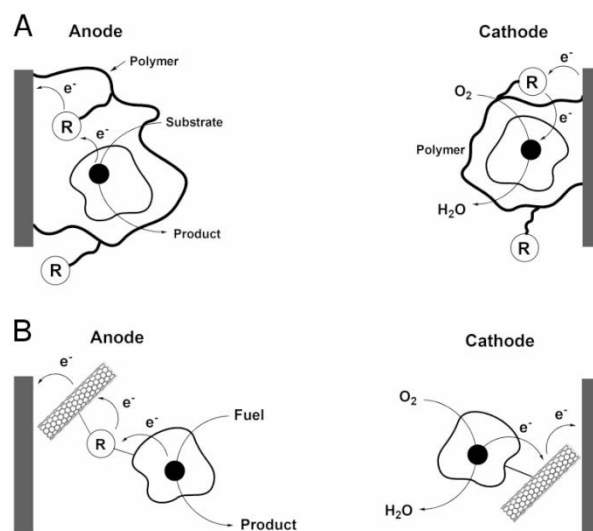


**Figure 6.** Electrode designs for enzymatic bio-fuel cells. (A) Redox-polymers form a hydrogel, immobilizing the enzyme within, while also acting as redox mediators. Substrate and product can diffuse through the hydrogel. (B) Immobilization of enzyme on carbon nanotubes or other nanomaterials, with or without redox-mediators. From Willner et al. (2009) [56].

Based on these progresses in electrode design, miniaturized enzymatic bio-fuel cells were suggested for application as a power source for sensor-transmitters implanted for a few weeks [59]. A number of prototypes have been implanted since then in rats and other living animals, employing DET and MET concepts [52,54,65–69]. One of those prototypes, consisting of two enzymatic bio-fuel cells, implanted in separate lobsters, and connected in series, could power a digital watch [52]. The major challenge of biocompatibility and operational stability was not taken into account in this preliminary proof of concept however. To address the issue of biocompatibility, Zebda et al. designed a compressed enzyme/carbon nanomaterial based bio-fuel cell packaged in a dialysis membrane, supported by a perforated silicon tube and sutured into a biocompatible Dacron® bag. The dialysis membrane served as barrier against diffusion of electrode material into, but also against potentially damaging macromolecules from, the host body. The Dacron® bag ensured biocompatibility of the implant. Maximum power density, tested 6-8 d after surgery, was  $194 \mu\text{W cm}^{-2}$  and the OCV was 0.57 V. This was enough to power a digital thermometer but due to wire breakage the fuel cells stopped being operational after around 9 days [65].

Further progress in the creation of biocompatible electrodes was achieved by developing diffusion optimized genipin cross-linked chitosan barriers, replacing the dialysis membrane. This barrier minimised inflammatory response in the initial two weeks and it was successfully integrated in the host body, still intact and not degraded after 167 d *in vivo* [70].

These examples show the considerable progress of early implantable enzymatic bio-fuel cell prototypes in recent years, based on novel materials and improved electrode design and implantation strategies. However, these implanted bio-fuel cell prototypes are mostly based on glucose dehydrogenase or glucose oxidase as anodic enzymes [54] and coulombic efficiency of those two enzymes is low. They harvest only 2 electrons per D-glucose molecule [55], which is 1/12 of the electrons gained from complete oxidation of D-glucose to 6 CO<sub>2</sub>. Moreover, while implantable applications, and therefore D-glucose as fuel, have been the focus of much of the current enzymatic bio-fuel cell research, also non-implanted applications have been suggested. With a potential power output in the  $\mu\text{W}$  to 10 mW range [71] enzymatic bio-fuel cells could be used to power small portable electronic devices. For these applications also alternative fuels, such as cellobiose, lactose or maltose could be used [53]. In those cases an alternative to glucose oxidase is needed with its narrow substrate selectivity for D-glucose [14]. Pyranose dehydrogenase ( $E^{\circ}$  (pH 7) = +92 mV) [25] with its broad substrate range, including D-glucose, and its capability of harvesting 4 electrons per sugar molecule, attracted attention as an alternative candidate [12,13]. Another advantage of PDH over glucose oxidase is its almost complete lack of disadvantageous H<sub>2</sub>O<sub>2</sub> formation [17].

Due to PDH's capability of dioxidation, one venue of research focused on improving coulombic efficiency. Increasing it by oxidizing multiple C positions of D-glucose could substantially improve fuel efficiency of enzymatic bio-fuel cells. Therefore bi-enzymatic bioanodes were studied, combining a C1 oxidizing enzyme and *Am*PDH1, which is capable of di-oxidation of C2 and C3 of D-glucose [55,72,73]. An optimised membraneless glucose/O<sub>2</sub> bio-fuel-cell with increased maximum current density and fuel efficiency was consequently reported by Shao et al. It was based on an *Am*PDH1/*Corynascus thermophilus* CDH dehydrogenase domain C310Y/Os-polymer modified graphite anode and a *Myrothecium verrucaria* bilirubin oxidase modified graphite cathode. This bio-fuel cell achieved a maximum power output of 20  $\mu\text{W cm}^{-2}$  at 300 mV cell voltage with 5 mM D-glucose in physiological buffer. Up to 6 electrons could be garnered per D-glucose molecule, and in presence of limited fuel, half-life of the mixed bio-fuel cell was increased 2-fold compared to an analogously designed single enzyme anode bio-fuel cell [74].

Another focus of research was on improving bioanode performance by using *in-vitro* deglycosylated enzyme for modification (see also Chapter 2.3: Enzyme performance can be improved by preventing or removing N-glycosylation). Based on research with *in-vitro* deglycosylated *Am*PDH1 [75–77], a glucose/O<sub>2</sub> bio-fuel cell (Figure 4) could be constructed with 10-fold maximum power output

compared to an analogue bio-fuel cell with glycosylated *AmPDH1*. It consisted of a deglycosylated *AmPDH1*/Os-polymer/multiwalled carbon nanotube modified graphite anode and a *Myrothecium verrucaria* bilirubin oxidase/gold nanoparticle modified gold cathode. At a cell voltage of 300 mV it achieved a maximum power output of  $73 \mu\text{W cm}^{-2}$  in whole human blood and  $275 \mu\text{W cm}^{-2}$  in PBS buffer with 5 mM D-glucose [51].

Although enzymes are such a central component of enzymatic bio-fuel cells, surprisingly, genetic engineering of enzymes has been rarely used for optimizing bio-fuel cells performance so far. Among the few reported examples are engineered cellobiose dehydrogenase [74,78] and pyranose 2-oxidase [37,79]. And in this work, rational engineering of *AmPDH1* for partial N-glycosylation was explored for improving maximum current densities of PDH modified anodes.

## **N-glycosylation: Function and engineering potential**

Understanding the role of N-glycosylation is the basis for engineering it. Like the majority of eukaryotic protein species, all known pyranose dehydrogenases are glycosylated [12,80]. Hereby, glycan groups are covalently attached to a protein [81], whereas 90% of the well characterized glycoproteins featured the asparagine (N) linked glycosylation type [80].

This chemically complex modification is serving a broad variety of biological functions. N-glycans are thought to influence protein folding by stabilizing local conformations, increasing the polarity, and limiting conformational freedom. Also a central role of N-glycans has been reported in the quality control mechanisms of protein folding in the ER and subsequent addressing towards translocation, secretion or degradation [82]. In the final protein N-glycosylation can improve thermostability and solubility and protect from proteolytic digest. Also cases of negative, and less commonly positive, influence of deglycosylation on catalytic activity of enzymes have been reported. N-glycans are furthermore important modulators of receptor binding affinities [82–85]. In higher organisms glycoconjugates such as N-glycans have been shown to influence cell morphology and cell developmental events. Moreover, cell adhesion and the immune system depend on them. [86–88].

### **Core oligosaccharides are pre-assembled and transferred to Asn within N-X-S/T sequons**

As diverse as its biological functions are, as complex is the process of N-glycosylation itself. It starts with the dolichol-pathway where core oligosaccharides are formed at the ER membrane and transferred to N-glycosylation sites of newly synthesized peptide chains as they enter the ER. Those core glycans are then modified further in the ER and also in the golgi apparatus [88]. The core

oligosaccharides are highly conserved in eukaryotic cells and are assembled by membrane bound glycosyltransferases in a bi-compartmental process with dolichol as membrane carrier for the oligomer.  $\text{Man}_5\text{GlcNAc}_2$  is formed on the cytosolic side of the ER membrane, translocated to the inside and completed to  $\text{Glc}_3\text{Man}_9\text{GlcNAc}_2$  (Figure 7) [82,89].

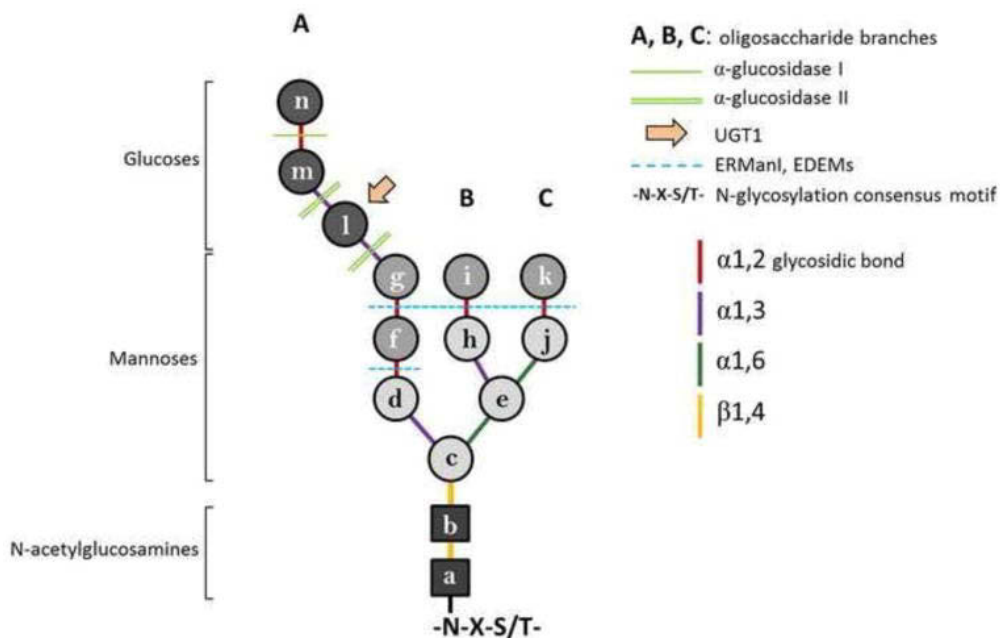


**Figure 7.** Core oligosaccharide transferred by oligosaccharyltransferase (OST) to the Asn of N-glycosylation sites, consisting of N-acetylglucosamine (GlcNAc), D-mannose (Man) and D-glucose (Glc). GlcNAc “a” is covalently linked to the Asn. Cleavage sites of selected glycosidases in the ER are shown. From Tannous et al. (2015) [90].

Oligosaccharyltransferase (OST) scans the translated peptide chain as it enters the ER for N-X-S/T sequons and attaches a core oligosaccharide via N-glycosidic bond to the Asn [82]. Whereas, X in the sequon can be any amino acid but proline. Glycosylation of asparagine, with amino acids other than serine or threonine in position +2 are the exception, although some cases have been reported in recent years. While the presence of the sequon is important, it is not sufficient for covalent linkage of glycans to Asn (N) [81,91–93]. The modification efficiency also depends, among others, on neighbouring amino acids, the location of the sequon in the gene [94], the rate of protein folding and the availability of precursors and glycosyltransferases [82]. It has been predicted that about 2/3 of the sequons are modified [80].

### N-glycosylation enhances and regulates glycoprotein folding in the ER

While not all N-glycosylation sites of a glycoprotein are required for efficient expression, some were shown to be essential [95]. N-glycans have been suggested to promote protein folding directly by

stabilizing local conformations. Also, interactions between N-glycan and peptide chain were reported to help in the formation of  $\beta$ -turns which are thought to act as folding nuclei [96,97,82].

Structure			Generated by		Signal for
Native	Misfolded	Immature	Mammals	<i>S. cerevisiae</i>	
			OST	OTase	N-glycan dependent protein folding and quality control
			Glucosidase I	Gls1p	Association with malectin
			Glucosidase II	Gls2p	Association with calnexin and/or calreticulin
			UGT1	-	Re-association with calnexin and/or calreticulin
			Glucosidase II	Gls2p	Prevents re-association with calnexin and/or calreticulin
			ERManI	Mns1p	ER exit
			ERManI	Mns1p	ERAD
			GH family 47 members	Htm1p	ERAD
			GH family 47 members	-	ERAD

**Figure 8.** Stages of N-glycan trimming in the ER and their signal function in protein folding and quality control. From Aebi et al. (2010) [98].

Oligosaccharides are also acting indirectly on protein folding as signals for chaperons and folding quality control which depend on subsequent trimming events of peptide chain linked N-glycans in the ER [90,98] (Figure 8). The terminal glucose residue is removed immediately after the transfer of the oligosaccharide to the protein [99]. The resulting N-glycan can be recognized by malectin [100], a lectin in higher eukaryotes, that is expressed under ER stress and thought to identify terminally misfolded proteins at an early stage [101].

Removal of the second glucose enables association of the glycoprotein with the ER chaperons calnexin and calreticulin [102–105] which bind to monoglucosylated N-glycans and facilitate protein folding. Other assisting proteins can associate with calnexin and calreticulin and are catalyzing the formation of disulfide bonds (disulfide isomerases; PDI family) or conformational changes in peptidyl-prolyl bonds (peptidyl-prolyl isomerases; PPI family) [90,106–108]. This calnexin/calreticulin assisted folding ends with the removal of the third glucose residue. The glycosyltransferase UGT1 acts as folding sensor and can detect proteins which retained a non-native

fold. By adding again a single glucose to the N-glycan it can initiate another round of the calnexin/calreticulin cycle. [102,109]. However, not all eukaryotes feature this mechanism. Among yeasts, *Schizosaccharomyces pombe* expresses under stress conditions a homologue to UGT1, but the model organism *Saccharomyces cerevisiae* does not [110,111].

Trimming of  $\alpha$ 1,2-mannoses (figure 7 and 8) is a timing mechanism to prevent endless folding attempts of terminally misfolded proteins and to eventually direct them to the ER assisted degradation pathway (ERAD) [112–115]. Proteins targeted by lectins to the ERAD machinery are ubiquitinated by E3 ubiquitin ligases like HRD1 and translocated to the cytosol where they are finally degraded by proteasomes [115,116]. Glycoproteins with correct conformation and high mannose N-glycans ( $\text{Man}_7\text{GlcNAc}_2$ ) however, exit the ER and are transported to the Golgi [90,115,117–119].

### Maturation in the Golgi yields a broad variety of N-glycan structures

Although most folding quality control events take place in the ER, some have been described in the Golgi as well [120]. Moreover, N-glycans are processed to their final form in the Golgi. Unlike the trimming events in the ER, those modifications are less conserved however, leading to distinct structures. High-mannose, hybrid and complex type are the major groups of mature N-glycan structures (Figure 9). Higher eukaryotes feature all three types but more commonly have glycoproteins with hybrid and complex N-glycans. The latter are formed from core oligosaccharide by trimming back to  $\text{Man}_3\text{GlcNAc}_2$  and subsequently adding antennary structures consisting of GlcNAc and terminal sugars such as D-galactose, N-acetylgalactosamine (GalNAc) fucose and sialic acid. In hybrid N-glycans these antennary structures are transferred to the precursor  $\text{Man}_5\text{GlcNAc}_2$  [88,121–123].

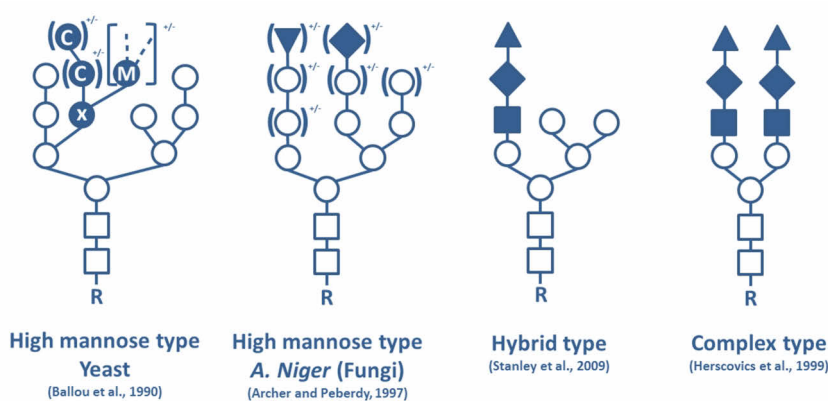


**Figure 9.** Exemplary mature N-glycans [N-acetylglucosamine ( $\square$ ;  $\blacksquare$ ), D-mannose ( $\circ$ ,  $\bullet$ ), galactofuranose ( $\blacklozenge$ ), N-acetylneuraminic acid ( $\blacktriangle$ ), D-glucose ( $\blacktriangledown$ )], sugar residues with filled symbols are added in the Golgi. Residues in brackets are commonly subject to variability between organisms or within the same organism. “X” marks the mannose residue added by Och1p in yeast, “C” shows core type glycosylation and “M” marks the starting point of chain-elongated glycosylation [121,122,125,127].

In this work, fungal enzymes were expressed in yeast systems and yeasts as well as filamentous fungi create glycoproteins with high-mannose type N-glycosylation (Figure 9) [124,125]. In yeasts, the core N-glycan is commonly not trimmed back beyond  $\text{Man}_8\text{GlcNAc}_2$ . The mannosyltransferase Och1p, or homologous enzymes, start the addition of mannose groups in the Golgi by adding a single  $\alpha$ 1-6 mannose as shown in Figure 9. Subsequently further hexose groups, mainly mannose, are added. This can lead to either core sized ( $\text{Man}_{<15}\text{GlcNAc}_2$ ) or, often much larger, chain-elongated high mannose N-glycans [124,126,127]. In the latter case, a  $\alpha$ 1-6 mannose backbone is formed with side chains that vary greatly between different yeast strains and can include terminal galactose and phosphomannose. If N-glycans remain core sized or are chain elongated is thought to depend not only on the strain but also the protein and the environment of the N-glycosylation site [124].

Hyperglycosylation of secreted glycoproteins produced in the yeast model organism *Saccharomyces cerevisiae* causes a less authentic recombinant product for proteins, which are not natively featuring chain elongated N-glycosylation. This is especially a problem for the recombinant production of mammalian proteins and for pharmaceutical purposes [128]. The chosen heterologous expression host in this work, *Pichia pastoris*, is also capable of chain-elongated N-glycosylation but uses it less frequently [129] and forms shorter chain elongated N-glycans than *Saccharomyces cerevisiae* [130]. Glycosylation patterns of *Pichia pastoris* varied substantially depending on the recombinantly expressed protein. Proteins were commonly modified entirely with the core sized type, predominantly in the range of  $\text{Man}_{4-12}\text{GlcNAc}_2$  [129,131–135]. However, some appeared to be hyperglycosylated by *Pichia pastoris*, as indicated by SDS-Page [136–139].

Filamentous fungi are the native producers of pyranose dehydrogenases, the engineering target of this work. Their high mannose type N-glycosylation often features shorter N-glycans than *Saccharomyces cerevisiae* as they may possess alternative core trimming  $\alpha$ 1,2-mannosidases and usually lack some of the mannosyltransferases involved in hyperglycosylation. Additionally, their N-glycans can be modified with terminal groups such as D-glucose and galactofuranose [140]. Fungal N-glycans of  $\text{Man}_{5-12}\text{GlcNAc}_2$  have been commonly described in literature but in some instances also smaller ones down to  $\text{Man}_1\text{GlcNAc}_2$  [141]. Even more unusual N-glycosylation patterns have been reported, such as modification of Asn with a single GlcNAc residue. The biological function of such single GlcNAc residues is still unknown but it was speculated that they may be the product of high mannose type N-glycans being exposed to native fungal Endo H or F [142].

### **Enzyme performance can be improved by preventing or removing N-glycosylation**

Reduced or completely removed N-glycosylation has been reported to impact glycoprotein secretion, function and stability. Positive as well as negative effects of it on enzymatic activity have been shown

[83]. In this thesis, the N-glycosylated pyranose dehydrogenase was engineered for improved current density of electrodes. Removal of N-glycosylation was previously demonstrated to be a successful strategy for improving electron transfer between oxidoreductase and electrode. Lindgren et al. tested horseradish peroxidase which was expressed in *Escherichia coli* and therefore non-glycosylated. It exhibited increased direct electron transfer to the electrode, compared to the native glycosylated enzyme. This was attributed to the reduced distance between active site and electrode surface and changed protein orientation, without the N-glycan [143]. A similar effect was reported with glucose oxidase where *in-vitro* deglycosylated protein produced an electric current on glassy carbon electrode, unlike the native glycosylated one [144].

*Agaricus meleagris* pyranose dehydrogenase 1 (*AmPDH1*) could not be expressed in *Escherichia coli* [34]. It was therefore recombinantly expressed in the N-glycosylating expression system *Pichia pastoris* and subsequently *in-vitro* deglycosylated. In line with previous work on other oxidoreductases, the deglycosylated variant yielded a 2-fold increase in maximal current density on Os-polymer modified graphite electrodes, compared to the glycosylated variant. Furthermore, direct electron transfer was reported, which could not be observed with glycosylated *AmPDH1* [75]. With this approach also catalytic current of cellobiose dehydrogenase based electrodes could be improved [145].

### **Effect of individual N-glycosylation sites can be studied by site-directed mutagenesis**

*In-vitro* deglycosylation techniques remove N-glycans from all N-glycosylation sites, indiscriminately. They are also introducing an additional modification step in enzyme preparation, employing costly deglycosylation enzymes, which pose a challenge in upscaling. An alternative approach, employed in this thesis, is to selectively knock out N-glycosylation sites via site-directed mutagenesis. Those sites are commonly eliminated by replacing the asparagine (Asn, N) of the N-X-S/T sequon with the structurally similar glutamine (Gln, G), or, less frequently, other amino acids. This enables the study of effects of individual N-glycosylation sites on the glycoprotein [83]. Grinnell et al. could show for example, that two N-glycosylation sites of human protein C were important for expression and intracellular modification, while knocking out the other two sites increased its activity [146]. With site-directed mutagenesis N-glycan elimination can be limited to those sites where it is beneficial while leaving the other sites glycosylated.

## References

- 1 Cavener DR (1992) GMC oxidoreductases: A newly defined family of homologous proteins with diverse catalytic activities. *J. Mol. Biol.* **223**, 811–814.
- 2 Dijkman WP, Gonzalo G de, Mattevi A & Fraaije MW (2013) Flavoprotein oxidases: classification and applications. *Appl. Microbiol. Biotechnol.* **97**, 5177–5188.
- 3 Kittl R, Sygmund C, Halada P, Volc J, Divne C, Haltrich D & Peterbauer CK (2008) Molecular cloning of three pyranose dehydrogenase-encoding genes from *Agaricus meleagris* and analysis of their expression by real-time RT-PCR. *Curr. Genet.* **53**, 117–127.
- 4 Zámocký M, Hallberg M, Ludwig R, Divne C & Haltrich D (2004) Ancestral gene fusion in cellobiose dehydrogenases reflects a specific evolution of GMC oxidoreductases in fungi. *Gene* **338**, 1–14.
- 5 Mattevi A (1998) The PHBH fold: Not only flavoenzymes. *Biophys. Chem.* **70**, 217–222.
- 6 Finn RD, Mistry J, Tate J, Coggill P, Heger A, Pollington JE, Gavin OL, Gunasekaran P, Ceric G, Forslund K, Holm L, Sonnhammer ELL, Eddy SR & Bateman A (2010) The Pfam protein families database. *Nucleic Acids Res.* **38**, D211–D222.
- 7 Kiess M, Hecht H-J & Kalisz HM (1998) Glucose oxidase from *Penicillium amagasakiense*. *Eur. J. Biochem.* **252**, 90–99.
- 8 Sygmund C, Kittl R, Volc J, Halada P, Kubátová E, Haltrich D & Peterbauer CK (2008) Characterization of pyranose dehydrogenase from *Agaricus meleagris* and its application in the C-2 specific conversion of D-galactose. *J. Biotechnol.* **133**, 334–342.
- 9 Volc J, Kubátová E, Wood DA & Daniel G (1997) Pyranose 2-dehydrogenase, a novel sugar oxidoreductase from the basidiomycete fungus *Agaricus bisporus*. *Arch. Microbiol.* **167**, 119–125.
- 10 Volc J, Kubátová E, Daniel G, Sedmera P & Haltrich D (2001) Screening of basidiomycete fungi for the quinone-dependent sugar C-2/C-3 oxidoreductase, pyranose dehydrogenase, and properties of the enzyme from *Macrolepiota rhacodes*. *Arch. Microbiol.* **176**, 178–186.
- 11 Kujawa M, Volc J, Halada P, Sedmera P, Divne C, Sygmund C, Leitner C, Peterbauer C & Haltrich D (2007) Properties of pyranose dehydrogenase purified from the litter-degrading fungus *Agaricus xanthoderma*. *FEBS J.* **274**, 879–894.
- 12 Peterbauer CK & Volc J (2010) Pyranose dehydrogenases: biochemical features and perspectives of technological applications. *Appl. Microbiol. Biotechnol.* **85**, 837–848.
- 13 Sedmera P, Halada P, Kubátová E, Haltrich D, Přikrylová V & Volc J (2006) New biotransformations of some reducing sugars to the corresponding (di)dehydro(glycosyl) aldoses or aldonic acids using fungal pyranose dehydrogenase. *J. Mol. Catal. B Enzym.* **41**, 32–42.
- 14 Keilin D & Hartree EF (1948) Properties of glucose oxidase (notatin). *Biochem. J.* **42**, 221–229.
- 15 Henriksson G, Johansson G & Pettersson G (2000) A critical review of cellobiose dehydrogenases. *J. Biotechnol.* **78**, 93–113.
- 16 Freimund S, Huwig A, Giffhorn F & Köpper S (1998) Rare Keto-Aldoses from Enzymatic Oxidation: Substrates and Oxidation Products of Pyranose 2-Oxidase. *Chem. – Eur. J.* **4**, 2442–2455.
- 17 Krondorfer I, Lipp K, Brugger D, Staudigl P, Sygmund C, Haltrich D & Peterbauer CK (2014) Engineering of Pyranose Dehydrogenase for Increased Oxygen Reactivity. *PLoS ONE* **9**, e91145.
- 18 Tan TC, Spadiut O, Wongnate T, Sucharitakul J, Krondorfer I, Sygmund C, Haltrich D, Chaiyen P, Peterbauer CK & Divne C (2013) The 1.6 Å Crystal Structure of Pyranose Dehydrogenase from *Agaricus meleagris* Rationalizes Substrate Specificity and Reveals a Flavin Intermediate. *PLoS ONE* **8**, e53567.

- 19 Marchler-Bauer A, Derbyshire MK, Gonzales NR, Lu S, Chitsaz F, Geer LY, Geer RC, He J, Gwadz M, Hurwitz DI, Lanczycki CJ, Lu F, Marchler GH, Song JS, Thanki N, Wang Z, Yamashita RA, Zhang D, Zheng C & Bryant SH (2015) CDD: NCBI's conserved domain database. *Nucleic Acids Res.* **43**, D222–D226.
- 20 Ander P & Marzullo L (1997) Sugar oxidoreductases and veratryl alcohol oxidase as related to lignin degradation. *J. Biotechnol.* **53**, 115–131.
- 21 Giffhorn F (2000) Fungal pyranose oxidases: occurrence, properties and biotechnical applications in carbohydrate chemistry. *Appl. Microbiol. Biotechnol.* **54**, 727–740.
- 22 Morin E, Kohler A, Baker AR, Foulongne-Oriol M, Lombard V, Nagye LG, Ohm RA, Patyshakuliyeva A, Brun A, Aerts AL, Bailey AM, Billette C, Coutinho PM, Deakin G, Doddapaneni H, Floudas D, Grimwood J, Hildén K, Kues U, LaButti KM, Lapidus A, Lindquist EA, Lucas SM, Murat C, Riley RW, Salamov AA, Schmutz J, Subramanian V, Wösten HAB, Xu J, Eastwood DC, Foster GD, Sonnenberg ASM, Cullen D, Vries RP de, Lundell T, Hibbett DS, Henrissat B, Burton KS, Kerrigan RW, Challen MP, Grigoriev IV & Martin F (2012) Genome sequence of the button mushroom *Agaricus bisporus* reveals mechanisms governing adaptation to a humic-rich ecological niche. *Proc. Natl. Acad. Sci.* **109**, 17501–17506.
- 23 Graf MMH, Bren U, Haltrich D & Oostenbrink C (2013) Molecular dynamics simulations give insight into d-glucose dioxidation at C2 and C3 by *Agaricus meleagris* pyranose dehydrogenase. *J. Comput. Aided Mol. Des.* **27**, 295–304.
- 24 Wongnate T, Sucharitakul J & Chaiyen P (2011) Identification of a Catalytic Base for Sugar Oxidation in the Pyranose 2-Oxidase Reaction. *ChemBioChem* **12**, 2577–2586.
- 25 Graf MMH, Sucharitakul J, Bren U, Chu DB, Koellensperger G, Hann S, Furtmüller PG, Obinger C, Peterbauer CK, Oostenbrink C, Chaiyen P & Haltrich D (2015) Reaction of pyranose dehydrogenase from *Agaricus meleagris* with its carbohydrate substrates. *FEBS J.* **282**, 4218–4241.
- 26 Mattevi A (2006) To be or not to be an oxidase: challenging the oxygen reactivity of flavoenzymes. *Trends Biochem. Sci.* **31**, 276–283.
- 27 Brugger D, Krondorfer I, Shelswell C, Huber-Dittes B, Haltrich D & Peterbauer CK (2014) Engineering Pyranose 2-Oxidase for Modified Oxygen Reactivity. *PLoS ONE* **9**, e109242.
- 28 Leferink NGH, Fraaije MW, Joosten H-J, Schaap PJ, Mattevi A & Berkel WJH van (2009) Identification of a Gatekeeper Residue That Prevents Dehydrogenases from Acting as Oxidases. *J. Biol. Chem.* **284**, 4392–4397.
- 29 Sucharitakul J, Prongjit M, Haltrich D & Chaiyen P (2008) Detection of a C4a-Hydroperoxyflavin Intermediate in the Reaction of a Flavoprotein Oxidase. *Biochemistry (Mosc.)* **47**, 8485–8490.
- 30 Sucharitakul J, Wongnate T & Chaiyen P (2011) Hydrogen Peroxide Elimination from C4a-hydroperoxyflavin in a Flavoprotein Oxidase Occurs through a Single Proton Transfer from Flavin N5 to a Peroxide Leaving Group. *J. Biol. Chem.* **286**, 16900–16909.
- 31 Volc J, Sedmera P, Halada P, Prikrylova V & Daniel G (1998) C-2 and C-3 oxidation of-Glc, and C-2 oxidation of-Gal by pyranose dehydrogenase from *Agaricus bisporus*. *Carbohydr. Res.* **310**, 151–156.
- 32 Volc J, Sedmera P, Halada P, Daniel G, Přikrylová V & Haltrich D (2002) C-3 oxidation of non-reducing sugars by a fungal pyranose dehydrogenase: spectral characterization. *J. Mol. Catal. B Enzym.* **17**, 91–100.
- 33 Pisanelli I, Kujawa M, Gschnitzer D, Spadiut O, Seiboth B & Peterbauer C (2009) Heterologous expression of an *Agaricus meleagris* pyranose dehydrogenase-encoding gene in *Aspergillus* spp. and characterization of the recombinant enzyme. *Appl. Microbiol. Biotechnol.* **86**, 599–606.
- 34 Szymund C, Gutmann A, Krondorfer I, Kujawa M, Glieder A, Pscheidt B, Haltrich D, Peterbauer C & Kittl R (2011) Simple and efficient expression of *Agaricus meleagris* pyranose dehydrogenase in *Pichia pastoris*. *Appl. Microbiol. Biotechnol.* **94**, 695–704.

- 35 Staudigl P, Krondorfer I, Haltrich D & Peterbauer CK (2013) Pyranose Dehydrogenase from *Agaricus campestris* and *Agaricus xanthoderma*: Characterization and Applications in Carbohydrate Conversions. *Biomolecules* **3**, 535–552.
- 36 Giffhorn F, Köpper S, Huwig A & Freimund S (2000) Rare sugars and sugar-based synthons by chemo-enzymatic synthesis. *Enzyme Microb. Technol.* **27**, 734–742.
- 37 Spadiut O, Pisanelli I, Maischberger T, Peterbauer C, Gorton L, Chaiyen P & Haltrich D (2009) Engineering of pyranose 2-oxidase: Improvement for biofuel cell and food applications through semi-rational protein design. *J. Biotechnol.* **139**, 250–257.
- 38 Volc J, Sedmera P, Kujawa M, Halada P, Kubátová E & Haltrich D (2004) Conversion of lactose to  $\beta$ -d-galactopyranosyl-(1 $\rightarrow$ 4)-d-arabino-hexos-2-ulose-(2-dehydrolactose) and lactobiono-1, 5-lactone by fungal pyranose dehydrogenase. *J. Mol. Catal. B Enzym.* **30**, 177–184.
- 39 Thévenot DR, Toth K, Durst RA & Wilson GS (2001) Electrochemical biosensors: recommended definitions and classification. *Biosens. Bioelectron.* **16**, 121–131.
- 40 Turner A, Karube I & Wilson GS (1987) *Biosensors : Fundamentals and Applications* Oxford University Press.
- 41 Borgmann S, Schulte A, Neugebauer S & Schuhmann W (2011) Amperometric Biosensors. In *Advances in Electrochemical Science and Engineering* pp. 1–83. Wiley-VCH Verlag GmbH & Co. KGaA.
- 42 Chaubey A & Malhotra BD (2002) Mediated biosensors. *Biosens. Bioelectron.* **17**, 441–456.
- 43 Clark LC & Lyons C (1962) Electrode Systems for Continuous Monitoring in Cardiovascular Surgery. *Ann. N. Y. Acad. Sci.* **102**, 29–45.
- 44 Cass AEG, Davis G, Francis GD, Hill HAO, Aston WJ, Higgins IJ, Plotkin EV, Scott LDL & Turner APF (1984) Ferrocene-mediated enzyme electrode for amperometric determination of glucose. *Anal. Chem.* **56**, 667–671.
- 45 Ghindilis AL, Atanasov P & Wilkins E (1997) Enzyme-catalyzed direct electron transfer: Fundamentals and analytical applications. *Electroanalysis* **9**, 661–674.
- 46 Newman JD & Setford SJ (2006) Enzymatic biosensors. *Mol. Biotechnol.* **32**, 249–268.
- 47 Tasca F, Timur S, Ludwig R, Haltrich D, Volc J, Antiochia R & Gorton L (2007) Amperometric Biosensors for Detection of Sugars Based on the Electrical Wiring of Different Pyranose Oxidases and Pyranose Dehydrogenases with Osmium Redox Polymer on Graphite Electrodes. *Electroanalysis* **19**, 294–302.
- 48 Cruys-Bagger N, Ren G, Tatsumi H, Baumann MJ, Spodsborg N, Andersen HD, Gorton L, Borch K & Westh P (2012) An amperometric enzyme biosensor for real-time measurements of cellobiohydrolase activity on insoluble cellulose. *Biotechnol. Bioeng.* **109**, 3199–3204.
- 49 Cruys-Bagger N, Badino SF, Tokin R, Gontsarik M, Fathalinejad S, Jensen K, Toscano MD, Sørensen TH, Borch K, Tatsumi H, Våljamäe P & Westh P (2014) A pyranose dehydrogenase-based biosensor for kinetic analysis of enzymatic hydrolysis of cellulose by cellulases. *Enzyme Microb. Technol.* **58–59**, 68–74.
- 50 Leech D, Kavanagh P & Schuhmann W (2012) Enzymatic fuel cells: Recent progress. *Electrochimica Acta* **84**, 223–234.
- 51 Ó Conghaile P, Falk M, MacAodha D, Yakovleva ME, Gonaus C, Peterbauer CK, Gorton L, Shleev S & Leech D (2016) Fully Enzymatic Membraneless Glucose|Oxygen Fuel Cell That Provides 0.275 mA cm<sup>-2</sup> in 5 mM Glucose, Operates in Human Physiological Solutions, and Powers Transmission of Sensing Data. *Anal. Chem.* **88**, 2156–2163.
- 52 MacVittie K, Halámek J, Halámková L, Southcott M, Jemison WD, Lobel R & Katz E (2013) From “cyborg” lobsters to a pacemaker powered by implantable biofuel cells. *Energy Env. Sci* **6**, 81–86.
- 53 Meredith MT & Minteer SD (2012) Biofuel Cells: Enhanced Enzymatic Bioelectrocatalysis. *Annu. Rev. Anal. Chem.* **5**, 157–179.

- 54 Cosnier S, Le Goff A & Holzinger M (2014) Towards glucose biofuel cells implanted in human body for powering artificial organs: Review. *Electrochem. Commun.* **38**, 19–23.
- 55 Tasca F, Gorton L, Kujawa M, Patel I, Harreither W, Peterbauer CK, Ludwig R & Nöll G (2010) Increasing the coulombic efficiency of glucose biofuel cell anodes by combination of redox enzymes. *Biosens. Bioelectron.* **25**, 1710–1716.
- 56 Willner I, Yan Y-M, Willner B & Tel-Vered R (2009) Integrated Enzyme-Based Biofuel Cells—A Review. *Fuel Cells* **9**, 7–24.
- 57 Zafar MN, Tasca F, Boland S, Kujawa M, Patel I, Peterbauer CK, Leech D & Gorton L (2010) Wiring of pyranose dehydrogenase with osmium polymers of different redox potentials. *Bioelectrochemistry* **80**, 38–42.
- 58 Kim J, Jia H & Wang P (2006) Challenges in biocatalysis for enzyme-based biofuel cells. *Biotechnol. Adv.* **24**, 296–308.
- 59 Heller A (2004) Miniature biofuel cells. *Phys. Chem. Chem. Phys.* **6**, 209.
- 60 Katz E, Willner I & Kotlyar AB (1999) A non-compartmentalized glucose | O<sub>2</sub> biofuel cell by bioengineered electrode surfaces. *J. Electroanal. Chem.* **479**, 64–68.
- 61 Winter M & Brodd RJ (2004) What Are Batteries, Fuel Cells, and Supercapacitors? *Chem. Rev.* **104**, 4245–4270.
- 62 Chen T, Barton SC, Binyamin G, Gao Z, Zhang Y, Kim H-H & Heller A (2001) A Miniature Biofuel Cell. *J. Am. Chem. Soc.* **123**, 8630–8631.
- 63 Mao F, Mano N & Heller A (2003) Long Tethers Binding Redox Centers to Polymer Backbones Enhance Electron Transport in Enzyme “Wiring” Hydrogels. *J. Am. Chem. Soc.* **125**, 4951–4957.
- 64 Holzinger M, Le Goff A & Cosnier S (2012) Carbon nanotube/enzyme biofuel cells. *Electrochimica Acta* **82**, 179–190.
- 65 Zebda A, Cosnier S, Alcaraz J-P, Holzinger M, Le Goff A, Gondran C, Boucher F, Giroud F, Gorgy K, Lamraoui H & Cinquin P (2013) Single Glucose Biofuel Cells Implanted in Rats Power Electronic Devices. *Sci. Rep.* **3**.
- 66 Halámková L, Halánek J, Bocharova V, Szczupak A, Alfonta L & Katz E (2012) Implanted Biofuel Cell Operating in a Living Snail. *J. Am. Chem. Soc.* **134**, 5040–5043.
- 67 Katz E & MacVittie K (2013) Implanted biofuel cells operating in vivo – methods, applications and perspectives – feature article. *Energy Environ. Sci.* **6**, 2791–2803.
- 68 Rasmussen M, Ritzmann RE, Lee I, Pollack AJ & Scherson D (2012) An Implantable Biofuel Cell for a Live Insect. *J. Am. Chem. Soc.* **134**, 1458–1460.
- 69 Szczupak A, Halánek J, Halámková L, Bocharova V, Alfonta L & Katz E (2012) Living battery – biofuel cells operating in vivo in clams. *Energy Environ. Sci.* **5**, 8891.
- 70 El Ichi S, Zebda A, Alcaraz J-P, Laaroussi A, Boucher F, Boutonnat J, Reverdy-Bruas N, Chaussy D, Belgacem MN, Cinquin P & Martin DK (2015) Bioelectrodes modified with chitosan for long-term energy supply from the body. *Energy Env. Sci* **8**, 1017–1026.
- 71 Bullen RA, Arnot TC, Lakeman JB & Walsh FC (2006) Biofuel cells and their development. *Biosens. Bioelectron.* **21**, 2015–2045.
- 72 Shao M, Nadeem Zafar M, Sygmund C, Guschin DA, Ludwig R, Peterbauer CK, Schuhmann W & Gorton L (2013) Mutual enhancement of the current density and the coulombic efficiency for a bioanode by entrapping bi-enzymes with Os-complex modified electrodeposition paints. *Biosens. Bioelectron.* **40**, 308–314.
- 73 Zafar MN, Shao M, Ludwig R, Leech D, Schuhmann W & Gorton L (2013) Improving the Current Density and the Coulombic Efficiency by a Cascade Reaction of Glucose Oxidizing Enzymes. *ECS Trans.* **53**, 131–143.

- 74 Shao M, Zafar MN, Falk M, Ludwig R, Sygmund C, Peterbauer CK, Guschin DA, MacAodha D, Ó Conghaile P, Leech D, Toscano MD, Shleev S, Schuhmann W & Gorton L (2013) Optimization of a Membraneless Glucose/Oxygen Enzymatic Fuel Cell Based on a Bioanode with High Coulombic Efficiency and Current Density. *ChemPhysChem* **14**, 2260–2269.
- 75 Yakovleva ME, Killyéni A, Ortiz R, Schulz C, MacAodha D, Conghaile PÓ, Leech D, Popescu IC, Gonaus C, Peterbauer CK & Gorton L (2012) Recombinant pyranose dehydrogenase—A versatile enzyme possessing both mediated and direct electron transfer. *Electrochem. Commun.* **24**, 120–122.
- 76 Yakovleva ME, Killyéni A, Seubert O, Ó Conghaile P, MacAodha D, Leech D, Gonaus C, Popescu IC, Peterbauer CK, Kjellstrom S & Gorton L (2013) Further Insights into the Catalytical Properties of Deglycosylated Pyranose Dehydrogenase from *Agaricus meleagris* Recombinantly Expressed in *Pichia pastoris*. *Anal. Chem.*, 130910071924000.
- 77 Killyéni A, Yakovleva ME, MacAodha D, Conghaile PÓ, Gonaus C, Ortiz R, Leech D, Popescu IC, Peterbauer CK & Gorton L (2013) Effect of deglycosylation on the mediated electrocatalytic activity of recombinantly expressed *Agaricus meleagris* pyranose dehydrogenase wired by osmium redox polymer. *Electrochimica Acta*.
- 78 Ludwig RD, Gorton L, Haltrich DD & DI Harreither W EP2223936 (EP2009-153889)/WO2010097462 (WO2010-EP52488). *Cloning, sequences and immobilization of fungal cellobiose dehydrogenases for use in glucose sensors and electrochemical cells*.
- 79 Spadiut O, Brugger D, Coman V, Haltrich D & Gorton L (2010) Engineered pyranose 2-Oxidase: Efficiently turning sugars into electrical energy. *Electroanalysis* **22**, 813–820.
- 80 Apweiler R, Hermjakob H & Sharon N (1999) On the frequency of protein glycosylation, as deduced from analysis of the SWISS-PROT database1. *Biochim. Biophys. Acta BBA - Gen. Subj.* **1473**, 4–8.
- 81 Marshall RD (1974) The nature and metabolism of the carbohydrate peptide linkages of glycoproteins. *Biochem. Soc. Symp.* **Vol. 40**, 17–26.
- 82 Helenius A & Aebi M (2004) Roles of N-linked glycans in the endoplasmatic reticulum. *Annu. Rev. Biochem.* **73**, 1019–1049.
- 83 Skropeta D (2009) The effect of individual N-glycans on enzyme activity. *Bioorg. Med. Chem.* **17**, 2645–2653.
- 84 Han M, Wang X, Ding H, Jin M, Yu L, Wang J & Yu X (2014) The role of N-glycosylation sites in the activity, stability, and expression of the recombinant elastase expressed by *Pichia pastoris*. *Enzyme Microb. Technol.* **54**, 32–37.
- 85 Petrescu A-J, Milac A-L, Petrescu SM, Dwek RA & Wormald MR (2004) Statistical analysis of the protein environment of N-glycosylation sites: Implications for occupancy, structure, and folding. *Glycobiology* **14**, 103–114.
- 86 Rademacher TW, Parekh RB & Dwek RA (1988) Glycobiology. *Annu. Rev. Biochem.* **57**, 785–838.
- 87 Haltiwanger RS & Lowe JB (2004) Role of Glycosylation in Development. *Annu. Rev. Biochem.* **73**, 491–537.
- 88 Kukuruzinska MA & Lennon K (1998) Protein N-glycosylation: Molecular genetics and functional significance. *Crit. Rev. Oral Biol. Med.* **9**, 415–448.
- 89 Burda P & Aebi M (1999) The dolichol pathway of N-linked glycosylation. *Biochim. Biophys. Acta BBA - Gen. Subj.* **1426**, 239–257.
- 90 Tannous A, Pisoni GB, Hebert DN & Molinari M (2015) N-linked sugar-regulated protein folding and quality control in the ER. *Semin. Cell Dev. Biol.* **41**, 79–89.
- 91 Bause E (1983) Structural requirements of N-glycosylation of proteins. Studies with proline peptides as conformational probes. *Biochem. J.* **209**, 331–336.
- 92 Pless DD & Lennarz WJ (1977) Enzymatic conversion of proteins to glycoproteins. *Proc. Natl. Acad. Sci. U. S. A.* **74**, 134–138.

- 93 Luke B (2012) Beyond the Sequon: Sites of N-Glycosylation. In *Glycosylation* (Petrescu S, ed), InTech.
- 94 Bañó-Polo M, Baldin F, Tamborero S, Marti-Renom MA & Mingarro I (2011) N-glycosylation efficiency is determined by the distance to the C-terminus and the amino acid preceding an Asn-Ser-Thr sequon. *Protein Sci.* **20**, 179–186.
- 95 Hebert DN, Zhang J-X, Chen W, Foellmer B & Helenius A (1997) The Number and Location of Glycans on Influenza Hemagglutinin Determine Folding and Association with Calnexin and Calreticulin. *J. Cell Biol.* **139**, 613–623.
- 96 O'Connor SE & Imperiali B (1996) Modulation of protein structure and function by asparagine-linked glycosylation. *Chem. Biol.* **3**, 803–812.
- 97 Imperiali B & Rickert KW (1995) Conformational implications of asparagine-linked glycosylation. *Proc. Natl. Acad. Sci. U. S. A.* **92**, 97–101.
- 98 Aebi M, Bernasconi R, Clerc S & Molinari M (2010) N-glycan structures: recognition and processing in the ER. *Trends Biochem. Sci.* **35**, 74–82.
- 99 Deprez P, Gautschi M & Helenius A (2005) More Than One Glycan Is Needed for ER Glucosidase II to Allow Entry of Glycoproteins into the Calnexin/Calreticulin Cycle. *Mol. Cell* **19**, 183–195.
- 100 Schallus T, Fehér K, Sternberg U, Rybin V & Muhle-Goll C (2010) Analysis of the specific interactions between the lectin domain of malectin and diglucosides. *Glycobiology* **20**, 1010–1020.
- 101 Galli C, Bernasconi R, Soldà T, Calanca V & Molinari M (2011) Malectin Participates in a Backup Glycoprotein Quality Control Pathway in the Mammalian ER. *PLOS ONE* **6**, e16304.
- 102 Hammond C, Braakman I & Helenius A (1994) Role of N-linked oligosaccharide recognition, glucose trimming, and calnexin in glycoprotein folding and quality control. *Proc. Natl. Acad. Sci.* **91**, 913–917.
- 103 Hebert DN, Foellmer B & Helenius A (1995) Glucose trimming and reglucosylation determine glycoprotein association with calnexin in the endoplasmic reticulum. *Cell* **81**, 425–433.
- 104 Ora A & Helenius A (1995) Calnexin Fails to Associate with Substrate Proteins in Glucosidase-deficient Cell Lines. *J. Biol. Chem.* **270**, 26060–26062.
- 105 Rodan AR, Simons JF, Trombetta ES & Helenius A (1996) N-linked oligosaccharides are necessary and sufficient for association of glycosylated forms of bovine RNase with calnexin and calreticulin. *EMBO J.* **15**, 6921–6930.
- 106 Jessop CE, Tavender TJ, Watkins RH, Chambers JE & Bulleid NJ (2009) Substrate Specificity of the Oxidoreductase ERp57 Is Determined Primarily by Its Interaction with Calnexin and Calreticulin. *J. Biol. Chem.* **284**, 2194–2202.
- 107 Kozlov G, Bastos-Aristizabal S, Määttänen P, Rosenauer A, Zheng F, Killikelly A, Trempe J-F, Thomas DY & Gehring K (2010) Structural Basis of Cyclophilin B Binding by the Calnexin/Calreticulin P-domain. *J. Biol. Chem.* **285**, 35551–35557.
- 108 Caramelo JJ & Parodi AJ (2015) A sweet code for glycoprotein folding. *FEBS Lett.* **589**, 3379–3387.
- 109 Sousa M & Parodi AJ (1995) The molecular basis for the recognition of misfolded glycoproteins by the UDP-Glc:glycoprotein glucosyltransferase. *EMBO J.* **14**, 4196–4203.
- 110 Fanchiotti S, Fernández F, D'Alessio C & Parodi AJ (1998) The UDP-Glc:Glycoprotein Glucosyltransferase Is Essential for *Schizosaccharomyces pombe* Viability under Conditions of Extreme Endoplasmic Reticulum Stress. *J. Cell Biol.* **143**, 625–635.
- 111 Fernández FS, Trombetta SE, Hellman U & Parodi AJ (1994) Purification to homogeneity of UDP-glucose:glycoprotein glucosyltransferase from *Schizosaccharomyces pombe* and apparent absence of the enzyme from *Saccharomyces cerevisiae*. *J. Biol. Chem.* **269**, 30701–30706.
- 112 Ayalon-Soffer M, Shenkman M & Lederkremer GZ (1999) Differential role of mannose and glucose trimming in the ER degradation of asialoglycoprotein receptor subunits. *J. Cell Sci.* **112**, 3309–3318.

- 113 Liu Y, Choudhury P, Cabral CM & Sifers RN (1999) Oligosaccharide Modification in the Early Secretory Pathway Directs the Selection of a Misfolded Glycoprotein for Degradation by the Proteasome. *J. Biol. Chem.* **274**, 5861–5867.
- 114 Spear ED & Ng DTW (2005) Single, context-specific glycans can target misfolded glycoproteins for ER-associated degradation. *J. Cell Biol.* **169**, 73–82.
- 115 Benyair R, Ogen-Shtern N & Lederkremer GZ (2015) Glycan regulation of ER-associated degradation through compartmentalization. *Semin. Cell Dev. Biol.* **41**, 99–109.
- 116 Hebert DN, Bernasconi R & Molinari M (2010) ERAD substrates: Which way out? *Semin. Cell Dev. Biol.* **21**, 526–532.
- 117 Kamiya Y, Kamiya D, Yamamoto K, Nyfeler B, Hauri H-P & Kato K (2008) Molecular Basis of Sugar Recognition by the Human L-type Lectins ERGIC-53, VIPL, and VIP36. *J. Biol. Chem.* **283**, 1857–1861.
- 118 Geva Y & Schuldiner M (2014) The Back and Forth of Cargo Exit from the Endoplasmic Reticulum. *Curr. Biol.* **24**, R130–R136.
- 119 Balch WE & Gist Farquhar M (1995) Beyond bulk flow. *Trends Cell Biol.* **5**, 16–19.
- 120 Ellgaard L & Helenius A (2003) Quality control in the endoplasmic reticulum. *Nat. Rev. Mol. Cell Biol.* **4**, 181–191.
- 121 Stanley P, Schachter H & Taniguchi N (2009) N-Glycans. In *Essentials of Glycobiology* (Varki A, Cummings RD, Esko JD, Freeze HH, Stanley P, Bertozzi CR, Hart GW, & Etzler ME, eds), 2nd ed. Cold Spring Harbor Laboratory Press, Cold Spring Harbor (NY).
- 122 Herscovics A (1999) Importance of glycosidases in mammalian glycoprotein biosynthesis. *Biochim. Biophys. Acta BBA - Gen. Subj.* **1473**, 96–107.
- 123 Roth J (2002) Protein N-Glycosylation along the Secretory Pathway: Relationship to Organelle Topography and Function, Protein Quality Control, and Cell Interactions. *Chem. Rev.* **102**, 285–304.
- 124 Gemmill TR & Trimble RB (1999) Overview of N- and O-linked oligosaccharide structures found in various yeast species. *Biochim. Biophys. Acta BBA - Gen. Subj.* **1426**, 227–237.
- 125 Archer DB & Peberdy JF (1997) The Molecular Biology of Secreted Enzyme Production by Fungi. *Crit. Rev. Biotechnol.* **17**, 273–306.
- 126 Nakayama K, Nakanishi-Shindo Y, Tanaka A, Haga-Toda Y & Jigami Y (1997) Substrate specificity of  $\alpha$ -1,6-mannosyltransferase that initiates N-linked mannose outer chain elongation in *Saccharomyces cerevisiae*. *FEBS Lett.* **412**, 547–550.
- 127 Ballou L, Hernandez LM, Alvarado E & Ballou CE (1990) Revision of the oligosaccharide structures of yeast carboxypeptidase Y. *Proc. Natl. Acad. Sci.* **87**, 3368–3372.
- 128 Malissard M, Zeng S & Berger EG (1999) The yeast expression system for recombinant glycosyltransferases. *Glycoconj. J.* **16**, 125–139.
- 129 Daly R & Hearn MTW (2005) Expression of heterologous proteins in *Pichia pastoris*: A useful experimental tool in protein engineering and production. *J. Mol. Recognit.* **18**, 119–138.
- 130 Grinna LS & Tschopp JF (1989) Size distribution and general structural features of N-linked oligosaccharides from the methylotrophic yeast, *Pichia pastoris*. *Yeast* **5**, 107–115.
- 131 Reddy ST & Dahms NM (2002) High-level expression and characterization of a secreted recombinant cation-dependent mannose 6-phosphate receptor in *Pichia pastoris*. *Protein Expr. Purif.* **26**, 290–300.
- 132 Montesino R, Nimtz M, Quintero O, García R, Falcón V & Cremata JA (1999) Characterization of the oligosaccharides assembled on the *Pichia pastoris*—expressed recombinant aspartic protease. *Glycobiology* **9**, 1037–1043.
- 133 Tull D, Gottschalk TE, Svendsen I, Kramhøft B, Phillipson BA, Bisgård-Frantzen H, Olsen O & Svensson B (2001) Extensive N-Glycosylation Reduces the Thermal Stability of a Recombinant Alkalophilic *Bacillus*  $\alpha$ -Amylase Produced in *Pichia pastoris*. *Protein Expr. Purif.* **21**, 13–23.

- 134 Khandekar SS, Silverman C, Wells-Marani J, Bacon AM, Birrell H, Brigham-Burke M, DeMarini DJ, Jonak ZL, Camilleri P & Fishman-Lobell J (2001) Determination of Carbohydrate Structures N-Linked to Soluble CD154 and Characterization of the Interactions of CD40 with CD154 Expressed in *Pichia pastoris* and Chinese Hamster Ovary Cells. *Protein Expr. Purif.* **23**, 301–310.
- 135 Trimble RB, Atkinson PH, Tschopp JF, Townsend RR & Maley F (1991) Structure of oligosaccharides on *Saccharomyces SUC2* invertase secreted by the methylotrophic yeast *Pichia pastoris*. *J. Biol. Chem.* **266**, 22807–22817.
- 136 Majerle A, Kidrič J & Jerala R (1999) Expression and Refolding of Functional Fragments of the Human Lipopolysaccharide Receptor CD14 in *Escherichia coli* and *Pichia pastoris*. *Protein Expr. Purif.* **17**, 96–104.
- 137 Martinet W, Saelens X, Deroo T, Neiryneck S, Contreras R, Min Jou W & Fiers W (1997) Protection of Mice Against a Lethal Influenza Challenge by Immunization with Yeast-Derived Recombinant Influenza Neuraminidase. *Eur. J. Biochem.* **247**, 332–338.
- 138 Paramasivam M, Saravanan K, Uma K, Sharma S, Singh TP & Srinivasan A (2002) Expression, purification, and characterization of equine lactoferrin in *Pichia pastoris*. *Protein Expr. Purif.* **26**, 28–34.
- 139 Ruitenbergh KM, Gilkerson JR, Wellington JE, Love DN & Whalley JM (2001) Equine herpesvirus 1 glycoprotein D expressed in *Pichia pastoris* is hyperglycosylated and elicits a protective immune response in the mouse model of EHV-1 disease. *Virus Res.* **79**, 125–135.
- 140 Deshpande N, Wilkins MR, Packer N & Nevalainen H (2008) Protein glycosylation pathways in filamentous fungi. *Glycobiology* **18**, 626–637.
- 141 Maras M, Die I van, Contreras R & Hondel CAMJJ van den (1999) Filamentous fungi as production organisms for glycoproteins of bio-medical interest. *Glycoconj. J.* **16**, 99–107.
- 142 Harrison MJ, Nouwens AS, Jardine DR, Zachara NE, Gooley AA, Nevalainen H & Packer NH (1998) Modified glycosylation of cellobiohydrolase I from a high cellulase-producing mutant strain of *Trichoderma reesei*. *Eur. J. Biochem.* **256**, 119–127.
- 143 Lindgren A, Tanaka M, Ruzgas T, Gorton L, Gazaryan I, Ishimori K & Morishima I (1999) Direct electron transfer catalysed by recombinant forms of horseradish peroxidase: insight into the mechanism. *Electrochem. Commun.* **1**, 171–175.
- 144 Courjean O, Gao F & Mano N (2009) Deglycosylation of Glucose Oxidase for Direct and Efficient Glucose Electrooxidation on a Glassy Carbon Electrode. *Angew. Chem. Int. Ed.* **48**, 5897–5899.
- 145 Ortiz R, Matsumura H, Tasca F, Zahma K, Samejima M, Igarashi K, Ludwig R & Gorton L (2012) Effect of Deglycosylation of Cellobiose Dehydrogenases on the Enhancement of Direct Electron Transfer with Electrodes. *Anal. Chem.* **84**, 10315–10323.
- 146 Grinnell BW, Walls JD & Gerlitz B (1991) Glycosylation of human protein C affects its secretion, processing, functional activities, and activation by thrombin. *J. Biol. Chem.* **266**, 9778–9785.

# **CHAPTER I**

## **Transcription analysis of pyranose dehydrogenase from the basidiomycete *Agaricus bisporus* and characterization of the recombinantly expressed enzyme**

Christoph Gonaus,<sup>a</sup> Roman Kittl,<sup>a</sup> Christoph Sygmund,<sup>a</sup> Dietmar Haltrich,<sup>a</sup>  
Clemens K. Peterbauer<sup>a\*</sup>

<sup>a</sup>Food Biotechnology Laboratory, Department of Food Sciences and Technology, University of Natural Resources and Life Sciences, Vienna, Austria

Published in 2016 in *Protein Expr. Purif.* **119**, 36–44.

## **Abstract**

*Agaricus bisporus* is a litter degrading basidiomycete commonly found in humic-rich environments. It is used as model organism and cultivated in large scale for food industry. Due to its ecological niche it produces a variety of enzymes for detoxification and degradation of humified plant litter. One of these, pyranose dehydrogenase, is thought to play a role in detoxification and lignocellulose degradation. It is a member of the glucose-methanol-choline family of flavin-dependent enzymes and oxidizes a wide range of sugars with concomitant reduction of electron acceptors like quinones.

In this work, transcription of *pdh* in *A. bisporus* was investigated with real-time PCR revealing influence of the carbon source on *pdh* expression levels. The gene was isolated and heterologously expressed in *Pichia pastoris*. Characterization of the recombinant enzyme showed a higher affinity towards disaccharides compared to other tested pyranose dehydrogenases from related *Agariceae*. Homology modeling and sequence alignments indicated that two loops of high sequence variability at substrate access site could play an important role in modulating these substrate specificities.

## **Abbreviations**

*AbPDH*, *Agaricus bisporus* pyranose dehydrogenase; ABTS, 2,2'-azino-bis(3-ethylbenzothiazoline-6-sulphonic acid); *AcPDH*, *Agaricus campestris* pyranose dehydrogenase; *AmPDH1*, *Agaricus meleagris* pyranose dehydrogenase 1; *AxPDH*, *Agaricus xanthoderma* pyranose dehydrogenase; PDH, pyranose dehydrogenase;  $\text{Fc}^+$ , ferrocenium hexafluorophosphate; *TmP2O*, *Trametes multicolor* pyranose oxidase

## **Introduction**

Oxidoreductases of free, non-phosphorylated carbohydrates are expressed by fungi of all classes, and ascomycetes as well as litter degrading basidiomycetes produce a variety of them. They commonly feature FAD as prosthetic group [1] and show different substrate preferences and regioselective oxidation patterns. Glucose 1-oxidase (EC 1.1.3.4) catalyzes oxidation of glucose at C-1 [2], cellobiose dehydrogenase (EC 1.1.99.18) oxidizes  $\beta$ -1,4-linked di- or oligosaccharides, also at C-1 [3] and [4]. Pyranose 2-oxidase (EC 1.1.3.10) forms ketoaldoses by oxidizing aldopyranoses at C-2 [5].

Some *Agaricaceae* and *Lycoperdaceae*, which do not form pyranose oxidase, produce pyranose dehydrogenase (PDH, EC 1.1.99.29). This quinone dependent dehydrogenase is capable of dioxygenation of C-2 and C-3 of a broad range of substrates. It was first purified from the non-wood litter degrading model organism *Agaricus bisporus* by Volc et al. [6] and [7].

The *in vivo* function of PDH and related oxidoreductases is not fully elucidated but for PDH a role in detoxification was suggested [8]. Another proposed biological function is preventing repolymerization of quinone degradation products as part of ligninolysis [8], [9], [10] and [11]. The secreted PDH could be part of an extracellular system where potentially toxic quinones do not have to be imported into the cell [8] and [12]. The presence of a *pdh* gene and expansion of detoxifying enzyme families in *A. bisporus*, compared to other fungi, point towards a better adaption to humic-acid rich habitats [13]. *A. bisporus* is the most commonly cultivated and traded mushroom, and about eight percent of the residual wheat straw in the UK are converted to mushroom compost annually [14]. Cultivation of edible mushrooms is still considered the only profitable way to utilize lignocellulosic waste material from agriculture and forestry [14]. Consequently, a better understanding of lignocellulose degradation and ecological adaptation in *A. bisporus* may offer opportunities to improve mushroom yields or simplify substrate preparation for commercial cultivation.

Several fungal enzymes involved in lignocellulose degradation have additionally attracted interest for biocatalytic or analytic applications. Pyranose oxidase has been already extensively studied for applications in carbohydrate conversion, clinical chemistry and process monitoring. Pyranose dehydrogenase's capability of dioxygenation of a broad substrate range makes it an interesting alternative [8], [15] and [16]. Furthermore, its lack of reactivity with O<sub>2</sub> and consequential H<sub>2</sub>O<sub>2</sub> formation, the broad substrate range and electron yield commend it for use in enzymatic biofuel cells [17] and [18].

PDH from *Agaricus xanthoderma* (*AxPDH*), *Agaricus campestris* (*AcPDH*) [19] and [20] and *Agaricus meleagris* (*AmPDH*) [18] and [21] have been characterized extensively but only limited

kinetic characterization of *A. bisporus* PDH (*AbPDH*) was published as part of investigations of its catalytic products [6] and [7]. In this work, substrate dependent transcription of *pdh* in *A. bisporus* was studied and the kinetic characteristics of *AbPDH* were elucidated and compared to *AxPDH*, *AcPDH* and *AmPDH1*.

## **Material and methods**

### **Chemicals and microorganisms**

All chemicals were purchased from Sigma–Aldrich (St. Louis, MO) unless stated otherwise, and were of the highest purity available. ABTS was from Amresco (Solon, OH) and D-glucose from Merck (Whitehouse Station, NJ). The Phenyl-Sepharose Fast Flow resin was purchased from GE Healthcare (Chalfont-St. Giles, UK) and the DEAE-Sepharose Fast Flow resin from Sigma–Aldrich (Steinheim, Germany). Restriction enzymes, polymerases and DNA modifying enzymes were obtained from Fermentas (now: Thermo Fisher Scientific, Waltham, MA) and used as recommended by the manufacturer. Nucleic acid amplifications were done using *Pfu* proof-reading polymerase, dNTP mix, oligonucleotide-primers (VBC Biotech, Vienna, Austria) and a Biometra TRIO thermocycler (Biometra, Göttingen, Germany). cDNA first strand synthesis was done using the First Strand cDNA Synthesis Kit (Fermentas).

Commercially used *A. bisporus* was purchased from Pielachtaler Champignon (Kirchberg/Pielach, Austria) and *A. bisporus* strain DSM 3056 was obtained from DSMZ (Braunschweig, Germany) The cultures were maintained on malt extract agar (1.5% malt extract, 0.15% peptone from soy bean, 2% agar agar) and transferred on new plates every 2 months. *E. coli* DH5 $\alpha$  cells from New England Biolabs (Ipswich, MA) were used for cloning and *Pichia pastoris* X33 from Invitrogen (Carlsbad, CA) as heterologous expression host.

### **Cultivation of *A. bisporus***

*A. bisporus* DSM 3056 was cultivated in static liquid cultures in Roux flasks for 1 week, harvested, and the mycelium washed in basal salts medium [22] containing no carbohydrate source. Mycelial samples for RNA extraction were prepared from petri dish cultivation in basal salts medium with 1% (w/v) cellobiose. Fruiting body samples for RNA extraction were taken from compost grown *A. bisporus* from a commercial mushroom producer (Pielachtaler Champignon). ( Supplementary Information S1.1).

## Transcription analysis of the *pdh* gene

Total RNA was extracted from mycelial samples and different parts of the fruiting body with the Spektrum Plant total RNA kit (Sigma) and reverse transcribed with the High Capacity cDNA Reverse Transcription Kit (Applied Biosystems/Life Technologies, Grand Island, NY) using random hexamers as primers. Specific primers for the *pdh* gene (5'-CTATCGACACTGTTCTCCAATTCG3' and 5'-CACACCATGCACGTAAGAAAAC-3') and the glyceraldehyde-3-phosphate dehydrogenase-encoding gene *gpd2* (5'-CGCAAGGCCGCTGAAGG-3' and 5'-GAGCGGCGCATTCAAGCAAC-3') [23] of *A. bisporus* were used to generate amplicons [24]. Dilutions of the cDNA samples were directly used as templates for quantitative real-time PCR with a MyIQ Real Time PCR Detection System (Bio-Rad Laboratories, Hercules, CA). Optimal baseline range and threshold values were calculated with the MyIQ v2.0 software (Bio-Rad), and fold changes of the *pdh* transcripts in the different samples versus control were calculated as described using the *gpd2* gene as internal control [25]. (Supplementary Information S1.2).

## Expression of *A. bisporus* pyranose dehydrogenase in *P. pastoris* and purification

Expression and purification of *A. bisporus* PDH was done as described in detail in supplementary information S1.3. RNA isolated from *A. bisporus* DSM 3056 mycelium was reverse transcribed with an oligo (dT) primer. The reaction product was used as a template for PCR with 5AbPDHPml1 (5'-ATACACGTGATGATACCTCGAGTGGCC-3') containing a *Pml*I restriction site and 3AbPDHXba1 (5'-ATATCTAGATTAGCTGTAGCTCTTCGC-3') containing an *Xba*I restriction site. The digested PCR product was ligated into the plasmid pPICZB ( Fig. S2) and propagated in *E. coli* DH5a cells. Electrocompetent *P. pastoris* cells were transformed with *Sac*I linearized plasmids according to Lin-Cereghino et al. [26]. The GenBank Accession number of the *A. bisporus* PDH used in this work is KM851045.

*A. bisporus* PDH was expressed in shaking flasks at 30 °C using BMGY medium with methanol induction starting after 24 h. Supernatant was harvested 143 h after start of induction and purified by subsequent hydrophobic interaction chromatography (750 mL Phenyl-Sepharose Fast Flow column) and anion exchange chromatography (60 mL DEAE-Sepharose Fast Flow column). Fractions with highest PDH activity were pooled, concentrated with Ultra-15 Centrifugal Filter Units 30 kDa and stored at 4 °C.

## Enzymatic assays

Enzymatic activity was determined spectrophotometrically by sugar dependent reduction of ferrocenium ( $\text{Fc}^+$ ) to ferrocene [19]. In the standard reaction 25 mM D-glucose as electron donor and

0.2 mM  $\text{Fc}^+$  ( $\epsilon_{300} = 4.3 \text{ mM}^{-1} \text{ cm}^{-1}$ ) as electron acceptor in 50 mM sodium phosphate buffer (pH 7.5) were used in a 3 min reaction at 30°. Reduction of 2  $\mu\text{mol Fc}^+$  to ferrocene per minute was defined as 1 Unit enzyme activity. ABTS cation radical ( $\epsilon_{420} = 43.2 \text{ mM}^{-1} \text{ cm}^{-1}$ ) [27], 2,6-dichloroindophenol (DCIP) ( $\epsilon_{520} = 6.8 \text{ mM}^{-1} \text{ cm}^{-1}$ ) and 1,4-benzoquinone ( $\epsilon_{290} = 2.24 \text{ mM}^{-1} \text{ cm}^{-1}$ ) [19] were used as alternative electron acceptors. Enzymatic activity in the temperature optimum assay was calculated within the range of constant substrate turnover and for kinetic constant measurements over 5 min. Enzymatic assays were conducted in triplicates, except for pH-profile and temperature stability assays which were measured in duplicates. Kinetic constants were calculated by fitting steady state kinetic data to the Michaelis Menten equation using nonlinear least-squares regression (SigmaPlot 11.0, Systat Software GmbH, Erkrath, Germany).

### **Protein characterization**

Bradford based protein assay from Biorad Laboratories, with bovine serum albumin as standard, was used for protein determination according to the manufacturer's instructions. The Precast Mini Protean TGX gel system with 4–20% resolving gels, unstained Precision Plus Protein Standard (Biorad) and Bio-safe Commassie staining were used for SDS-Page. Enzymatic deglycosylation was done with 1  $\mu\text{g}$  Endo Hf (New England Biolabs) per 100  $\mu\text{g}$  PDH in sodium citrate buffer (100 mM, pH 5.5) incubated at 30 °C for 22 h. Covalent linkage of FAD was investigated according to Scrutton [28] with a modified excitation wavelength of 302 nm (GelDoc 2000, Biorad).

## **Results**

### **Analysis of *pdh* cds of *A. bisporus***

The *A. bisporus pdh* cds was aligned to *A. bisporus var. bisporus* genome (H97, “Agabi2masked”) and *A. bisporus var. burnettii* genome (JB137-S8, “Abisporus\_varburnettii”) using the BLASTN algorithm with a Blossum 62 scoring [13] and [29]. Both genomes carried one *pdh* gene, each, consisting of 10 exons. Exon 1 of *A. bisporus pdh* cds, containing the signal sequence, was identical to the homolog sequence of the *A. bisporus var. burnettii* genome. The rest of the *A. bisporus pdh* cds was closer related to *A. bisporus var bisporus* genome with 5 non-identical nucleotides (at positions 549, 606, 613, 1722, 1775), only 2 of them causing amino acid changes (I205L, V592A).

Related genes of *A. bisporus pdh* were identified using the BLASTN algorithm [30]. Genes with sequence identity of 77% or higher were previously isolated from *A. xanthoderma* (*Axpdh*, KF534751.1), *A. campestris* (*Acpdh*, KF534750.1) [20] and *A. meleagris* (*Ampdh1*, AY753307.1; *Ampdh2*, AY753309.1; *Ampdh3*, DQ117578) [24].

## Homology model of *A. bisporus* PDH

Comparative structural models of *A. bisporus* PDH (*Ab*PDH), *A. campestris* PDH (*Ac*PDH) and *A. xanthoderma* PDH (*Ax*PDH) were created with the SWISS model server in automated mode [31], [32], [33] and [34] based on *Am*PDH1 crystal structure 4H7U [35].

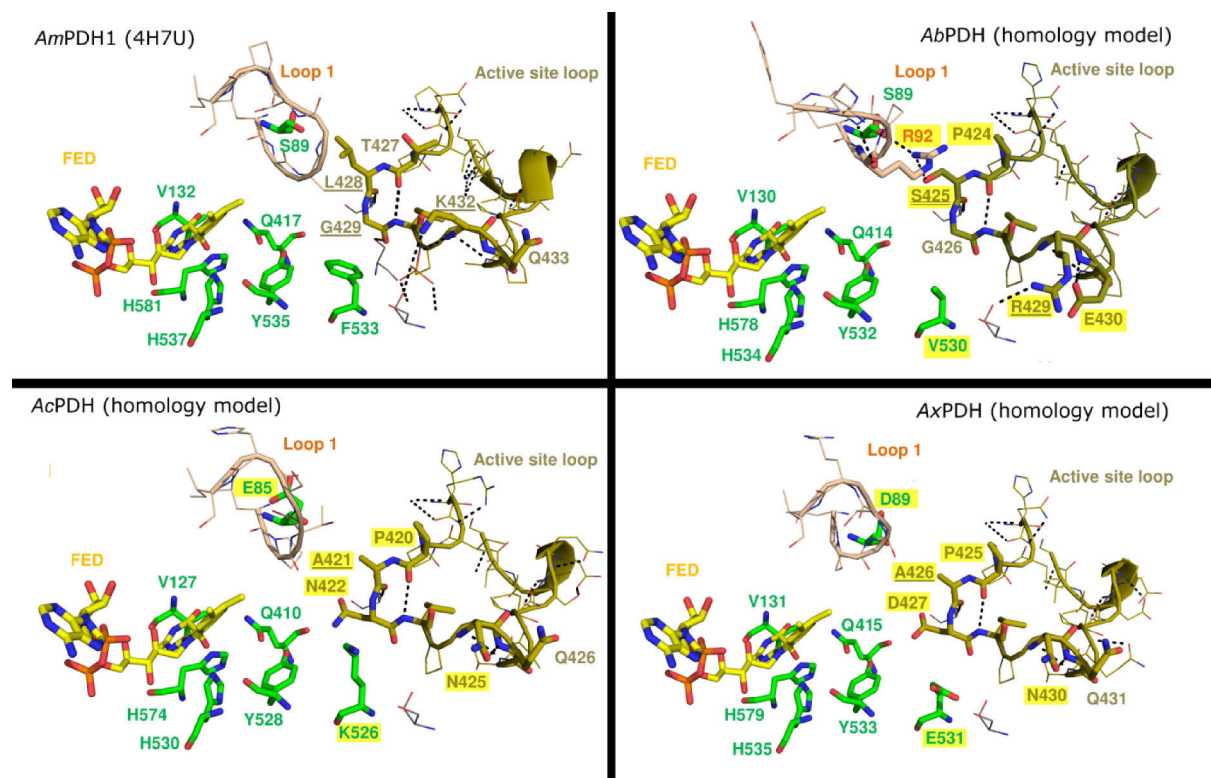


Fig. 1. Homology models (Swiss model server, automated mode) of *Ab*PDH, *Ac*PDH and *Ax*PDH based on crystal structure of *Am*PDH1 4H7U. FED, active side residues, loop 1 and active site loop are shown. Labelled residues that are not conserved are highlighted in yellow. Active site loop residues which are predicted to anchor the loop via H-bonds are underlined.

Of the active side residues, homologous to those previously described for *Am*PDH1 [36], and the related *Aspergillus niger* Glucose Oxidase [37], only *Am*PDH1 Phe<sup>533</sup> was not conserved in *Ab*PDH and replaced by the smaller Val<sup>530</sup> (Fig. 1). Deviations of the *Ab*PDH model in its peptide backbone from the template were only visible in two loops. Loop 1 (*Ab*PDH: <sup>91</sup>LRPRY<sup>95</sup>) is located at the entrance of the substrate pocket in direct vicinity to the isoalloxazine ring of the catalytic co-factor FAD. This loop's predicted structural deviations between compared PDHs were also supported by the low sequence identity (Fig. 2). Loop 2 (*Ab*PDH: <sup>273</sup>ENG<sup>275</sup>) is surface exposed and distant to the active site and substrate pocket. Another loop which is homolog to the gating active site loop reported in the related *Trametes multicolor* Pyranose Oxidase (*Tmp*2O) [38] could be modeled to the template backbone but had high sequence variability in 3 areas ( Fig. 1 and Fig. 2). These were the residues

directly oriented towards the active site (*AbPDH*<sup>424</sup>PSG<sup>426</sup>), <sup>429</sup>RE<sup>430</sup> and the more distant surface exposed C-terminal part of the loop.

Polar interactions of active site residues with other residues and within the loop were predicted using Pymol 1.3 and are shown in Fig. 1. In *AmPDH* 4H7U there were 3 active site residues predicted to be involved in non-covalent interactions anchoring the loop in the elucidated conformation. *AmPDH* Leu<sup>428</sup> and Gly<sup>429</sup>, at the beta-turn facing the FAD, were predicted to form H-bonds via their backbone C=O groups and Lys<sup>432</sup> to form H-bonds or a salt bridge via a coordinated phosphate anion which was resolved in the x-ray structure. The *AmPDH* Leu<sup>428</sup> H-bond was conserved in all homology models (*AbPDH* Ser<sup>425</sup>, *AcPDH* Ala<sup>421</sup>, *AxPDH* Ala<sup>426</sup>). However none of the Gly<sup>429</sup> homologs formed an H-bond because the interacting *AmPDH* Ser<sup>352</sup> is replaced by non-polar amino acids in the other PDHs. The Phosphate was not included in the homology models. *AbPDH* Arg<sup>429</sup> apparently formed an H-bond also in its absence while *AcPDH* Asn<sup>425</sup> and *AxPDH* Asn<sup>430</sup> did not. Setting *AbPDH* apart from the others, Ser<sup>425</sup> showed a second H-bond formed by its side chain with Arg<sup>92</sup> from loop 1. The other PDHs lacked this Arg as well as a polar residue at the homolog active site position for this interaction.

		Loop 1																							
<i>AmPDH1</i>	Q3L245	80	F	V	T	R	V	P	G	L	A	S	T	L	G	A	G	S	P	I	D	W	N	Y	101
<i>AbPDH</i>	K9H463	80	F	E	T	R	V	P	G	L	S	S	E	L	R	P	-	-	R	Y	D	W	N	Y	99
<i>AcPDH</i>	V5NDL4	76	F	A	T	R	V	P	G	L	A	E	T	L	P	T	-	S	H	I	D	W	N	Y	96
<i>AxPDH</i>	V5NC32	80	P	E	T	R	V	P	G	L	A	D	S	L	P	G	-	S	R	T	D	W	N	Y	100

		Active Site Loop																							
<i>AmPDH1</i>	Q3L245	423	P	Q	V	P	-	T	L	G	V	P	K	Q	A	P	L	P	A	A	N	S	Y	R	443
<i>AbPDH</i>	K9H463	420	H	Q	L	P	-	P	S	G	V	P	R	E	A	P	I	P	S	E	A	S	I	D	440
<i>AcPDH</i>	V5NDL4	416	H	R	I	P	-	P	A	N	V	P	N	Q	V	A	L	P	S	Q	D	S	I	G	436
<i>AxPDH</i>	V5NC32	421	H	Q	L	P	-	P	A	D	V	P	N	Q	V	Q	L	P	D	P	D	S	I	G	441
<i>TmP2O</i>	Q7ZA32	450	H	R	D	A	F	S	Y	G	A	V	Q	Q	S	-	I	D	S	R	-	-	-	-	466

Fig. 2. Sequence alignment of loop 1 and active site loop of *AmPDH1*, *AbPDH*, *AcPDH* and *AxPDH*, using Clustalw2 algorithm.

Five Asn residues of *AbPDH* were predicted to be N-glycosylated, using NetNGlyc 1.0 Server [39]. Four of them corresponded to N-glycosylation sites of *AmPDH1* described by Yakovleva et al. [40] (*AbPDH* N<sup>98</sup>, N<sup>198</sup>, N<sup>274</sup> and N<sup>341</sup> corresponding to *AmPDH1* N<sup>100</sup>, N<sup>200</sup>, N<sup>277</sup>, N<sup>344</sup>, respectively). N<sup>98</sup> and N<sup>198</sup>, their *AmPDH1* homologs, and N<sup>113</sup>, which has no *AmPDH1* counterpart, are located next to the active site access. N<sup>274</sup> is located at the deviating loop 2.

### Transcript analysis of the *A. bisporus* pdh and the gpd1 gene

Several carbon sources were already tested for inducing dehydrogenase activity in *A. bisporus* by Morrison et al. [41]. High activity was found on media with cellobiose as the sole carbon source, less with D-glucose, low activities were found with different forms of cellulose and no activity with D-

mannitol, d-xylose and d-fructose. Considering these results *A. bisporus* was cultivated as described in Material and Methods on minimal medium containing D-glucose and d-cellobiose as carbon sources, respectively. Samples were taken over 23 days of cultivation. As expected the PDH activity was higher on cellobiose. The cultures showed similar growth on both carbon sources with a maximum of biomass after 14 days, when the sugar concentration reached low levels. (Fig. 3A and B). A fraction of cellobiose was hydrolyzed to D-glucose by the  $\beta$ -glucosidase activity of the fungus.

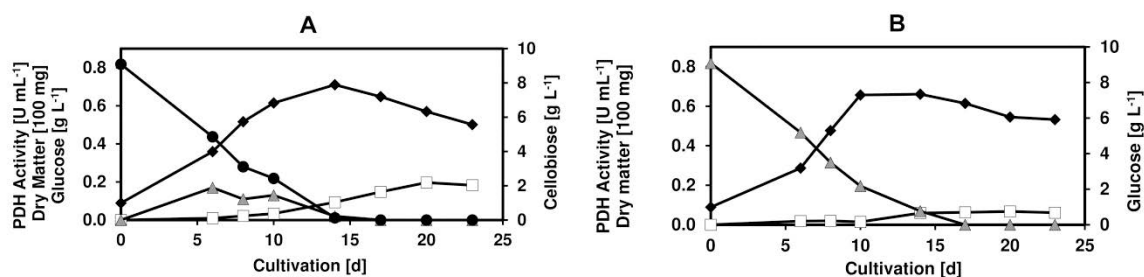


Fig. 3. Biomass production, carbon source consumption and PDH activity of *A. bisporus* on two carbon sources [A: cellobiose; B: D-glucose; dry matter (♦), PDH activity (□), d-glucose (▲), cellobiose (●)].

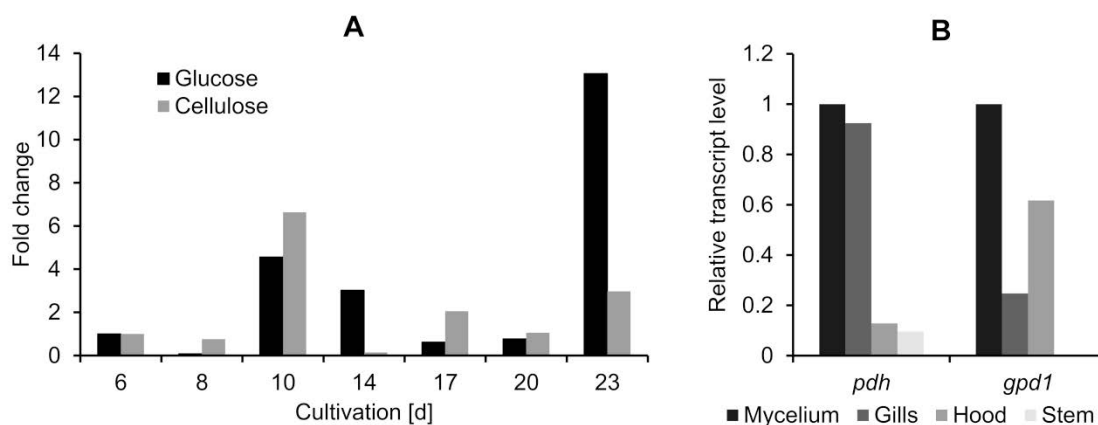


Fig. 4. Transcript analysis of the PDH-encoding gene of *A. bisporus* during the cultivation on D-glucose and cellobiose (A) and in different tissues of the fruiting body (B).

For transcriptional analysis mycelial samples were taken at the indicated time points during the 23-day cultivation. Changes of the mRNA levels were compared to the first sample of both cultivations taken on day 6, when growth on the surface could be detected. Samples of different tissues of the fruiting body of *A. bisporus* as well as from mycelium grown on soil used for commercial production were taken and the transcript levels of *pdh* were compared. The *gpd2* transcript was used for normalization of the expression levels. The mRNA levels of *pdh* showed a significant rise at day 10. On D-glucose the level stayed high throughout day 14. During that time most of the enzyme was produced. The spike in mRNA concentration at the end of the cultivation, when the dry weight of the mycelium was

already decreasing, did not result in additional PDH activity. On cellobiose the mRNA level dropped when the carbon source concentration was very low on day 14, but normalized afterwards corresponding to an increase of activity. The mRNA levels on cellobiose were generally higher than on D-glucose (Fig. 4A). Very low *pdh* transcript levels could be detected in the stem and the hood of the fruiting bodies, but the transcript level of *pdh* in the gills was within the variations of the transcripts in the mycelium ( Fig. 4B).

### Expression and purification of recAbPDH

For extracellular expression of the *pdh* gene from *A. bisporus* under control of the inducible AOX1 promoter, the full-length open reading frame of the gene including the native prepro leader sequence and stop codon was cloned into the vector plasmid pPICZB. Using the plasmid-encoded alpha factor leader sequence instead did not result in detectable amounts of secreted PDH (data not shown) as was described previously for *A. meleagris pdh* expression [18]. The resulting construct was transformed into *P. pastoris* X33 and a confirmed clone was chosen for recAbPDH production in 12 shaking flasks filled with 200 mL BMGY medium each. The fermentation resulted after 143 h of induction in a total of 1065 U of recAbPDH.

The enzyme was purified from the supernatant by hydrophobic interaction chromatography followed by anion exchange chromatography (Table 1). Chromatography fractions were restrictively pooled and purification yielded recAbPDH with a specific activity of 24 U mg<sup>-1</sup>. One third of initial total activity could be recovered with an about 4-fold increase in specific activity. Anion exchange-chromatography caused a loss of more than half of total activity while specific activity slightly decreased.

The resulting pool of recAbPDH was analyzed by SDS-Page with Coomassie Blue staining ( Fig. 5A), and showed a broad smear between 75 and 100 kDa, compared to approximately 75 kDa of native AbPDH [6]. However, after deglycosylation with Endo Hf the recAbPDH pool after anion exchange chromatography was found to be electrophoretically pure with a single band at ~70 kDa. As estimated by SDS-Page, the glycosyl moiety of recAbPDH amounted therefore to 7–33% of the enzyme mass.

Table 1. Purification of heterologously expressed AbPDH.

	Volume [mL]	Total activity [U]	Total protein [mg]	Specific activity [U mg <sup>-1</sup> ]	Recovery rate [%]	Purification [-fold]
Culture supernatant	2710	1065	189.7	5.6	100	1
Phenyl sepharose FF	290	903	31.9	28.3	85	5.1
DEAE sepharose FF & ultrafiltration	0.78	345	14.3	24.1	32	4.3

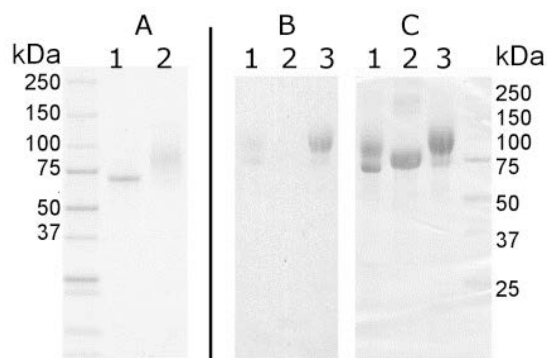


Fig. 5. A: SDS PAGE stained with Coomassie Blue; Precision Plus Protein Standards (Bio-Rad), *recAbPDH* deglycosylated with Endo Hf (New England Biolabs) (1) and N-glycosylated (2); B and C: 10  $\mu$ g *recAbPDH* (1), *Aspergillus niger* glucose oxidase (2) and *recAmPDH1* (3), visualized by excitation at 302 nm (B) and by being stained with Coomassie Blue (C).

Recombinant *AbPDH* showed two fluorescent bands which were identical with the two coomassie stained protein bands, indicating a covalent FAD linkage to the apoprotein ( Fig. 5B and C). Recombinant *A. meleagris* PDH with covalently bound FAD [18] and [21] was used as positive and native *A. niger* glucose oxidase (Sigma Aldrich) with non-covalently bound FAD as negative control [37].

### Influence of pH and temperature on *recAbPDH*

*recAbPDH* was stable in 100 mM Britton Robinson buffer from pH 4 to 8 ( $\geq 75\%$  remaining activity after 1 week at 25  $^{\circ}$ C, optimum at pH 6) and was rapidly inactivated in more acidic and alkaline conditions ( Fig. 6A). pH profiles of *recAbPDH* and *recAmPDH* with ferrocenium hexafluorophosphate were determined ( Fig. 7) between pH 3 and pH 8.5. More basic environments than pH 9 were complicated by enzyme stability and limitations of the ferrocenium based photometric assay [21]. Both enzymes showed a continuous rise in activity with increasing pH with comparable specific activities. The choice of pH 7.5 for the photometric standard assay was a compromise of high specific activity and enzyme stability.

The temperature optimum of *recAbPDH* at standard conditions was 49  $^{\circ}$ C ( Fig. 6B). pH was observed to have a strong impact on enzyme stability at higher temperatures. After 30 min at 50  $^{\circ}$ C and standard assay pH (7.5) only  $\sim 10\%$  of initial *recAbPDH* activity was left but at pH 6 more than 90% remained active ( Fig. 6C).

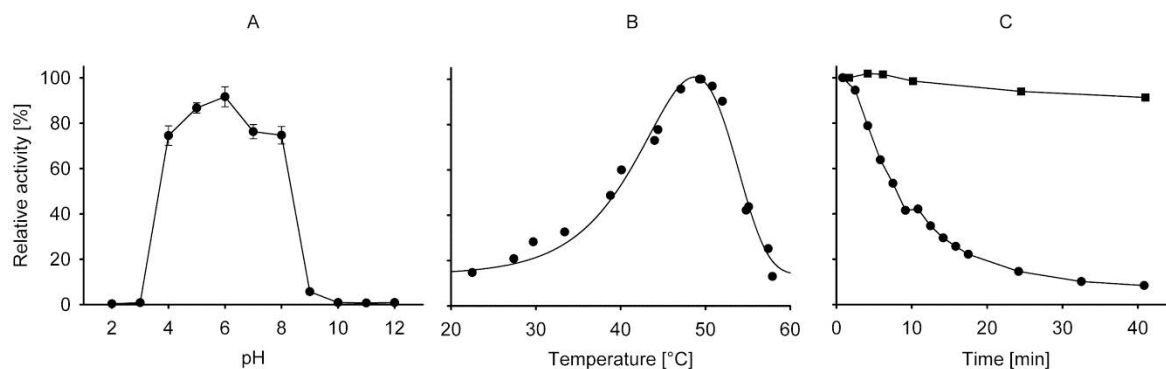


Fig. 6. A: pH stability of *recAbPDH* ( $0.023 \text{ mg mL}^{-1}$ ), remaining activity in % after 1 week at  $22 \text{ }^\circ\text{C}$  in  $28 \text{ mM}$  Britton-Robinson-buffer pH 2–12; B: temperature optimum of *recAbPDH*, single measurements from two independent experiments; C: temperature stability of *recAbPDH* at  $50 \text{ }^\circ\text{C}$  in sodium phosphate buffer pH 6 (■) and pH 7.5 (●); all measurements conducted with  $25 \text{ mM}$  D-glucose and  $0.2 \text{ mM}$  ferrocenium hexafluorophosphate.

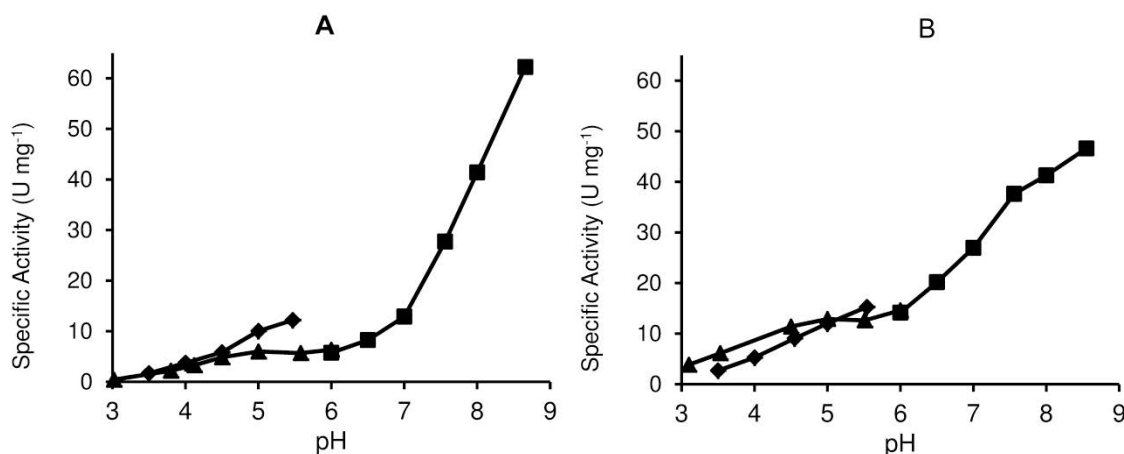


Fig. 7. A: pH-profiles of *recAmPDH1* (A) and *recAbPDH* (B), measured in duplicates with  $25 \text{ mM}$  D-glucose and  $0.2 \text{ mM}$  ferrocenium hexafluorophosphate [pH 3–6.5: sodium malonate buffer (▲); pH 3.5–5.5: sodium acetate buffer (●); pH 6–8.6: sodium phosphate buffer (■)].

### Kinetic parameters of electron acceptors and donors

Kinetic constants were determined for electron acceptors which were previously used for characterization of other PDHs [18] and [19] (Table 2). ABTS cation radical and DCIP had the highest catalytic efficiency but ABTS cation radical was instable in neutral and alkaline environments and DCIP inhibited *recAbPDH* at higher concentrations. 1,4 benzoquinone exhibited the least favorable kinetic characteristics of the tested electron acceptors. Ferrocenium hexafluorophosphate was therefore the preferred electron acceptor for photometric activity assays.

Selected mono-, di- and trisaccharides were tested for affinity and catalytic turnover with *recAbPDH* (Table 2). D-glucose and l-arabinose were the substrates with the highest catalytic efficiency. d-xylose and d-galactose were also good substrates but with an approximately 3-fold higher  $K_m$ . Di- and trisaccharides showed about 30–80% of the  $k_{cat}$  of D-glucose. Cellobiose and maltose had a  $K_m$  similar to D-glucose, whereas lactose and raffinose had a 26-fold and 7-fold increased  $K_m$ , respectively.

Table 2. Apparent kinetic constants of *recAbPDH* for electron acceptors with 25 mM D-glucose at respective pH (100 mM sodium acetate pH 4, 100 mM sodium phosphate pH 7.5) and for mono-, di- and tri-saccharides with 0.2 mM ferrocenium hexafluorophosphate at pH 7.5

<b>Electron acceptor</b>	$K_m$ [ $\mu\text{M}$ ]	$k_{cat}$ [ $\text{s}^{-1}$ ]	$k_{cat}/K_m$ [ $\text{mM}^{-1} \text{s}^{-1}$ ]
Ferrocenium hexafluorophosphate (1 e <sup>-</sup> ) (pH 7.5)	170 ±10	111.1 ±3.8	326
ABTS cation radical (1 e <sup>-</sup> ) (pH 4)	79 ±1.6	101.2 ±2.2	768
2,6-Dichloroindophenol (2 e <sup>-</sup> ) (pH 4)	60 ±22	57.6 ±10.2	958
1,4-Benzoquinone (2 e <sup>-</sup> ) (pH 4)	566 ±72	44.2 ±2.1	78

<b>Substrate</b>	$K_m$ [ $\mu\text{M}$ ]	$k_{cat}$ [ $\text{s}^{-1}$ ]	$k_{cat}/K_m$ [ $\text{mM}^{-1} \text{s}^{-1}$ ]
D-Glucose	1.54 ±0.22	33.7 ±0.6	22
D-Xylose	4.75 ±0.08	36.9 ±0.1	7.8
L-Arabinose	1.33 ±0.22	29.6 ±1.1	22
D-Galactose	4.19 ±0.01	28.7 ±0.7	6.9
D-Mannose	109.1 ±4.3	13.31 ±0.31	0.1
Cellobiose	2.45 ±0.40	24.63 ±0.60	10
Maltose	2.16 ±0.18	27.26 ±0.91	13
Lactose	40.51 ±0.31	15.95 ±0.35	0.4
Raffinose	10.79 ±1.97	19.61 ±0.87	1.8

## **Discussion**

*AbPDH* was the first discovered pyranose dehydrogenase and described by Volc et al. [6] and [7]. However, only limited kinetic data was published in these works in form of relative activities of selected electron acceptors and substrates and a pH profile with 1,4-benzoquinone. Morrison et al. [41] reported the steady state kinetics of a range of sugars with a glucose 3-dehydrogenase from *A. bisporus*, which had an N-terminus identical to that of mature *AbPDH* (AITYQNPT ...). This enzyme was however considerably smaller and featured a different oxidation pattern of D-glucose than the *AbPDH* described by Volc et al. [7]. *A. bisporus* has only one *pdh* gene, as was suggested by

Peterbauer and Volc [8] and now confirmed on genomic level. As the full sequence of this glucose 3-dehydrogenase was not elucidated its identity and degree of sequence similarity to *AbPDH* could not be clarified however.

To address these uncertainties and further elucidate the role of PDH in *A. bisporus* and possible applications of the enzyme, a more detailed investigation of transcription and protein characteristics of confirmed *AbPDH* was conducted. We studied transcription of *pdh* from *A. bisporus* in submerged and solid substrate culture. The successful recombinant expression of *AbPDH* in *P. pastoris* was reported and purified protein was characterized and compared to previously studied *A. xanthoderma* PDH, *A. campestris* PDH [20] and *A. meleagris* PDH1 [18], which have sequence identities of 77–78% to *AbPDH*. For the also related *AmPDH2* and *AmPDH3* there are no kinetic data available to this date.

### Homologous transcription and expression

*AbPDH* activity and transcription levels of *Abpdh* were monitored in a batch cultivation of *A. bisporus* with D-glucose and cellobiose, which supported the formation of PDH activity in *A. meleagris* [24], as substrates. Biomass yields were similar with both substrates. Very little *pdh* was transcribed during the exponential growth phase, which corresponded well to the low activity. An increase in transcription took place after the onset of substrate limitation on day 10, and continued on a lower level after substrate depletion. The strong increase of the mRNA level on day 23 could be explained by a stress reaction to prolonged cell starvation. Cultivation with cellobiose led to higher PDH activity than with D-glucose and also generally higher transcription of *pdh*. These findings are similar to those of Kittl et al. [24] with PDH of *A. meleagris*, and in agreement with the proposed function of PDH as detoxification enzyme with a role in degradation of humic compounds [13]. It is intriguing, however, that the single *pdh* gene in *A. bisporus* displays a similar transcription pattern as the two “secondary” *pdh* genes *pdh2* and *pdh3* in *A. meleagris*, whose transcription level is significantly lower than that of *pdh1* and which lack the sharp increase of transcription of *pdh1* upon transfer to fresh culture vessels, possibly associated with oxygen depletion. Both these enzymes are also far less abundant than PDH1. This discrepancy indicates that PDH is a non-essential or redundant enzyme whose function can be substituted by other, catalytically related enzymes, and which consequently can evolve to take over diverse functions in different fungi. The amount of transcript in the fruiting bodies was approximately equal (gills) or significantly lower (stem, cap) than in the vegetative mycelium and does not indicate a particular role during fruiting.

### Protein characterization

*AbPDH* was successfully heterologously expressed in *P. pastoris* and purified to a specific activity of 24 U mg<sup>-1</sup> and homogeneity on SDS-page. It was generally less stable than *AmPDH1*, more sensitive

to a moderately alkaline environment (pH 8–10) and had a lower temperature optimum of 49 °C compared to 63 °C of *Am*PDH1 [21] and 75 °C of *Ax*PDH [19]. These data support the idea that PDH is not necessarily a vital enzyme under many growth conditions. However, it proved stable at physiological pH and temperature and the reduced stability at basic conditions and high temperatures is of little consequence for suggested applications like biofuel cells.

The co-factor FAD was shown to be covalently bound to *Ab*PDH, like in *Am*PDH1 [21]. SDS-Page revealed two distinct bands for *Ab*PDH which were both fluorescent. This change from the single band in the initial SDS-Page after purification can be explained by the previously observed spontaneous degradation or autoproteolysis of PDH [21], leading to two fragments under denaturing SDS-Page conditions. The additional band at ~70 kDa still contained the FAD prosthetic group. The reduced intensity of the fluorescence could be due to the greater spreading of the enzyme on the gel.

PDH is a secretory glycoprotein, and in *Am*PDH1 the carbohydrate moiety amounts for approximately seven percent of the molecular mass in the protein purified from culture supernatant. Heterologously produced *Am*PDH1 (*P. pastoris*), however, was found to be significantly overglycosylated, resulting in a total molecular mass of around 100 kDa [18] and [21]. This observation was also made for the recombinantly produced *Ab*PDH.

### **Kinetic properties**

The pH dependency of *Ab*PDH with the electron acceptors 1,4-benzoquinone [6] and ferrocenium hexafluorophosphate were similar to those reported for other PDHs [19], [20] and [21]. It had the highest catalytic turnover rates with ABTS cation radical and ferrocenium hexafluorophosphate. Because of limitations in the use of other electron acceptors, and to obtain comparable results to previous publications, ferrocenium hexafluorophosphate was chosen as electron acceptor for further kinetic analyses. Even though quinones are likely biological electron acceptors for PDH [8], the catalytic efficiency of 1,4-benzoquinone was 2–3 lower than for the tested alternatives. This is in agreement to previous results with *Am*PDH1 and *Ax*PDH. However, *Ac*PDH has its highest catalytic turnover with 1,4-benzoquinone [19], [20] and [21].

Affinity of monosaccharides to *Ab*PDH, *Ac*PDH and *Ax*PDH were similar and slightly lower than to *Am*PDH1 (Table S3). A change in orientation of the C2 hydroxyl group increased the  $K_m$  approximately 100-fold compared to D-glucose, as was already observed with *Am*PDH1, while it did not prevent catalysis. C4 D-glucose epimers had an up to three-fold decreased affinity to *Ab*PDH and *Am*PDH1 at similar catalytic activities as D-glucose. Interestingly, *Ab*PDH showed comparable affinities and catalytic turnover numbers with D-glucose and its disaccharides maltose and cellobiose, in contrast to *Am*PDH1 which also had comparable  $k_{cat}$  values but an 8–11 fold higher  $K_m$  for these

disaccharides than for D-glucose. For applications in enzymatic biofuel cells, this may be an advantage for *AbPDH* in certain cases when, e.g., plant biomass hydrolysates containing incompletely hydrolyzed polysaccharides are employed as fuel. Compared to the other recently characterized recombinant PDHs (*AcPDH* and *AxPDH*), *AbPDH* and *AmPDH1* showed significantly higher catalytic turnover numbers for tested sugars and electron acceptors [19], [20] and [21].

Like the other PDHs described so far, *AbPDH* oxidizes a broad range of sugars, not only cellobiose, which is the strongest known inducer of its transcription. The number of e-acceptors is limited however and includes quinones, phenols and organometallic-compounds [7]. Steady state kinetics with 1,4 benzoquinone but also with the other tested e-acceptors varied significantly between PDHs. These observations support the reported detoxification function of PDHs [8] but also point towards specialization towards different reduction targets for different PDHs.

### Structural analysis

So far, *AmPDH1* is the only PDH with a resolved x-ray crystallography structure (4H7U) [35]. As *AbPDH*, *AcPDH* and *AxPDH* share sufficient sequence identity (>70%) with *AmPDH1*, automated homology modeling could be employed to predict structural differences. The strong conservation of active site residues between *AbPDH* and *AmPDH1* is in line with the high similarity of apparent kinetic characteristics of both enzymes. There were differences however in the larger active site pocket. Replacement of Phe<sup>533</sup> (*AmPDH1*) with the smaller Val<sup>530</sup> (*AbPDH*) apparently enlarged the substrate pocket.

Of the two deviant loops that could be identified, loop 1 (<sup>91</sup>LRPRY<sup>95</sup>) is at a peculiar position as it forms one side of the active site access. The active site loop on the other side had been described to play a key role in substrate binding and specificity in the related oxidoreductase Pyranose 2-Oxidase (P2O) [38]. PDHs replaced the gating segment <sup>454</sup>FSY<sup>456</sup> of this P2O active site loop, whereas polarity of the structurally homologous segment was varying between the different PDHs. In *AmPDH1* the side chains oriented towards the FAD are all non-polar, while there is one polar residue (Ser<sup>425</sup>) in the *AbPDH* homolog pointing to the FAD. *AcPDH* and *AxPDH* feature even a glutamine and aspartate, respectively ( Fig. 1). The predicted active site loop anchoring H-bond network in *AbPDH* differed substantially from that in other studied PDHs. The hydrogen bond directly at the FAD facing segment (*AbPDH* Ser<sup>425</sup>/Gln<sup>444</sup>) was however conserved in all of them. Interestingly, *AbPDH* was the only studied PDH which showed polar interactions between the active site loop and loop 1. This interaction takes place between two residues which have no polar homolog in the other PDHs.

It is unknown, to this date, if the active site loop in PDHs also serves the central gating function that it has in P2O with an open and closed conformation. However, in the crystal structure 4H7U, and

consequently in the homology models the FAD facing segment and loop 1 are determining factors for the dimensions and nature of the substrate access site. Changes in the affinity towards disaccharides with only modest changes in catalytic turnover are in line with the highly conserved set of residues around the isoalloxazine ring but high variability in the substrate access site at the surface. Furthermore, Val<sup>530</sup> in *AbPDH* could also make the active site sterically less stringent, favoring the binding of larger substrates.

Loop 1, FAD facing segment residues, and amino acids putatively involved in anchoring the active site loop as well as Val<sup>530</sup> are therefore promising targets for site directed mutagenesis studies with the aim of modulating substrate specificities of PDHs and improving the understanding of its substrate binding. Additionally, mutagenesis studies on the more basic amino acid residues around the active site of *AcPDH* appear promising to elucidate the altered electron acceptor preferences. Such studies are, however, hampered by the difficulties in heterologous expression of *AcPDH* as reported recently [20].

## **Conclusion**

The flavoenzyme *AbPDH* was expressed by *A. bisporus* mainly at the onset of substrate limitation and is proposed to be a non-essential detoxification enzyme. It is closely related to PDHs from *A. meleagris*, *A. campestris* and *A. xanthoderma* but displayed some significantly different properties. While enzyme stability was lower for basic and high temperature conditions, compared to *AmPDH1*, it showed higher affinity towards disaccharides. *AbPDH* is therefore an interesting candidate for biofuel cells powered by plant biomass hydrolysates and could be an alternative to other PDHs for implantable biofuel cells. Gene shuffling experiments could be used to combine higher affinity towards larger substrates of *AbPDH* with the higher stability of *AmPDH1*. Further study of the active site loop and less conserved active site residues could improve the understanding of the substrate binding and specificity.

## **Acknowledgments**

This work was supported by the Austrian Science Fund (FWF) (grant TRP218 to CKP). CG is a member of the doctoral program “BioTop – Biomolecular Technology of Proteins” (FWF W1224). The authors declare no conflict of interest.

## References

- [1] E.W. van Hellemond, N.G.H. Leferink, D.P.H.M. Heuts, M.W. Fraaije, W.J.H. van Berkel, Occurrence and biocatalytic potential of carbohydrate oxidases, in: S. S, G.M.G. Allen, I. Laskin (Eds.), *Adv. Appl. Microbiol.*, Academic Press, 2006, pp. 17e54. <http://www.sciencedirect.com/science/article/pii/S0065216406600026>.
- [2] M. Kiess, H.-J. Hecht, H.M. Kalisz, Glucose oxidase from *Penicillium amagasakiense*, *Eur. J. Biochem.* 252 (1998) 90e99, <http://dx.doi.org/10.1046/j.1432-1327.1998.2520090.x>.
- [3] G. Henriksson, V. Sild, I.J. Szab\_o, G. Pettersson, G. Johansson, Substrate specificity of cellobiose dehydrogenase from *Phanerochaete chrysosporium*, *Biochim. Biophys. Acta BBA e Protein Struct. Mol. Enzymol.* 1383 (1998) 48e54, [http://dx.doi.org/10.1016/S0167-4838\(97\)00180-5](http://dx.doi.org/10.1016/S0167-4838(97)00180-5).
- [4] C.W. Higham, D. Gordon-Smith, C.E. Dempsey, P.M. Wood, Direct <sup>1</sup>H NMR evidence for conversion of b-d-cellobiose to cellobionolactone by cellobiose dehydrogenase from *Phanerochaete chrysosporium*, *FEBS Lett.* 351 (1994) 128e132, [http://dx.doi.org/10.1016/0014-5793\(94\)00847-7](http://dx.doi.org/10.1016/0014-5793(94)00847-7).
- [5] C. Leitner, J. Volc, D. Haltrich, Purification and characterization of pyranose oxidase from the white rot fungus *Trametes multicolor*, *Appl. Environ. Microbiol.* 67 (2001) 3636e3644, <http://dx.doi.org/10.1128/AEM.67.8.3636-3644.2001>.
- [6] J. Volc, E. Kub\_atov\_a, D.A. Wood, G. Daniel, Pyranose 2-dehydrogenase, a novel sugar oxidoreductase from the basidiomycete fungus *Agaricus bisporus*, *Arch. Microbiol.* 167 (1997) 119e125.
- [7] J. Volc, P. Sedmera, P. Halada, V. Prikrylova, G. Daniel, C-2 and C-3 oxidation of-Glc, and C-2 oxidation of-Gal by pyranose dehydrogenase from *Agaricus bisporus*, *Carbohydr. Res.* 310 (1998) 151e156.
- [8] C.K. Peterbauer, J. Volc, Pyranose dehydrogenases: biochemical features and perspectives of technological applications, *Appl. Microbiol. Biotechnol.* 85 (2009) 837e848, <http://dx.doi.org/10.1007/s00253-009-2226-y>.
- [9] T.R. Green, Significance of glucose oxidase in lignin degradation, *Nature* 268 (1977) 78e80, <http://dx.doi.org/10.1038/268078a0>.
- [10] G. Szklarz, A. Leonowicz, Cooperation between fungal laccase and glucose oxidase in the degradation of lignin derivatives, *Phytochemistry* 25 (1986) 2537e2539, [http://dx.doi.org/10.1016/S0031-9422\(00\)84503-3](http://dx.doi.org/10.1016/S0031-9422(00)84503-3).
- [11] M. Samejima, K.-E.L. Eriksson, A comparison of the catalytic properties of cellobiose: quinone oxidoreductase and cellobiose oxidase from *Phanerochaete chrysosporium*, *Eur. J. Biochem.* 207 (1992) 103e107, <http://dx.doi.org/10.1111/j.1432-1033.1992.tb17026.x>.
- [12] J.D. Stahl, S.J. Rasmussen, S.D. Aust, Reduction of quinones and radicals by a plasma membrane redox system of *Phanerochaete chrysosporium*, *Arch. Biochem. Biophys.* 322 (1995) 221e227, <http://dx.doi.org/10.1006/abbi.1995.1455>.
- [13] E. Morin, A. Kohler, A.R. Baker, M. Foulongne-Oriol, V. Lombard, L.G. Nagye, et al., Genome sequence of the button mushroom *Agaricus bisporus* reveals mechanisms governing adaptation to a humic-rich ecological niche, *Proc. Natl. Acad. Sci.* 109 (2012) 17501e17506, <http://dx.doi.org/10.1073/pnas.1206847109>.
- [14] M.J. Carlile, S.C. Watkinson, G.W. Gooday, The Fungi, second ed., *Academic Press*, London, 2001. <http://www.sciencedirect.com/science/article/pii/B9780127384450500198>.
- [15] F. Giffhorn, Fungal pyranose oxidases: occurrence, properties and biotechnical applications in carbohydrate chemistry, *Appl. Microbiol. Biotechnol.* 54 (2000) 727e740.

- [16] F. Giffhorn, S. Köpper, A. Huwig, S. Freimund, Rare sugars and sugar-based synthons by chemo-enzymatic synthesis, *Enzyme Microb. Technol.* 27 (2000) 734e742, [http://dx.doi.org/10.1016/S0141-0229\(00\)00293-3](http://dx.doi.org/10.1016/S0141-0229(00)00293-3).
- [17] M.N. Zafar, F. Tasca, S. Boland, M. Kujawa, I. Patel, C.K. Peterbauer, et al., Wiring of pyranose dehydrogenase with osmium polymers of different redox potentials, *Bioelectrochemistry* 80 (2010) 38e42.
- [18] C. Sygmund, A. Gutmann, I. Krondorfer, M. Kujawa, A. Glieder, B. Pscheidt, et al., Simple and efficient expression of *Agaricus meleagris* pyranose dehydrogenase in *Pichia pastoris*, *Appl. Microbiol. Biotechnol.* 94 (2011) 695e704, <http://dx.doi.org/10.1007/s00253-011-3667-7>.
- [19] M. Kujawa, J. Volc, P. Halada, P. Sedmera, C. Divne, C. Sygmund, et al., Properties of pyranose dehydrogenase purified from the litter-degrading fungus *Agaricus xanthoderma*, *FEBS J.* 274 (2007) 879e894.
- [20] P. Staudigl, I. Krondorfer, D. Haltrich, C.K. Peterbauer, Pyranose dehydrogenase from *Agaricus campestris* and *Agaricus xanthoderma*: characterization and applications in carbohydrate conversions, *Biomolecules* 3 (2013) 535e552, <http://dx.doi.org/10.3390/biom3030535>.
- [21] C. Sygmund, R. Kittl, J. Volc, P. Halada, E. Kubátová, D. Haltrich, et al., Characterization of pyranose dehydrogenase from *Agaricus meleagris* and its application in the C-2 specific conversion of D-galactose, *J. Biotechnol.* 133 (2008) 334e342.
- [22] K. Manning, D.A. Wood, Production and regulation of extracellular endocellulase by *Agaricus bisporus*, *J. Gen. Microbiol.* 129 (1983) 1839e1847, <http://dx.doi.org/10.1099/00221287-129-6-1839>.
- [23] M. Harmsen, F.J. Schuren, S. Moukha, C. Zuilen, P. Punt, J.H. Wessels, Sequence analysis of the glyceraldehyde-3-phosphate dehydrogenase genes from the basidiomycetes *Schizophyllum commune*, *Phanerochaete chrysosporium* and *Agaricus bisporus*, *Curr. Genet.* 22 (1992) 447e454, <http://dx.doi.org/10.1007/BF00326409>.
- [24] R. Kittl, C. Sygmund, P. Halada, J. Volc, C. Divne, D. Haltrich, et al., Molecular cloning of three pyranose dehydrogenase-encoding genes from *Agaricus meleagris* and analysis of their expression by real-time RT-PCR, *Curr. Genet.* 53 (2008) 117e127, <http://dx.doi.org/10.1007/s00294-007-0171-9>.
- [25] M. Pfaffl, A new mathematical model for relative quantification in real-time RT-PCR, *Nucleic Acids Res.* 29 (2001), <http://dx.doi.org/10.1093/nar/29.9.e45> e45.
- [26] J. Lin-Cereghino, W.W. Wong, S. Xiong, W. Giang, L.T. Luong, J. Vu, et al., Condensed protocol for competent cell preparation and transformation of the methylotrophic yeast *Pichia pastoris*, *BioTechniques* 38 (2005) 44e48.
- [27] C. Leitner, J. Volc, D. Haltrich, Purification and characterization of pyranose oxidase from the white rot fungus *Trametes multicolor*, *Appl. Environ. Microbiol.* 67 (2001) 3636e3644, <http://dx.doi.org/10.1128/AEM.67.8.3636-3644.2001>.
- [28] N.S. Scrutton, Identification of covalent flavoproteins and analysis of the covalent link, in: *Methods Mol. Biol*, Humana Press, Totowa, NJ, 1999, pp. 181e193.
- [29] I.V. Grigoriev, H. Nordberg, I. Shabalov, A. Aerts, M. Cantor, D. Goodstein, et al., The Genome portal of the department of energy joint genome institute, *Nucleic Acids Res.* 40 (2012) D26-D32, <http://dx.doi.org/10.1093/nar/gkr947>.
- [30] S.F. Altschul, W. Gish, W. Miller, E.W. Myers, D.J. Lipman, Basic local alignment search tool, *J. Mol. Biol.* 215 (1990) 403e410, [http://dx.doi.org/10.1016/S0022-2836\(05\)80360-2](http://dx.doi.org/10.1016/S0022-2836(05)80360-2).

- [31] T. Schwede, J. Kopp, N. Guex, M.C. Peitsch, SWISS-MODEL: an automated protein homology-modeling server, *Nucleic Acids Res.* 31 (2003) 3381e3385, <http://dx.doi.org/10.1093/nar/gkg520>.
- [32] K. Arnold, L. Bordoli, J. Kopp, T. Schwede, The SWISS-MODEL workspace: a web-based environment for protein structure homology modelling, *Bioinform. Oxf. Engl.* 22 (2006) 195e201, <http://dx.doi.org/10.1093/bioinformatics/bti770>.
- [33] F. Kiefer, K. Arnold, M. Künzli, L. Bordoli, T. Schwede, The SWISS-MODEL repository and associated resources, *Nucleic Acids Res.* 37 (2009) D387eD392, <http://dx.doi.org/10.1093/nar/gkn750>.
- [34] M. Biasini, S. Bienert, A. Waterhouse, K. Arnold, G. Studer, T. Schmidt, et al., SWISS-MODEL: modelling protein tertiary and quaternary structure using evolutionary information, *Nucleic Acids Res.* 42 (2014) W252eW258, <http://dx.doi.org/10.1093/nar/gku340>.
- [35] C.T. Tan, O. Spadiut, T. Wongnate, J. Sucharitakul, I. Krondorfer, C. Sygmund, et al., The 1.6 Å crystal structure of pyranose dehydrogenase from *Agaricus meleagris* rationalizes substrate specificity and reveals a flavin intermediate, *PLoS ONE* 8 (2013) art. no. e53567.
- [36] M.M.H. Graf, U. Bren, D. Haltrich, C. Oostenbrink, Molecular dynamics simulations give insight into d-glucose dioxidation at C2 and C3 by *Agaricus meleagris* pyranose dehydrogenase, *J. Comput. Aided Mol. Des.* 27 (2013) 295e304, <http://dx.doi.org/10.1007/s10822-013-9645-7>.
- [37] G. Wohlfahrt, S. Witt, J. Hendle, D. Schomburg, H.M. Kalisz, H.-J. Hecht, 1.8 and 1.9 Å resolution structures of the *Penicillium amagasakiense* and *Aspergillus niger* glucose oxidases as a basis for modelling substrate complexes, *Acta Crystallogr. Sect. D.* 55 (1999) 969e977, <http://dx.doi.org/10.1107/S09074444999003431>.
- [38] O. Spadiut, T.-C. Tan, I. Pisanelli, D. Haltrich, C. Divne, Importance of the gating segment in the substrate-recognition loop of pyranose 2-oxidase, *FEBS J.* 277 (2010) 2892e2909, <http://dx.doi.org/10.1111/j.1742-4658.2010.07705.x>.
- [39] NetNGlyc 1.0 Server, (n.d.). <http://www.cbs.dtu.dk/services/NetNGlyc/> (accessed 09.09.14).
- [40] M.E. Yakovleva, A. Killy\_eni, O. Seubert, P. \_OConghaile, D. MacAodha, D. Leech, et al., Further Insights into the catalytical properties of deglycosylated pyranose dehydrogenase from *Agaricus meleagris* recombinantly expressed in *Pichia pastoris*, *Anal. Chem.* (2013), <http://dx.doi.org/10.1021/ac4023988>, 130910071924000.
- [41] S.C. Morrison, D.A. Wood, P.M. Wood, Characterization of a glucose 3-dehydrogenase from the cultivated mushroom (*Agaricus bisporus*), *Appl. Microbiol. Biotechnol.* 51 (1999) 58e64.

## **CHAPTER II**

### **Engineering of pyranose dehydrogenase for application to enzymatic anodes in biofuel cells**

Maria E. Yakovleva,<sup>‡a</sup> Christoph Gonaus,<sup>‡b</sup> Katharina Schropp,<sup>ab</sup> Peter O'Conghaile,<sup>c</sup> Dónal Leech,<sup>c</sup> Clemens K. Peterbauer<sup>b</sup> and Lo Gorton<sup>\*a</sup>

<sup>a</sup> Department of Analytical Chemistry/Biochemistry and Structural Biology, Lund University, PO Box 124, SE-221 00 Lund, Sweden.

<sup>b</sup> Department of Food Sciences and Technology, BOKU-University of Natural Resources and Applied Life Sciences, Muthgasse 18, A-1190 Wien, Austria

<sup>c</sup> School of Chemistry, National University of Ireland Galway, University Road, Galway, Ireland

<sup>‡</sup> These authors contributed equally.

E-mail: lo.gorton@biochemistry.lu.se

Electronic supplementary information (ESI) available: Information concerning purification of mutant PDHs. See DOI: 10.1039/c5cp00430f

Published in 2015 in Phys. Chem. Chem. Phys. 17, 9074–9081.

## **Abstract**

In the search for improved glucose oxidising enzymes for biofuel cells, a number of *Agaricus meleagris* (*Am*) pyranose dehydrogenase mutants (mPDHs) exhibiting different degrees of glycosylation were produced using site-directed mutagenesis and electrochemically characterised. The response of electrodes modified with different mPDHs is compared in a mediated electron transfer mode, where the electrodes are modified with each of the mutants covalently attached to redox polymers based on polyvinylimidazole-bound osmium complexes using a cross-linking agent. Coating of each of the enzymes onto the graphite electrode surface is also used to screen for their capacity for direct electron transfer. The double mutant PDH exhibits the highest response to glucose at physiological pH in both direct and mediated electron transfer modes, producing a  $J_{\max}$  of  $\approx 800 \mu\text{A cm}^{-2}$  at room temperature and when “wired” to the Os-polymer having the highest formal potential. From the results obtained the double mPDH is proposed as the most suitable candidate for application to bioanode fabrication.

## **Introduction**

An enzymatic biofuel cell (EBFC) is a specific class of fuel cells, which converts the energy of enzymatic redox reactions into electrical energy as long as fuel is supplied to it. The development of EBFCs became more extensive during the last few years due to their beneficial properties. Compared to conventional fuel cells, EBFCs can operate in physiological conditions and utilise fuels and oxidants present in vivo even at low concentrations.<sup>1-9</sup> These features make EBFCs applicable for construction of miniaturised implantable devices, which can be used as continuous power supplies with the energy derived from physiological sugars.

An obvious example of such a device would be an EBFC powering a cardiac pacemaker – medical devices currently powered by lithium-iodine batteries invented by Wilson Greatbatch and his team in 1972, with a life time of about 10 years.<sup>10</sup> EBFCs can also be applied as implantable self-powered sensors, for instance in monitoring of the glucose concentration in blood for diabetes management.<sup>11</sup>

One of the reasons why EBFCs still did not yet reach the market is the low power output, which is directly related to the current generated in the anodic part, where sugar is oxidised at the anode, onto which the biocatalyst is immobilised, and the cathodic part, where oxygen is reduced. In order to produce an EBFC with a sufficient power capacity it is important to maximise the current density generated in both parts of the cell. This can be done by a variety of methods.

One of the most efficient ways is to improve the electrical communication between the redox enzyme and the electrode, which to a large degree determines the current output. This can be done by “wiring”

the enzyme to osmium redox polymers, which will facilitate the electron transfer between the enzyme's active site and electrode surface.<sup>12-16</sup> Such an approach was demonstrated in a number of recent publications, where various oxidising enzymes were cross-linked with redox polymers based on polyvinylimidazole-bound osmium complexes in order to improve the current density of both bioanodes<sup>17-19</sup> and biocathodes.<sup>20,21</sup>

Another way to increase the current output of the bioanode and the biocathode is to downsize the dimensions of the enzyme.<sup>22</sup> This can be achieved by employing whole deglycosylated enzymes or by utilising separate enzyme domains responsible for the catalytic activity. By removing the carbohydrate shell from glycosylated redox enzymes it is possible to physically bring the enzyme's active site closer to the electrode surface or mediator matrix, which will increase the electron transfer rate according to the Marcus theory.<sup>23</sup> This has been previously demonstrated for horseradish peroxidase (HRP),<sup>24,25</sup> glucose oxidase (GOx),<sup>26,27</sup> cellobiose dehydrogenase (CDH)<sup>28,29</sup> and pyranose dehydrogenase (PDH).<sup>30-32</sup> Shao et al. proposed a bioanode based on the separately expressed deglycosylated dehydrogenase domain of CDH (DH<sub>CDH</sub>).<sup>33,34</sup> When using only DH<sub>CDH</sub> instead of the whole enzyme for construction of EBFCs, a greater load of the biocatalyst can be packed onto the electrode surface due to the smaller size of DH<sub>CDH</sub> resulting in higher currents. Downsizing the redox enzyme for improved current density was also demonstrated for deglycosylated PDH, which spontaneously loses a part of its C-terminus and forms a fragmented product with excellent electrocatalytic performance.<sup>35</sup>

PDH (EC 1.1.99.29) is a glycosylated extracellular enzyme produced by a group of litter-degrading basidiomycete *Agaricales*. It is a monomeric enzyme, which carries one flavin adenine dinucleotide (FAD) prosthetic group covalently bound to the polypeptide chain of the protein<sup>36</sup> in contrast to other glucose oxidising enzymes carrying their cofactor only through non-covalent linkages. PDH belongs to the glucose-methanol-choline oxidoreductase superfamily,<sup>37</sup> which also includes GOx (EC 1.1.3.4), pyranose oxidase (POx, EC 1.1.3.10), and CDH (EC 1.1.99.18).<sup>38</sup> In contrast to other members of the same family, which can only monooxidise sugars at the C-1 position, PDH (as well as POx) is able to mono- and dioxidise a variety of substrates at the C-2 and/or C-3 to their corresponding aldonolactones, or (di)dehydrosugars (aldos(di)uloses) and it is thus anomericly insensitive.<sup>36,39,40</sup> Unlike many sugar oxidising oxidoreductases PDH does not show reactivity towards molecular oxygen but makes use of other electron acceptors/mediators instead.<sup>41</sup> Together with a broad substrate tolerance and regioselectivity, this lack of electron donation to oxygen can be explained by a unique structure of the flavin pocket specific for the members of VAO [6-S-cysteinyl-8 $\alpha$ -(N1-histidyl)-FAD] family.<sup>42</sup> These three properties make the enzyme attractive for construction of EBFCs, where a broad substrate tolerance is not considered a disadvantage, the covalently bound cofactor increases the long-term stability of the enzyme in its immobilised state and the inability to utilise oxygen prevents

competition with  $O_2$  as electron acceptor as well as any damaging effects of hydrogen peroxide, which is otherwise formed when oxygen-dependent oxidoreductases are employed (e.g., GOx or POx).

The suitability of PDH for bioanode fabrication was first demonstrated for naturally occurring glycosylated *Agaricus meleagris* enzyme when “wired” to osmium redox polymers on the surface of graphite electrodes.<sup>43</sup> The electrodes modified with PDH showed a higher current response to glucose in flow-injection amperometry compared to those modified with GOx. It was possible to oxidise the substrate at potentials close to the formal potential of the enzyme in near-physiological conditions.<sup>18</sup> However, low production levels of PDH purified from the natural source hindered widespread application of the enzyme for fabrication of EBFCs and other biotechnological purposes. The problem was solved by heterologous expression of the enzyme in several host organisms, of which *Pichia pastoris* was shown to be most suitable, resulting in production of active recombinant enzyme (recAmPDH) with 30% glycosylation.<sup>44</sup> A further step in engineering of recAmPDH was achieved through enzymatic deglycosylation of the overglycosylated enzyme, which resulted in improved electrocatalytical performance of deglycosylated PDH compared to its glycosylated analogue.<sup>30–32</sup> Time-consuming and generally expensive production of enzymatically deglycosylated enzyme suggested that other approaches for engineering of PDH should be implemented. In the present study we utilise a novel approach for engineering PDH, based on a recent report,<sup>35</sup> as follows: asparagine residues (N) carrying the glycan moieties in the enzyme were first assigned using MALDI-MS measurements in combination with endoglycosidase treatment and tryptic digestion.<sup>35</sup> Three of the five possible glycosylation positions: N<sup>75</sup>, N<sup>175</sup> and N<sup>252</sup> were confirmed to carry carbohydrate moieties. Using site-directed mutagenesis it was then possible to exchange glycosylated asparagine (N) residues and express an enzyme in *Pichia pastoris* that lacks part of the glycosyl moiety. Two single mutant PDHs (mPDHs) (SM) with asparagine residues exchanged to glycine (G), N75G, and glutamine (Q), N175Q, one double mutant with N exchanged to G in N<sup>75</sup> and to Q in N<sup>175</sup> position (DM; N75G N175Q) and one triple mutant with N exchanged to G, Q and Q in positions N<sup>75</sup>, N<sup>175</sup> and N<sup>252</sup>, respectively (TM; N75G N175Q N252Q) were produced. In the work described herein all four mutants were electrochemically “wired” to three polyvinylimidazole-bound osmium complexes with different formal potentials ( $E^{\circ'}$  = 140 mV, 320 mV and 420 mV vs. NHE) and the electrocatalytic properties of the enzyme electrodes studied using flow-injection amperometry and cyclic voltammetry. The mPDHs were also directly adsorbed onto the working electrodes in order to study their ability to directly communicate with the electrode surface in a mediator-less mode.

### **Enzyme engineering**

Four mutant PDHs from *Agaricus meleagris* were recombinantly expressed in *Pichia pastoris* (volumetric activity 0.1–0.4 U mL<sup>-1</sup>; specific activity 0.3–3.7 U mg<sup>-1</sup>, protein concentration 0.03–0.8

mg mL<sup>-1</sup>). The enzymes were stored at -20 °C in order to preserve their catalytic activity and were slowly thawed on ice prior to analysis. The volumetric activity of the mutants was determined on a UV-2401 PC spectrophotometer (Shimadzu Deutschland GmbH, Duisburg, Germany) at 20 °C in the presence of ferricinium (Fc<sup>+</sup>) as electron acceptor and glucose as substrate.<sup>45</sup> One unit of enzyme activity was equal to the amount of enzyme required for reduction of 2 µmol of Fc<sup>+</sup> per 1 min at 20 °C.

Oligonucleotides were synthesised by VBC Biotech (Vienna, Austria) and polymerase chain reactions were conducted in a BioRad (Hercules, CA, USA) C1000 Thermal Cycler. Molecular biology reagents were obtained from Thermo Scientific (Waltham, MA, USA) and used according to the manufacturer's recommendations. Chemically competent *E. coli* NEB5α from New England Biolabs (Ipswich, MA, USA) was used for vector constructions and *P. pastoris* X33 from Invitrogen (Carlsbad, CA, USA) for expression. Chromatography resins were purchased from GE Healthcare (Little Chalfont, UK). Endo Hf (1 000 000 U mL<sup>-1</sup>; 232 000 U mg<sup>-1</sup>) was supplied by New England Biolabs (Ipswich, MA, USA).

### Site saturation and site directed mutagenesis

Numbering of amino acid residues refers to the mature protein starting with the sequence AITYQ.<sup>46</sup> The site saturation mutagenesis library was created using Phusion PCR polymerase (Thermo Scientific) according to the manufacturer's recommendations and the oligonucleotide primers fwAmPDHN75 and rvAmPDHN75X (Table S1, ESI†). Chemically competent *E. coli* NEB5α was transformed with the DpnI digested amplicon. All transformants were washed from the plate surface with 5 mL of LB medium containing 25 mg mL<sup>-1</sup> Zeocin™ and the suspension was incubated for 90 min at 37 °C on a shaker. Recovered plasmids were linearised with MssI and electroporated into *P. pastoris* X33 according to the manufacturer's recommendations. Two hundred clones were picked for 96-deep-well plate expression as described by Sygmund et al.<sup>36</sup> The supernatant was screened for enzymatic activity with Fc<sup>+</sup> and 2,6-dichlorophenolindophenol (DCIP) in 96-well plates.

Overlap extension PCR was used for site directed mutagenesis. Two amplicons were generated using Phusion DNA polymerase (Thermo Scientific) and one mutating oligonucleotide (Table S2, ESI†) with the complementary AOX oligonucleotide each (3'AOX: 5'-GCAAATGGCATTCTGACATCC-3', 5'AOX: 5'-GACTGGTTCCAATTGACAAG-3'). In a subsequent polymerase chain reaction with 5'AOX and 3'AOX the two amplicons were fused. The resulting DNA fragment was ligated into the XbaI and KpnI restriction sites of pPICZ-B. The vector was amplified in *E. coli* NEB5α, recovered and electroporated into *P. pastoris* according to the manufacturer's recommendations.

AmPDH1 [GeneBank: AY753307.1] glycosylation sites were previously predicted from the sequence in silico. Five consensus sites NXS/T are found, one (N<sup>313</sup>) is ruled out by the presence of proline at the middle position, another one (N<sup>319</sup>) was judged to have a low probability of glycosylation by the

prediction software NetNGlyc 1.0. Positions N<sup>75</sup>, N<sup>175</sup> and N<sup>252</sup> were since confirmed by mass spectrometry analysis of tryptic fragments.<sup>35</sup> The locations of these sites, and of the additional site at N<sup>319</sup>, are shown in Fig. 1a, based on the *AmpDH1* crystal structure.<sup>42</sup> N<sup>319</sup> is located in a surface cavity but the other sites are well exposed. N<sup>75</sup> is located next to the largest active site access and close to the covalently bound catalytic co-factor FAD. N<sup>175</sup> is situated on the other side of the active site access. The fragmentation site into the ~46 kDa and ~20 kDa fragments is between residues 416 and 417, positioned between N<sup>75</sup> (~34 Å away) and N<sup>175</sup> (~24 Å away) (Fig. 1b). N<sup>252</sup> is on the far side of the protein. N<sup>75</sup> and N<sup>175</sup> were selected for elimination due to the expected effect of reducing the distance from the active site and the FAD co-factor to the electrode surface when the enzyme is immobilised on the electrode. The third site, N<sup>252</sup>, was eliminated to additionally reduce the overall size of the enzyme. The *AmpDH1* N75X site saturation mutagenesis library was created from *Ampdh1* in pPICZ-B (Invitrogen, Life Technologies) with the primers fw*AmpDHN75* and rv*AmpDHN75X*. 10% of the screened clones expressed active PDH and were rescreened in triplicates, and 14 mutants with expression of active enzyme were sequenced. Half of the clones were wild type, while the others were mutated to N75G, Q, K or H. These four mutants were expressed in shake flasks with *AmpDH1* wild type (wt) as positive control and purified in a simplified 2-step chromatography scheme (Table S1, ESI†). *AmpDH1* N75G showed the best expression at almost wild type levels and was chosen for further study. The other N-glycosylation site mutants were constructed by site directed mutagenesis (Table S2, ESI†). *AmpDH1* N75G/N175Q could be expressed in shake flasks to twice the volumetric activity of *AmpDH1* N75G/N175G. Gln was therefore chosen as replacement for Asn at N<sup>175</sup> and N<sup>252</sup>.

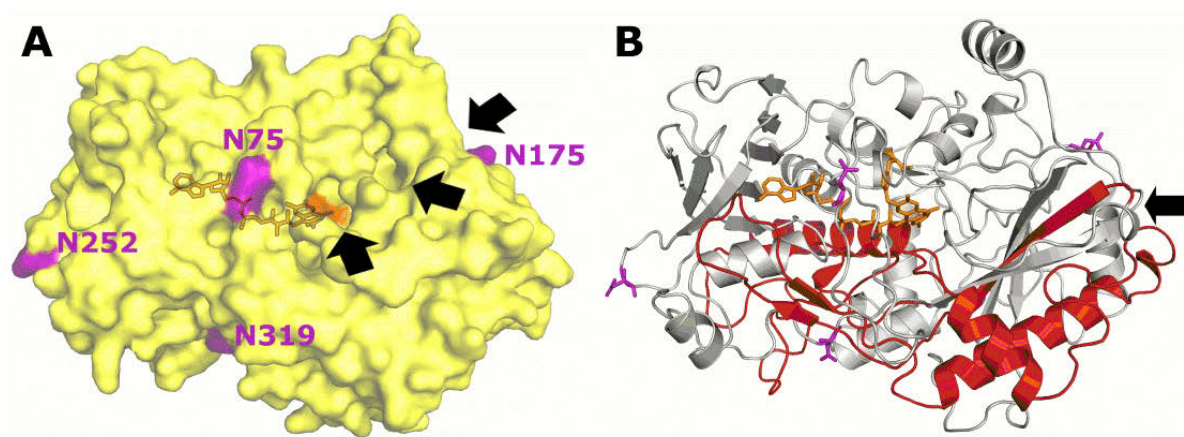


Fig. 1 *AmpDH1* X-ray crystal structure (Tan et al. 2013), the FAD co-factor shown as stick structure and N-glycosylated Asn in purple. (a) Black arrows indicate access to the active site. (b) Cleavage position (arrow) of ~46 kDa (grey) and C-terminal ~20 kDa fragment (red).

### **Expression and purification of *A. meleagris* pyranose dehydrogenase 1 in *P. pastoris***

Methanol induced expression in *P. pastoris* was done according to the Invitrogen “Pichia Fermentation Process Guidelines” in a 5 L stirred-tank bioreactor (MBR, Wetzikon, Switzerland) (see ESI†).

The enzyme was purified from the harvested supernatant by salt precipitation ((NH<sub>4</sub>)<sub>2</sub>SO<sub>4</sub>) followed by hydrophobic interaction chromatography at room temperature (750 mL of Phenyl-Sepharose fast flow, 15 mL min<sup>-1</sup>). The eluted fractions of the enzyme were subjected to buffer exchange with Bis-Tris buffer (50 mM, pH 6.5) and subsequent anion exchange chromatography (60 mL of DEAE-Sepharose fast flow, 10 mL min<sup>-1</sup>) was conducted. The fractions with high enzyme activity were pooled and subjected to a second purification step, which included salt precipitation and hydrophobic interaction chromatography. The resulting fractions were pooled for highest specific activity, washed with sodium phosphate buffer (50 mM, pH 6.5) and concentrated by ultracentrifugation (10 kDa Amicon Ultra-15 Centrifugal Filter Units, Millipore Corp.). If necessary, the resulting enzyme solution was further purified by gel filtration (180 mL of Superose12, 1 mL min<sup>-1</sup>). Purified and concentrated enzyme solutions were stored at -20 °C.

The recombinant expression of N-glycosylation site mutants and the wt enzyme were compared in simultaneous expression in an Infors HT Multifors 6 × 0.5 L bioreactor system, according to the Invitrogen “Pichia Fermentation Process Guidelines”. Wet biomass, protein concentration and enzyme activity at standard conditions were determined (see ESI†).

### **Expression of *AmPDH1* N-glycosylation mutants**

The single mutant N75G and the multiple mutants N75G/N175Q (DM) and N75G/N175Q/N252Q (TM) were expressed in *P. pastoris* in Infors HT Multifors bioreactors in parallel and in three repeats to compare expression efficiency (Fig. 2). Due to limitations in the aeration with pressurised air, oxygen supply was limited in the bioreactors and a methanol feed rate of 0.4 mL h<sup>-1</sup> could not be exceeded. There was no significant difference in the protein concentration in the supernatant between wild type and mutant PDH producers after 96 h. *AmPDH1* N75G showed a similar volumetric activity yield as that of the wild type, whereas *AmPDH1* DM and TM had a lower volumetric activity yield of ~50% of that of the wild type (Fig. 2).

The not optimised expression yielded 0.1–0.4 U mL<sup>-1</sup> (0.3–3.7 U mg<sup>-1</sup>) in the supernatant. Purification was done by a 3-step chromatography scheme (Phenyl-Sepharose, DEAE-Sepharose, Phenyl-Source), whereas *AmPDH1* DM was polished in an additional gel filtration step with Superose12 resin (Table S3, ESI†). An eight- to 115-fold increase in specific activity could be achieved with a purification

yield of 11–30%, due to strict pooling. In parallel production experiments of mutant enzymes with wild type enzyme, the single mutation N75G had no significant impact on expression efficiency. The mutation at N<sup>175</sup> in *AmPDH1* DM, however, decreased the volumetric and specific yield by half. An additional mutation at N<sup>252</sup> in *AmPDH1* TM did not lead to a further decrease in yield. The single mutation N175Q showed an ambiguous picture with expression levels between wt/N75G and *AmPDH1* DM (data not shown). This suggests a different importance of the particular glycosylation sites, in this case namely that position N<sup>175</sup> requires intact N-glycosylation for proper folding and/or secretion of the enzyme. *AmPDH1* N175Q, DM and TM showed sufficient expression levels in 5 L stirred-tank bioreactors and *AmPDH1* N75G in shake flasks (0.1–0.4 U mL<sup>-1</sup>) for subsequent characterisation of the purified enzyme.

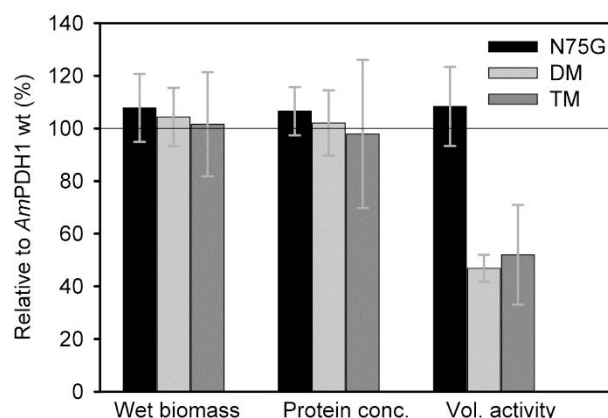


**Fig. 2** Recombinant expression of *AmPDH1* N75G, DM, TM and wt in *P. pastoris* in Infors Multifors bioreactor: wet biomass, protein concentration and volumetric activity after 96 h relative to the wild type reference.

### Protein characterisation

The fragmentation of purified *AmPDH1* into a ~46 kDa and a ~20 kDa fragment (observed on SDS-PAGE) was described by Sygmond et al.<sup>36</sup> Yakovleva et al.<sup>35</sup> observed complete fragmentation of enzymatically deglycosylated *AmPDH1* (dg*AmPDH1*) within 2 months at 4 °C, with a concomitant ~6-fold increase in specific activity. All tested *AmPDH1* N-glycosylation mutants also formed these two fragments in a glycosylation-dependent pattern (Fig. S1, ESI†). *AmPDH1* DM and TM were fragmented to a large degree immediately after purification, and completely within 1–2 months, and showed an increase in specific activity similar to dg*AmPDH1*. *AmPDH1* N175Q fragmentation was slower with a less pronounced activity increase, and *AmPDH1* wt and N75G only started to fragment in this time frame without any increase in specific activity. As observed for expression efficiency, there is no significant effect by the mutation of N<sup>75</sup> alone, a larger influence of N<sup>175</sup> alone, and a significant effect to levels observed for dg*AmPDH1* by a combination of these two mutations. A third

mutation, eliminating the distant site 252, does not increase any of the observed effects further. Therefore, the N-glycosylation sites in proximity to the active site appear to influence correct folding and expression/secretion efficiency. The mechanism of cleavage at S416/Y417 is not known and appears to be a spontaneous or autocatalytic process, as it is observed in protein preparations that are purified to homogeneity. It has to be noted that, despite the appearance of two distinct fragments originating from the same protein on SDS-PAGE (confirmed by peptide sequencing, not shown), an actual separation of the two fragments is highly unlikely, if not impossible, as the smaller fragment contains amino acids considered essential to catalysis.<sup>47</sup> Mass spectrometric investigation of the mutants, including DM and TM, also did not reveal any large missing fragments (not shown). This indicates that the peptide chain is “nicked” upon storage, but the two fragments remain attached to each other, as is suggested by their close interaction (Fig. 1b), and only separate under denaturing conditions. Nevertheless, the presence of glycosyl moieties on the two N-glycosylation sites in near vicinity, particularly the closest one, exerts a strong influence. It is also interesting to note that the elimination of one and two glycosylation sites (N<sup>75</sup>, N<sup>175</sup>, or both) does not visibly reduce the molecular mass of the purified protein, suggesting heavier glycosylation of the remaining site(s). Only knock-out of N<sup>75</sup>, N<sup>175</sup> and N<sup>252</sup> results in a sharp band at ~65 kDa on the SDS-PAGE, indistinguishable from the enzymatically deglycosylated wt *AmPDH1*.

## **Electrochemical methods**

All chemicals were purchased from Sigma-Aldrich Chemie GmbH (Steinheim, Germany) if not stated otherwise. Synthesis of osmium redox polymers: [Os(dmoby)<sub>2</sub>(PVI)<sub>10</sub>Cl]<sup>+2/+</sup> ( $E^{\circ'} = 140$  mV vs. NHE), [Os(dmbpy)<sub>2</sub>(PVI)<sub>10</sub>Cl]<sup>+2/+</sup> ( $E^{\circ'} = 320$  mV vs. NHE) and [Os(bpy)<sub>2</sub>(PVI)<sub>10</sub>Cl]<sup>+2/+</sup> ( $E^{\circ'} = 420$  mV vs. NHE), where dmoby is 4,4'-dimethoxy-2,2'-bipyridine, dmbpy is 4,4'-dimethyl-2,2'-bipyridine, bpy is 2,2'-bipyridine, and PVI is poly(N-vinylimidazole), was performed according to the protocol described in.<sup>48,49</sup> The osmium polymers were dissolved in deionised water to obtain a concentration of 5 mg mL<sup>-1</sup>. Sodium phosphate buffer with a total phosphate concentration of 50 mM (pH 7.4) containing 137 mM NaCl was used throughout all experiments. It was degassed prior to the measurements in order to avoid bubble formation in the FIA system. Calibration solutions of D(+)-glucose were prepared daily by diluting a 40 mM stock solution with buffer. All aqueous solutions were prepared using deionised water purified with a Milli-Q purification system (EMD Millipore Corporation, Billerica, MA, USA).

## **Preparation of enzyme-modified graphite electrodes**

The electrodes were prepared from graphite rods with a diameter of 3.05 mm and 13% porosity (Ringsdorff Werke GmbH, Bonn, Germany). Rods were cut into 3 cm pieces, polished on wet emery

paper (grit number P1200), washed with water and dried in an air flow prior to modification. For chemical cross-linking poly(ethyleneglycol)(400)diglycidyl ether (PEGDGE) was diluted to a final concentration of 68% (v/v) with deionised water. Two microliters of PEGDGE solution were then mixed with 5  $\mu\text{L}$  of Os-polymer solution on the surface of the graphite electrode and left for 10 min before drop-coating of the enzyme. Five microliter of each enzyme solution (N75G: 26.3 mg  $\text{mL}^{-1}$ /1440 U  $\text{mL}^{-1}$ ; N175Q: 24.1 mg  $\text{mL}^{-1}$ /1103 U  $\text{mL}^{-1}$ ; DM: 17.0 mg  $\text{mL}^{-1}$ /624 U  $\text{mL}^{-1}$ ; TM: 16.1 mg  $\text{mL}^{-1}$ /820 U  $\text{mL}^{-1}$ ) were added to the mixture of PEGDGE-Os-polymer and left overnight at 4  $^{\circ}\text{C}$  in a humid atmosphere for completion of cross-linking. For direct electron transfer (DET) experiments 5  $\mu\text{L}$  of solutions containing the various mPDHs were directly drop-coated onto the surface of working electrodes and stored overnight under the same conditions as described for mediated electron transfer (MET). The modified electrodes were rinsed with the running buffer prior to the measurements in order to remove loosely attached material. All experiments were performed at room temperature.

### Flow-injection amperometry

The current response of the enzyme-modified electrodes towards the substrate (glucose) was measured using a flow-injection (FI) system described elsewhere.<sup>50,51</sup> The electrodes were pressfitted into a teflon holder and mounted into a wall-jet type flow-through electrochemical cell.<sup>52</sup> The graphite rods served as the working electrode, an Ag|AgCl (0.1 M KCl, 288 mV vs. NHE) as the reference electrode and a platinum wire as the counter electrode. A constant potential was applied onto the working electrode controlled by a three-electrode potentiostat (Zäta Electronics, Höör, Sweden). Glucose solutions of different concentrations (50  $\mu\text{l}$  volume) were introduced into the system by a six-port injection valve (Rheodyne, type 7125 LabPR, Cotati, CA, USA) at a constant flow rate of 0.5  $\text{mL min}^{-1}$  controlled by a peristaltic pump (Minipuls 3, Gilson, Villier-le Bel, France). The change in current was then registered with a BD 112 recorder (Kipp & Zonen, Utrecht, The Netherlands). The concentrations of all injected samples were corrected for a dispersion factor of the FI system equal to 1.08. Values for the apparent Michaelis–Menten constant ( $K^{\text{app}}_{\text{M}}$ ) and saturating current densities ( $J_{\text{max}}$ ) were obtained by fitting the data with the Michaelis–Menten equation.

### Cyclic voltammetry

All voltammograms were recorded using a BAS CV-50W potentiostat (Bioanalytical Systems, West Lafayette, IN, USA) in 50 mM phosphate buffer at pH 7.4 (137 mM NaCl) at room temperature in the absence of oxygen. The response to 25 mM glucose was measured with the enzyme-modified graphite electrodes at a scan rate of 1 or 5  $\text{mV s}^{-1}$ . A saturated calomel electrode (244 mV vs. NHE) was used as the reference electrode and a platinum foil as the counter electrode.

## **Results and discussion**

### **Catalytic performance of Os-polymer/mPDH-modified electrodes**

In our recently reported study the glycosylation positions in PDH were assigned using MALDI-MS in combination with Endo H treatment and tryptic digestion.<sup>35</sup> The obtained information was used for production of the mPDHs lacking part of the glycosylation. This was accomplished by destroying a typical glycosylation pattern N-X-S/T/C (where X can be any amino acid except for proline<sup>53</sup>) in the protein polypeptide chain. N in the tripeptide consensus sequon was exchanged to either G or Q and two single, one double and one triple mPDH with different degrees of deglycosylation were engineered. The study of the use of these enzymes focuses on their bioelectrochemical characterisation when co-immobilised with the polyvinylimidazole-bound Os-complexes exhibiting different  $E^{\circ'}$ -values defined by the electron donating/accepting radical in the 4,4'-position of the 2,2'-bipyridine ligands of the polymer.<sup>48</sup> For provision of anodes for EBFCs, redox polymers demonstrating glucose oxidation at lower redox potentials provide the possibility of power production at higher overall cell voltages.<sup>54,55</sup> However, this advantage may be offset by the loss in catalysis as the redox potential approaches the potential of the PDH active site.<sup>18</sup> The applied potential for characterisation of the mediator/enzyme couples was selected based on previously reported data.<sup>30–32,35,43</sup> Os(dmoby)PVI/mPDH-modified electrodes were characterised at an applied potential of 288 mV vs. NHE, at which a steady state current is obtained. An applied potential of 444 mV vs. NHE was selected for electrodes coated with Os(dmbpy)PVI/mPDH and Os(bpy)PVI/mPDH.

The electrocatalytic response of the films containing the different Os-polymer/mPDHs couples to glucose were measured in the flow injection system in 50 mM phosphate buffer pH 7.4 (137 mM NaCl) (Fig. S2, ESI<sup>†</sup>). The current densities obtained for the oxidation of glucose by the mPDHs-containing films increase with a shift in  $E^{\circ'}$ -values of the Os-polymer towards more positive values as a function of the ligand used: Os(dmoby)PVI < Os(dmbpy)PVI < Os(bpy)PVI (Table 1).

This result is expected considering that the driving force for electron transfer is increasing with the increase in potential difference between the bound FAD of mPDH and the Os-polymer. Maximum response is obtained for each of the mPDHs electrochemically “wired” with the Os(bpy)PVI-based polymer. The  $K^{\text{app}}_{\text{M}}$ -values obtained from the curve fitting of the results are displayed in Table 1 and the smallest  $K^{\text{app}}_{\text{M}}$ -values are obtained for the electrodes containing mPDH “wired” to the Os(dmoby)PVI polymer exhibiting the lowest  $E^{\circ'}$ .

The CVs recorded in the absence of substrate (Fig. 3) indicate that films of the DM and TM enzyme contain approximately half the amount of redox-active polymer compared to films of the N75G and N175Q enzyme, whilst providing higher maximum current densities (Table 1). Osmium coverage

alone therefore does not determine glucose oxidation current response. The cyclic voltammetry results presented in Fig. 3 are in a good agreement with the FIA data (Fig. S2, ESI†).

**Table 1** Summary of kinetic data obtained in the flow mode using Os-polymer/mPDH- and mPDH-modified electrodes

Type of ET <sup>a</sup>		MET			DET
mPDH	Kin. param. <sup>b</sup>	Os(dmoby)-PVI	Os(dmbpy)-PVI	Os(bpy)-PVI	-
N75G	$J_{\max}/\mu\text{A cm}^{-2}$	$0.5 \pm 0.02$	$2.5 \pm 0.09$	$22.2 \pm 1.8$	$1 \pm 0.06$
N175Q		$6.2 \pm 0.2$	$20.9 \pm 0.7$	$152.7 \pm 2.8$	$1.8 \pm 0.05$
DM		$9.8 \pm 0.3$	$290.1 \pm 15.9$	$802.4 \pm 101.07$	$7.8 \pm 0.7$
TM		$35.2 \pm 0.5$	$51.7 \pm 0.6$	$215 \pm 2.5$	$6.6 \pm 0.2$
N75G	$K^{\text{app}}_{\text{M}}/\text{mM}$	$1.9 \pm 0.1$	$5.9 \pm 0.2$	$6.7 \pm 0.1$	$4.5 \pm 0.4$
N175Q		$0.7 \pm 0.1$	$3.8 \pm 0.4$	$7.6 \pm 1.3$	$2.1 \pm 0.4$
DM		$0.2 \pm 0.06$	$2.1 \pm 0.2$	$1.7 \pm 0.1$	$5.2 \pm 0.4$
TM		$0.7 \pm 0.1$	$4.4 \pm 0.6$	$10.2 \pm 2.4$	$3.9 \pm 0.9$

<sup>a</sup> ET – electron transfer. <sup>b</sup> Kin. param. – kinetic parameter.

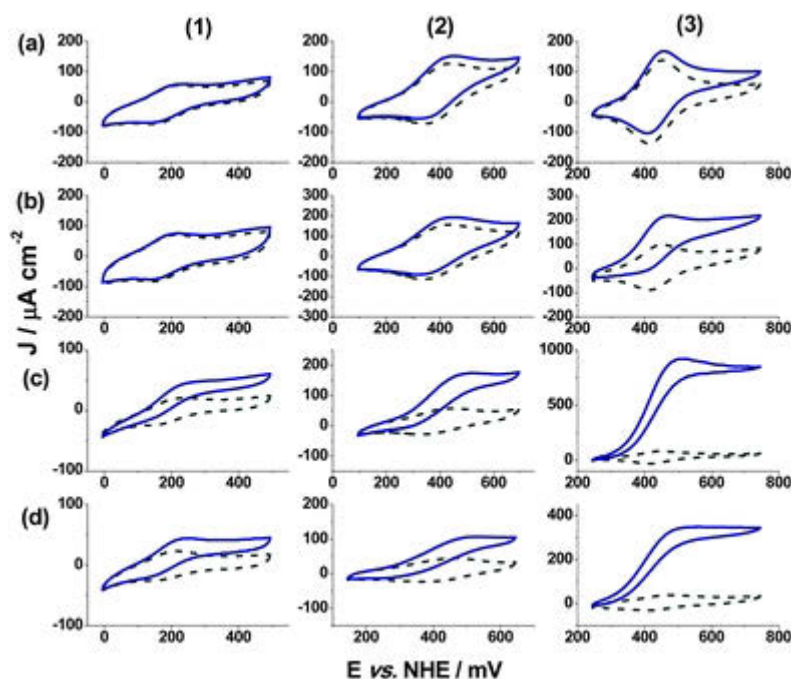


**Fig. 3** Cyclic voltammograms of a series of Os-polymer/mPDH-drop-coated graphite electrodes recorded at a scan rate of  $1 \text{ mV s}^{-1}$  in 50 mM phosphate buffer (137 mM NaCl, pH 7.4) in inert atmosphere in (grey dotted line) the absence and (blue solid line) the presence of 25 mM glucose: (a) N75G-; (b) N175Q-; (c) DM-; (d) TM-modified electrodes. Os-polymers used for cross-linking with various mPDHs: (1) Os(dmoby)PVI-; (2) Os(dmbpy)PVI-; (3) Os(bpy)PVI-based polymer.

When comparing the various mPDHs a clear correlation between the electrocatalytic response and the degree of deglycosylation can be observed for the SMs and the DM (Fig. 3 and Fig. S2, ESI†). The DM co-immobilised with the different Os-polymers generates current densities greater than those obtained for either of the SMs covalently bound to the corresponding Os-polymers. The concentration in terms of  $\text{mg mL}^{-1}$  is higher for the SMs (N75 g:  $26.3 \text{ mg mL}^{-1}$ ; N175Q:  $24.1 \text{ mg mL}^{-1}$ ) than for the DM ( $17.0 \text{ mg mL}^{-1}$ ) and the TM ( $16.1 \text{ mg mL}^{-1}$ ). Even though the specific activity of the enzyme solutions (N75G:  $1440 \text{ U mL}^{-1}$ ; N175Q:  $1103 \text{ U mL}^{-1}$ ; DM:  $624 \text{ U mL}^{-1}$ ; TM:  $820 \text{ U mL}^{-1}$ ) is around twice as high for the SMs, the current densities obtained for the oxidation of glucose increase in the following order:  $\text{N75} < \text{N175} < \text{DM}$  (Table 1). The explanation may be that the electron transfer rate between the two electroactive species is increased by bringing them closer to each other.<sup>23</sup> The glycan shell of DM is smaller than that of the SMs. Therefore, the active site of the DM is more accessible to be “wired” to the Os-polymer compared to mPDHs with a higher glycosylation degree and the electron transfer will hence become faster.

Taking these observations into consideration, it is expected that the TM should outperform both the DM and the SMs when “wired” with the various Os-polymers, because the TM has less carbohydrates attached to its polypeptide chain. Surprisingly, the opposite effect is observed. Analysis of the biological functions of carbohydrates indicates that the latter play an important role in the physical maintenance and the catalytic performance of the whole glycoprotein. Moreover, it is difficult to predict a priori an effect of elimination of the glycan on the properties of the glycoprotein.<sup>56</sup> This may explain why the DM shows much better catalytic response to glucose compared to the TM in both flow injection and cyclic voltammetric measurements, when the same mass of enzymes is co-immobilised with the mediator on the surface of the working electrodes. Apparently, glycosylation in N<sup>252</sup> is needed for retaining a high activity of mPDH using the osmium polymers as mediators, and exchanging N to Q in the protein polypeptide chain does not further improve the catalytic efficiency of mPDH.

The onset of the oxidation current is observed for all of the enzyme electrodes starting at a potential close to the  $E^{\circ'}$  of each redox polymer. The films modified with cross-linked Os(bpy)PVI/DM display the highest current densities (Table 1) compared to the other mPDHs prepared using the same redox polymer. With an increase in  $E^{\circ'}$  of the mediator the catalytic response of the Os-polymer/mPDH-modified electrodes becomes more clearly observed in the cyclic voltammograms, as expected considering the increase in the thermodynamic driving force of the electron transfer reaction.

The performance of the Os(dmbpy)PVI/DM electrode exhibiting the highest response to glucose in the FI and the CV studies was compared with the previously reported data on films prepared by co-immobilisation of an Os-polymer with enzymatically deglycosylated recombinantly expressed

*Am*PDH (dgPDH)<sup>31,32</sup> or the more active fragmented form of the same enzyme (fdgPDH).<sup>35</sup> Equal mass amounts of the enzyme, mediator and cross-linker were utilised for drop-coating onto the electrodes and the obtained films were screened under similar experimental conditions (buffer composition, applied potential, glucose as a substrate). The Os(dmbpy)PVI/DM-based films reported here produce a higher catalytic response ( $J_{\max} = 290 \mu\text{A cm}^{-2}$ ) compared to the  $J_{\max}$  of  $146 \mu\text{A cm}^{-2}$  and  $248 \mu\text{A cm}^{-2}$  for the Os(dmbpy)PVI/dgPDH- and the Os(dmbpy)PVI/fdgPDH-based films, respectively.<sup>32,35</sup>

Comparison with results of other sugar-oxidising enzyme electrodes is difficult due not only to considerable differences in the testing conditions such as glucose concentration, temperature and pH selected, but also to the effect of the electrode preparation methodologies, variability in experimental approaches and the method used to measure current density. For example, Murata et al.<sup>57</sup> recently reported that deglycosylated FAD-dependent glucose dehydrogenase from *Aspergillus terreus*, co-immobilised, through diepoxide crosslinking with an Os-polymer on glassy carbon electrodes, rotated at 5000 rpm, yields glucose oxidation current densities of  $0.95 \text{ mA cm}^{-2}$  and  $4 \text{ mA cm}^{-2}$  in 5 mM and 200 mM glucose, respectively, at 0.5 V vs. Ag|AgCl in pH 7.0 buffered solution at 25 °C.

Due to the drawbacks associated with general use of mediators,<sup>2,3,9</sup> DET approach for construction of bioanodes and cathodes is quite appealing. In the present study current output from mPDH-modified electrodes was studied using CV and FI (see ESI†). Although all of the films containing mPDHs possess an ability to directly communicate with the electrode surface, DET takes place at high overpotentials and current densities produced are much lower in comparison with the MET mode (Fig. S3 and S4, ESI†). Therefore, application of mPDH-modified films in fabrication of bioanodes is still limited.

## **Conclusions**

A number of recombinantly expressed mPDHs with different degrees of glycosylation produced by site-directed mutagenesis are screened in order to select the mutant enzyme exhibiting properties required for further application in the fabrication of bioanodes. The enzymes are co-immobilised with Os(dmoby)PVI, Os(dmbpy)PVI and Os(bpy)PVI-based redox polymers ranging in  $E^{\circ'}$  and co-precipitated on the surface of graphite working electrodes. An equal mass of all film components is utilised for electrode preparation and comparison. The Os-polymer/mPDH-modified film electrodes are characterised using flow-injection amperometry and CV. The Os(bpy)PVI/DM-based films reported here produce the higher catalytic response ( $J_{\max} = 802 \mu\text{A cm}^{-2}$ ) compared to those films prepared using the Os-polymers with a lower  $E^{\circ'}$  and with a different degree of glycosylation. The greater current densities generated by those biocatalytic films containing DM co-immobilised with

Os(bpy)PVI and the less laborious and relatively fast production of the enzyme makes it easier to integrate the enzyme into an EBFC.

All forms of the mutant enzyme possess an ability to directly communicate with the electrode surface with DM having the highest and the most stable current response to glucose ( $J_{\max} = 7.8 \mu\text{A cm}^{-2}$ ).

## **Acknowledgements**

The following agencies are acknowledged for financial support: CKP, The Austrian Science Fund FWF (grant TRP218); CG, The Austrian Science Fund FWF (CG is a member of the doctoral program Biomolecular Technology of Proteins, grant W1224); LG and MY, The Swedish Research Council, grant 2010-5031; LG and DL The European Commission “Bioenergy” FP7-PEOPLE-2013-ITN-607793.

## **References**

1. S. C. Barton, J. Gallaway and P. Atanassov, *Chem. Rev.*, 2004, 104, 4867–4886.
2. M. T. Meredith and S. D. Minter, in *Annual Review of Analytical Chemistry*, ed. R. G. Cooks and E. S. Yeung, *Annual Reviews*, Palo Alto, 2012, vol. 5, pp. 157–179.
3. D. Leech, P. Kavanagh and W. Schuhmann, *Electrochim. Acta*, 2012, 84, 223–234.
4. Y. Liu, Y. Du and C. M. Li, *Electroanalysis*, 2013, 25, 815–831.
5. Y. Song, V. Penmasta and C. Wang, in *Biofuel's Engineering Process Technology*, ed. M. A. D. S. Bernardes, 2011, ch. 28, pp. 657–684.
6. S. A. Neto, J. C. Forti and A. R. De Andrade, *Electrocatalysis*, 2010, 1, 87–94.
7. P. Kavanagh and D. Leech, *Phys. Chem. Chem. Phys.*, 2013, 15, 4859–4869.
8. M. Falk, C. W. Narváez Villarrubia, S. Babanova, P. Atanassov and S. Shleev, *ChemPhysChem*, 2013, 14, 2045–2058.
9. M. Falk, Z. Blum and S. Shleev, *Electrochim. Acta*, 2012, 82, 191–202.
10. W. Greatbatch and C. F. Holmes, *Pacing Clin. Electrophysiol.*, 1992, 15, 2034–2036.
11. N. Mano, *Chem. Commun.*, 2008, 2221–2223.
12. A. Heller, *J. Phys. Chem.*, 1992, 96, 3579–3587.
13. A. Heller, *Phys. Chem. Chem. Phys.*, 2004, 6, 209–216.
14. A. Heller, *Curr. Opin. Chem. Biol.*, 2006, 10, 664–672.
15. A. Heller, *Anal. Bioanal. Chem.*, 2006, 385, 469–473.
16. A. Heller and B. Feldman, *Chem. Rev.*, 2008, 108, 2482–2505.
17. D. MacAodha, P. ÓConghaile, B. Egan, P. Kavanagh, C. Sygmund, R. Ludwig and D. Leech, *Electroanalysis*, 2013, 25, 94–100.

18. F. Tasca, L. Gorton, M. Kujawa, I. Patel, W. Harreither, C. K. Peterbauer, R. Ludwig and G. Nöll, *Biosens. Bioelectron.*, 2010, 25, 1710–1716.
19. F. Tasca, L. Gorton, W. Harreither, D. Haltrich, R. Ludwig and G. Nöll, *J. Phys. Chem. C*, 2008, 112, 13668–13673.
20. F. Barriere, P. Kavanagh and D. Leech, *Electrochim. Acta*, 2006, 51, 5187–5192.
21. P. Kavanagh, S. Boland, P. Jenkins and D. Leech, *Fuel Cells*, 2009, 9, 79–84.
22. O. Courjean, V. Flexer, A. PrévotEAU, E. Suraniti and N. Mano, *ChemPhysChem*, 2010, 11, 2795–2797.
23. R. A. Marcus and N. Sutin, *Biochim. Biophys. Acta*, 1985, 811, 265–322.
24. E. E. Ferapontova, V. G. Grigorenko, A. M. Egorov, T. Borchers, T. Ruzgas and L. Gorton, *Biosens. Bioelectron.*, 2001, 16, 147–157.
25. A. Lindgren, M. Tanaka, T. Ruzgas, L. Gorton, I. Gazaryan, K. Ishimori and I. Morishima, *Electrochem. Commun.*, 1999, 1, 171–175.
26. S. Demin and E. A. H. Hall, *Bioelectrochemistry*, 2009, 76, 19–27.
27. A. PrévotEAU, O. Courjean and N. Mano, *Electrochem. Commun.*, 2010, 12, 213–215.
28. R. Ortiz, H. Matsumura, F. Tasca, K. Zahma, M. Samejima, K. Igarashi, R. Ludwig and L. Gorton, *Anal. Chem.*, 2012, 84, 10315–10323.
29. S. C. Feifel, R. Ludwig, L. Gorton and F. Lisdat, *Langmuir*, 2012, 28, 9189–9194.
30. M. E. Yakovleva, A. Killyéni, R. Ortiz, C. Schulz, D. MacAodha, P. ÓConghaile, D. Leech, I. C. Popescu, C. Gonaus, C. K. Peterbauer and L. Gorton, *Electrochem. Commun.*, 2012, 24, 120–122.
31. A. Killyéni, M. E. Yakovleva, D. MacAodha, P. ÓConghaile, C. Gonaus, R. Ortiz, D. Leech, I. C. Popescu, C. K. Peterbauer and L. Gorton, *Electrochim. Acta*, 2014, 126, 61–67.
32. A. Killyéni, M. E. Yakovleva, C. K. Peterbauer, D. Leech, L. Gorton and I. C. Popescu, *Stud. Univ. Babeş-Bolyai, Chem.*, 2012, 57, 87–99.
33. M. Shao, M. N. Zafar, C. Sygmund, D. A. Guschin, R. Ludwig, C. K. Peterbauer, W. Schuhmann and L. Gorton, *Biosens. Bioelectron.*, 2013, 40, 308–314.
34. M. Shao, M. N. Zafar, M. Falk, R. Ludwig, C. Sygmund, C. K. Peterbauer, D. A. Guschin, D. MacAodha, P. ÓConghaile, D. Leech, M. D. Toscano, S. Shleev, W. Schuhmann and L. Gorton, *ChemPhysChem*, 2013, 14, 2260–2269.
35. M. E. Yakovleva, A. Killyéni, O. Seubert, P. ÓConghaile, D. MacAodha, D. Leech, C. Gonaus, I. C. Popescu, C. K. Peterbauer, S. Kjellström and L. Gorton, *Anal. Chem.*, 2013, 85, 9852–9858.
36. C. Sygmund, R. Kittl, J. Volc, P. Halada, E. Kubátová, D. Haltrich and C. K. Peterbauer, *J. Biotechnol.*, 2008, 133, 334–342.
37. D. R. Cavener, *J. Mol. Biol.*, 1992, 223, 811–814.
38. C. K. Peterbauer and J. Volc, *Appl. Microbiol. Biotechnol.*, 2010, 85, 837–848.
39. W. Harreither, C. Sygmund, M. Augustin, M. Narciso, M. L. Rabinovich, L. Gorton, D. Haltrich and R. Ludwig, *Appl. Environ. Microbiol.*, 2011, 77, 1804–1815.
40. R. Ludwig, W. Harreither, F. Tasca and L. Gorton, *ChemPhysChem*, 2010, 11, 2674–2697.
41. R. Baron, C. Riley, P. Chenprakhon, K. Thotsaporn, R. T. Winter, A. Alfieri, F. Forneris, W. J. H. van Berkel, P. Chaiyen, M. W. Fraaije, A. Mattevi and J. A. McCammon, *Proc. Natl. Acad. Sci. U. S. A.*, 2009, 106, 10603–10608.
42. T. C. Tan, O. Spadiut, T. Wongnate, J. Sucharitakul, I. Kronendorfer, C. Sygmund, D. Haltrich, P. Chaiyen, C. K. Peterbauer and C. Divne, *PLoS One*, 2013, 8, e53567.

43. M. N. Zafar, F. Tasca, S. Boland, M. Kujawa, I. Patel, C. K. Peterbauer, D. Leech and L. Gorton, *Bioelectrochemistry*, 2010, 80, 38–42.
44. I. Pisanelli, M. Kujawa, D. Gschnitzer, O. Spadiut, B. Seiboth and C. Peterbauer, *Appl. Microbiol. Biotechnol.*, 2010, 86, 599–606.
45. M. Kujawa, J. Volc, P. Halada, P. Sedmera, C. Divne, C. Sygmund, C. Leitner, C. Peterbauer and D. Haltrich, *FEBS J.*, 2007, 274, 879–894.
46. R. Kittl, C. Sygmund, P. Halada, J. Volc, C. Divne, D. Haltrich and C. K. Peterbauer, *Curr. Genet.*, 2008, 53, 117–127.
47. I. Krondorfer, K. Lipp, D. Brugger, P. Staudigl, C. Sygmund, D. Haltrich and C. K. Peterbauer, *PLoS One*, 2014, 9, e91145.
48. R. J. Forster and J. G. Vos, *Macromolecules*, 1990, 23, 4372–4377.
49. E. M. Kober, J. V. Caspar, B. P. Sullivan and T. J. Meyer, *Inorg. Chem.*, 1988, 27, 4587–4598.
50. J. Ružička and E. H. Hansen, *Anal. Chim. Acta*, 1975, 78, 145–157.
51. K. Štulík and P. Pacáková, *Electroanalytical Measurements in Flowing Liquids*, John Wiley and Sons, New York, 1987
52. R. Appelqvist, G. Marko-Varga, L. Gorton, A. Torstensson and G. Johansson, *Anal. Chim. Acta*, 1985, 169, 237–247.
53. E. Bause, *Biochem. J.*, 1983, 209, 331–336.
54. P. ÓConghaile, D. MacAodha, B. Egan, P. Kavanagh and D. Leech, *J. Electrochem. Soc.*, 2013, 160, G3165–G3170.
55. D. MacAodha, P. ÓConghaile, B. Egan, P. Kavanagh and D. Leech, *ChemPhysChem*, 2013, 14, 2302–2307.
56. A. Varki, *Glycobiology*, 1993, 3, 97–130.
57. K. Murata, W. Akatsuka, T. Sadakane, A. Matsunaga and S. Tsujimura, *Electrochim. Acta*, 2014, 136, 537–541.

## **Chapter III**

### **Comprehensive analysis of *Agaricus meleagris* pyranose dehydrogenase N-glycosylation sites and the performance of partially non-glycosylated enzymes**

Christoph Gonaus,<sup>ad</sup> Daniel Maresch,<sup>b</sup> Katharina Schroppa,<sup>d</sup> Peter O'Conghaile,<sup>c</sup> Dónal Leech,<sup>c</sup> Lo Gorton,<sup>d</sup> Clemens K. Peterbauer<sup>a\*</sup>

<sup>a</sup> Department of Food Sciences and Technology, BOKU-University of Natural Resources and Life Sciences, Muthgasse 18, A-1190 Wien, Austria

<sup>b</sup> Department of Chemistry, BOKU-University of Natural Resources and Life Sciences, Muthgasse 18, A-1190 Wien, Austria

<sup>c</sup> School of Chemistry, National University of Ireland Galway, University Road, Galway, Ireland

<sup>d</sup> Department of Analytical Chemistry/Biochemistry and Structural Biology, Lund University, PO Box 124, SE-221 00 Lund, Sweden.

## **Abstract**

Pyranose Dehydrogenase 1 from the basidiomycete *Agaricus meleagris* (*AmPDH1*) is an oxidoreductase capable of oxidizing a broad variety of sugars. Due to this and its ability of dioxidation of substrates and no side production of H<sub>2</sub>O<sub>2</sub>, it is studied for use in enzymatic bio-fuel cells.

*In-vitro* deglycosylated *AmPDH1* as well as knock-out mutants of the N-glycosylation sites N<sup>75</sup> and N<sup>175</sup> near the active site entrance were previously shown to improve achievable current densities of graphite electrodes modified with *AmPDH1* and an osmium redox polymer acting as a redox mediator, up to 10-fold. For a better understanding of the role of N-glycosylation of *AmPDH1*, a systematic set of N-glycosylation site mutants was investigated in this work, regarding expression efficiency, enzyme activity and stability. Furthermore, the site specific extend of N-glycosylation was compared between native and recombinant *wild type AmPDH1*.

Knocking out the site N<sup>252</sup> prevented detectable enzyme overglycosylation on SDS-Page, but did not substantially alter enzyme performance on modified electrodes. This suggests that not the molecule size but other factors like accessibility of the active site improved performance of deglycosylated *AmPDH1*/Os-polymer modified electrodes. A fourth N-glycosylation site of *AmPDH1* could be confirmed by HPLC-ESI-MS at N<sup>319</sup>, which appeared to be conserved in related fungal pyranose dehydrogenases but not in other members of the glucose-methanol-choline oxidoreductase structural family. It was shown to be the only essential one for functional recombinant expression of the enzyme.

## **Abbreviations**

*AmPDH1*, *A. meleagris* pyranose dehydrogenase 1; AOX, alcohol oxidase; CDH, cellobiose dehydrogenase; GMC, glucose-methanol-choline; Fc<sup>+</sup>, ferrocenium hexafluorophosphate; FIA, flow injection analysis; GlcNAc, N-acetylglucosamine; GOx, glucose 1-oxidases; HexNAc, N-acetylhexosamine; PDH, pyranose dehydrogenase; P2O, pyruvate 2-oxidase

## **Introduction**

The secreted fungal oxidoreductase pyranose dehydrogenase (PDH; EC 1.1.99.29) was first described by Volc et al. [1], and the main variant from *Agaricus meleagris* (*AmPDH1*) by Sygmund et al. [2]. PDH oxidizes a broad range of mono- and disaccharides at C1-C4, depending on the substrate, and is capable of dioxidation. Quinones and metallo-complexes serve as electron acceptors but not molecular oxygen [3,4]. Its biological function is not well understood but hypothesized to include a role in fungal response against quinones used by plants as defence and in lignin degradation by reducing quinones [4].

PDH has been studied for use in carbohydrate chemistry and bioconversion [2,3,5,6] but also successfully wired to, and optimized on, modified electrodes for use in biosensors or in enzymatic bio-fuel cells [7–13]. In the latter case, electrodes are modified with oxidoreductases to generate electric current by oxidizing substrates at the anode while usually reducing molecular oxygen to water at the cathode. The broad substrate range, lack of production of H<sub>2</sub>O<sub>2</sub> and ability of dioxidation make PDH a promising candidate for the anodic half reaction [4]. Shao et al. [14] reported a membraneless enzymatic bio-fuel cell prototype with a mixed *AmPDH1*/cellobiose dehydrogenase flavodomain anode. Recently, another prototype had been constructed, which operated in human physiological solution and powered transmission of sensing data ( $j_{\max}=0.275 \text{ mA cm}^{-2}$ ) [15].

*AmPDH1* belongs to the glucose-methanol-choline (GMC) structural family alongside glucose 1-oxidases (GOx; EC 1.1.3.4), cellobiose dehydrogenases (CDH; EC 1.1.99.18), pyranose 2-oxidases (P2O; EC 1.1.3.10) and alcohol oxidases (AOX; EC 1.1.3.13) [16,17]. It is to date the only pyranose dehydrogenase, which has been structurally resolved in X-ray crystallography (PDB-ID: **4H7U**, [18]) and features two tightly interwoven conserved domains, a Rossmann-fold (PRK07364, GMC\_oxred\_N: pfam00732), which covalently binds the FAD co-factor via H103, and a substrate binding domain (GMC\_oxred\_C: pfam05199), which features H512, the only catalytic base of *AmPDH1* [18–20]. As a secreted fungal enzyme, native *AmPDH1* is N-glycosylated and was estimated to have a sugar content of 7% (m/m) [2].

To enable expression of enzyme variants, heterologous expression in *Pichia pastoris* was established. *Pichia pastoris* is known to be less prone to over-glycosylate heterologous proteins than the yeast model system *Saccharomyces cerevisiae*, but was observed to do so [21]. Indeed the purified recombinant product featured a comparable specific activity but also a more extensive and heterogeneous N-glycosylation pattern with a sugar content of approximately 30% [22].

Yakovleva et al. [9] found that recombinant *AmPDH1*/Os-polymer-modified graphite electrodes yielded higher currents when PDH was deglycosylated *in-vitro* prior to use. This created interest in producing PDH with no or reduced N-glycosylation. As expression in *Escherichia coli* yielded only

non-functional enzyme in form of inclusion bodies [22], knock out mutants, with a focus on N-glycosylation sites around the active site access, were expressed in *Pichia pastoris*. The mutant *AmpDH1* N75G/N175Q, showed a higher  $j_{\max}$  ( $290 \mu\text{A cm}^{-1}$ ) compared to the glycosylated recombinant wild type enzyme [9,23]. Interestingly, however, this double mutant largely retained the over-glycosylation pattern of recombinant *AmpDH1* wt. When all three glycosylation sites, which were at this point confirmed by mass spectrometry, were knocked out, the purified enzyme formed a well-defined band close to deglycosylated *AmpDH1*. However, the current output of electrodes modified with this triple mutant was not improved compared to the wild type ( $52 \mu\text{A cm}^{-1}$ ) [23]. These results suggest a site specific heterogenous N-glycosylation of *AmpDH1*, with differential effects of individual N-glycosylation moieties on enzyme performance and stability. In this work this was investigated further by elucidating the N-glycosylation pattern of native and recombinant *AmpDH1* and the impact of individual N-glycosylation sites on the recombinantly expressed enzyme. To this end a systematic set of N-glycosylation site knock-out mutants was expressed and characterized.

## **Material and methods**

### **Chemicals**

Chemicals were of the highest grade and purchased from Sigma Aldrich (St. Louis, MO, USA) unless stated otherwise. GE Healthcare (Chalfont-St. Giles, UK) was the supplier for the Phenyl-Sepharose FF chromatography resin and Thermo Fisher Scientific (Waltham, MA, USA) for restriction enzymes and Phusion polymerase. NEB-5 $\alpha$  competent *Escherichia coli* from New England Biolabs (Ipswich, MA, USA) was used for cloning and *Pichia pastoris* X33 from Invitrogen (Carlsbad, CA, USA) for heterologous expression. Alfa Aesar & Co KG (Karlsruhe, Germany) graphite rods (AGKSP grade, Ultra "F" purity, ASTM C-6, 3.81 cm, 3.05 mm diameter) were used as working electrodes and the polymer  $[\text{Os}(4,4'\text{-dimethyl-2,2'\text{-bipyridine)}_2(\text{poly}(1\text{-vinylimidazole})_{10})\text{Cl}_2]^{+2/+}$  ( $[\text{Os}(\text{dmbpy})_2(\text{PVI})_{10}\text{Cl}]^{+2/+}$ ,  $E^{0\ominus} = 320 \text{ mV vs. NHE}$ ) for electrode modification.

### **Mutagenesis and microtiter plate screening**

Site directed mutagenesis was done by overlap extension PCR, with Phusion PCR Polymerase (Thermo Fisher Scientific, Waltham, MA, USA), as reported elsewhere [23].

The site saturation library of transformed *Pichia pastoris* X33 was created according to previously described protocols [23] and screened by a modified microtiter plate expression protocol based on Weis et al. [22,24]. 300  $\mu\text{l}$  BMD1 medium (100 mM potassium phosphate buffer pH 6, 1.34% yeast nitrogen base without amino acids, 0.4  $\mu\text{g mL}^{-1}$  biotin, 1% D-glucose) per well were inoculated and after 64 h of incubation (25°C, 360 rpm, 80% humidity) 300  $\mu\text{l}$  BMM2 medium (100 mM potassium phosphate buffer pH 6, 1.34% yeast nitrogen base without amino acids, 0.4  $\mu\text{g mL}^{-1}$  biotin, 1%

methanol) were added. 70  $\mu\text{l}$  BMM10 medium (100 mM potassium phosphate buffer pH 6, 1.34% yeast nitrogen base without amino acids, 0.4  $\mu\text{g mL}^{-1}$  biotin, 5% methanol) were added at 73 h, 89 h and 112 h after inoculation. After 136 h the supernatant was harvested by plate centrifugation (3500 rpm, 4°C, 10 min) and transferred to a new plate. Enzymatic activity was determined by measuring 50  $\mu\text{l}$  of supernatant per well in a  $\text{Fc}^+$ -96-well-microtiter assay (100 mM sodium phosphate buffer pH 7.5, 0.2 mM ferrocenium hexafluorophosphate, 25 mM D-glucose, 30°C, total volume: 200  $\mu\text{l}$ ).

### **Shake flask expression screening**

Shake flask expression screening was done by modifying the microtiter plate protocol from Weis et al. [24] for 50-150 ml shake flasks. Per shake flask, 10 ml BMD1 medium was inoculated and incubated at 30°C and 130 rpm. Induction was started by adding 2.2 ml BMM2 after 64 h. 2.2 ml, 2,4 ml and 2,4 ml BMM10 were added after 73 h, 88 h and 112 h after inoculation, respectively. The supernatant was harvested 136 h after inoculation (centrifuging cell suspension for 20 min at 4000 rpm) and measured for volumetric activity in a standard ferrocenium assay, as described below, with a modified measuring time. After 100 s of incubation at 30°C measurement was conducted for 900 s.

### **Shake flask expression re-screening**

Chosen mutants were expressed at 1 L shake flask scale together with *AmPDH1* wt as positive control and with pPICZ-B without gene insert as negative control. 100 ml BMGY (100 mM potassium phosphate buffer pH 6, 2% peptone, 1% yeast extract, 1.34% yeast nitrogen base without amino acids, 0.4  $\mu\text{g mL}^{-1}$  biotin, 1% glycerol) were inoculated with pre-culture (10 ml BMGY incubated for 24 h at 30°C and 130 rpm after inoculation) and induction was started after 27 h (1 ml 50% methanol 4 times a day). Incubation temperature was reduced to 25°C after induction. Cell suspension samples were taken 24 h and 95 h after induction. 15 ml of the sample supernatant (4000 rpm, 20 min) were concentrated in 10 kDa Amicon ultrafiltration filter units (Millipore Corp., Billerica, MA, USA) at 4000 rpm to 0.24-0.45 ml. Volumetric activity of the concentrated supernatant was determined by standard ferrocenium assay.

### **Enzyme expression and purification**

PDH was expressed in methanol induced *Pichia pastoris* in a stirred-tank bioreactor (7L, MBR, Wetzikon, Switzerland) and purified by Hydrophobic Interaction Chromatography and Ion Exchange Chromatography according to a protocol described elsewhere [23]. Some modifications were applied. Glycerol batch/fed-batch phase lasted for 23-28 h and induction with methanol for 75-94 h. Elution with Anion Exchange Chromatography was done by gradients of 6-13% elution buffer (Bis-Tris 50 mM, pH 6.5, 1 M NaCl) in 7-10 column volumes. Purified enzyme was stored in sodium phosphate buffer pH 6.5 (50 mM) at -30°C.

Native *Am*PDH1 wt was purified like recombinantly expressed enzyme except for the 3<sup>rd</sup> purification step, which was done using a Superdex 75 10/300 GL column instead of a Phenyl-Source column. Enzyme solution from the previous purification step was prepared for this gel filtration by concentrating with 10 kDa Amicon ultrafiltration filter units (Millipore Corp., Billerica, MA, USA) to 1.2 ml.

### **Protein characterization**

Samples were denatured with Laemmli buffer and analysed on precast 4-20% acrylamide gels (Mini Protean TGX gel system, Biorad, Hercules, CA, USA) according to manufacturer's guidelines. Coomassie was used for staining and unstained Precision Plus Protein Standard (Biorad) was applied as reference.

*In-vitro* deglycosylation of PDH was done with Endo Hf (New England Biolabs) according to a non-denaturing protocol [25]. Native *Am*PDH1 was *in-vitro* deglycosylated with PNGase F (New England Biolabs) according to the producer's denaturing protocol.

The thermal unfolding variable  $T_m$  was determined by the ThermoFAD protocol [26,27] based on the change in fluorescence by the PDH cofactor upon unfolding. A Biorad MyIQ Single Color Real-Time PCR Detection system (excitation filter: 475-495, emission filter: 515-545 nm) was used to measure the fluorescence of 2 mg ml<sup>-1</sup> protein in sodium phosphate buffer (app. 80 mM) at pH 5.5, 6.5 and 7.5. A temperature gradient was run from 20-95°C (1 min 20°C, afterwards an increase by 0.5°C every 30 s). All measurements were done in triplicates and  $T_m$  was the peak of the first derivation of the fluorescence signal.

### **HPLC-ESI-MS**

Glycopeptide analysis, of Endo Hf digested and undigested protein samples, was done by HPLC-ESI-MS. For deglycosylation, sample protein (1 mg mL<sup>-1</sup>) was treated with Endo Hf as described above. Deglycosylated and glycosylated protein samples were reduced with 5 mM DTT in 100 mM NH<sub>4</sub>HCO<sub>3</sub> at 56°C for 45 min. Subsequently, samples were carbamidomethylated with 25 mM Iodoacetamide in the same buffer at room temperature for 30 min. After acetone precipitation (80% acetone, -20°C, 45 min) 20 µg of sample protein were digested with 0.4 µg of trypsin (Promega, Fitchburg, WI, USA) in 100 mM NH<sub>4</sub>HCO<sub>3</sub> at 37°C over night. Where a secondary chymotrypsin digestion was applied, trypsin was inactivated at 96°C for 6 min and 15 µg of sample were incubated with 0.3 µg of chymotrypsin (Promega) in the same buffer at 37°C over night. Thus prepared protein samples were analysed in a Dionex UltiMate 3000 LC-system (C18 column: Thermo Scientific 150 x 0.32 mm BioBasic-18, Particle Sz. (u) 5) coupled with a Bruker maXis 4G ETD MS-system. A modified "peptide mining by LC-ESI-MS/MS" protocol of Pabst et al. [28] was applied. The gradient was changed from 1% to 80% acetonitrile over 60 min at 6 µl min<sup>-1</sup> flow rate and a maXis 4G ETD in

positive mode was used (ion cooler transfer time: 100  $\mu$ s, ion cooler pre pulse storage time: 10  $\mu$ s, low mass: 300.00 m/z, spectra rate 1 Hz). Auto MS2 in data dependant acquisition mode (switching to MS/MS mode for eluting peaks) was performed for 8 dominant precursor peaks (active exclusion=on, exclusion activation=4 spectra, exclusion release= 120 s, absolute threshold: 2500). MS-scans were recorded in a range of 150-2200 m/z. Instrument calibration was performed using ESI calibration mixture (Agilent).

Manual glycopeptide searches were made using DataAnalysis 4.0 (Bruker). For the quantification of the different glycoforms, the peak areas of EIC (Extracted Ion Chromatograms) of the first 4 isotopic peaks were summed. Adduct formation (mainly ammonium) and different charge states of the ions were taken into account.

### Enzymatic assays

The redox dye ferrocenium hexafluorophosphate ( $\text{Fc}^+$ ) ( $\epsilon_{300} = 4.3 \text{ mM}^{-1} \text{ cm}^{-1}$ ) was used for spectrophotometric activity assays [29]. Unless mentioned otherwise, enzymatic activity was measured with 0.2 mM  $\text{Fc}^+$  and 25 mM D-glucose at 30°C for 5 min. One Unit was defined as reduction of 2  $\mu$ mol of  $\text{Fc}^+$  to ferrocene per min. Apparent kinetic constants were determined in triplicate measurements and non-linear regression was done with SigmaPlot 11.0.

### Flow Injection Amperometry

The Os polymer  $[\text{Os}(\text{dmbpy})_2(\text{PVI})_{10}\text{Cl}]^{2+/+}$  was dissolved in deionised water by ultrasonification at a concentration of 5 mg  $\text{ml}^{-1}$ . Graphite rods of 3.05 mm diameter were polished on wet emery paper (P1200) and air-dried. 5  $\mu$ l of an  $[\text{Os}(\text{dmbpy})_2(\text{PVI})_{10}\text{Cl}]^{2+/+}$  solution and 2  $\mu$ l of a freshly prepared 68% (w/v) poly(ethyleneglycol)(400)diglycidyl ether in water solution were mixed on the electrode surface and left for 8-10 min at room temperature before adding 5  $\mu$ l of (*Am*PDH1 N252Q: 20.4  $\mu\text{g } \mu\text{l}^{-1}$ , *Am*PDH1 N75G/N252Q: 17.1  $\mu\text{g } \mu\text{l}^{-1}$ ) or 7.5  $\mu$ l of (*Am*PDH1 N175Q/N252Q: 13.6  $\mu\text{g } \mu\text{l}^{-1}$ ) enzyme solution, respectively. Modified electrodes were stored at 4°C in saturated atmosphere overnight and rinsed with deionised water before use.

Flow-injection amperometry was conducted in a wall-jet flow-through electrochemical cell as previously described [23,30–32]. *Am*PDH-modified graphite working electrodes were fitted into a Teflon holder and measured for current response after injection of D-glucose. A platinum counter-electrode and Ag-AgCl (0.1 mM KCl, 288 mV vs. NHE) reference-electrode were used in this setting and a constant potential of 444 mV vs. NHE was applied to the working electrode by a three electrode potentiostat from Zäta Electronics (Höör, Sweden). The peristaltic pump (Minipuls 3, Gilson, Villier-le Bel, France). was set to a flow rate of 0.5  $\text{ml min}^{-1}$ , 50  $\mu$ l of substrate was injected by a 6-port valve (Rheodyne, type 7125 LabPR, Cotati, CA, USA) and the running buffer was a sodium phosphate buffer (50 mM, pH 7.4) with 137 mM NaCl. The current output was recorded by a BD 112 recorder

from Kipp & Zonen (Utrecht, The Netherlands). Injected substrate concentrations were corrected by a dispersion factor of 1.23 and the Michaelis-Menten equation was fitted to the data to derive apparent  $K_m^{app}$  and saturating current densities ( $j_{max}$ ). Measurements were conducted with three or more independent repeats using different electrode preparations for each repeat.

## **Results**

### **Site directed and site saturation mutagenesis of *AmPDH1* N-glycosylation sites**

A set of N-glycosylation site knock out mutants of *AmPDH1* had been studied already by Yakovleva et al. [23] (*AmPDH1* N75G, N175Q, N75G/N175Q and N75G/N175Q/N252Q). In this work the remaining knock out mutants involving N<sup>252</sup> were constructed (*AmPDH1* N252Q, N75G/N252Q and N175Q/N252Q) by site directed mutagenesis of the templates *AmPDH1* wt [22], *AmPDH1* N75G and *AmPDH1* N175Q [23] in pPICZ-B, with the primers fwAmPDHN252Q and rvAmPDHN252Q (Table S1). Additionally, a fourth glycosylation site at N<sup>319</sup>, which was previously only predicted but could not be verified by mass spectroscopy, was knocked out as well. This was done by site directed and site saturation mutagenesis. The site saturation mutagenesis library was created from the *pdh1* gene of *Agaricus meleagris* in pPICZ-B [22] by mutating position N319 with the primers fwAmPDHN319 and rvAmPDHN319X. 200 clones of transformed *Pichia pastoris* were screened in microtiter plates for functional expression of PDH with *AmPDH1* wt as positive control and empty pPICZ-B vector as negative control. Due to generally low enzymatic activity, compared to the negative control, the results of the microtiter plate screening were ambiguous (data not shown). 9 clones of the apparent best producers and 10 randomly chosen clones were sequenced. From those, 5 different mutants could be identified (N319L, R, T, P and A). The remaining 14 mutants were created by site directed mutagenesis using the primers fwAmPDHN319 and rvAmPDHN319, respectively, and the complementary mutating primers listed in Table S1.

For improved expression conditions, compared to the microtiter plates, screening was also conducted in shake flasks. All 19 *AmPDH1* N319 variants were expressed in *Pichia pastoris* and compared to a positive (*AmPDH1* wt) and a negative control (pPICZ-B without *pdh1* gene). Supernatant from all mutant expressing clones showed very low or no discernible enzymatic activity in a ferrocenium ion based assay. The only variants with a relative activity of more than 0.3%, compared to the wild type enzyme, were *AmPDH1* N319G (1.2%) and C (0.8%). These two variants, together with N319Q, were chosen for rescreening in 1 L shake flask scale (Table 1). While overall yields were even lower than in the previous screening, and decreased during longer expression duration, *AmPDH1* N319G was confirmed as poorly, but relatively best, expressed N319 variant.

**Table 1: Expression rescreening of *AmPDH1* N319 C, G and Q in *Pichia pastoris* in 1 L shake flasks**

Sample	Neg. control corrected vol. activity		Rel. activity to pos. control	
	24h after induction	95h after induction	24h after induction	95h after induction
	[U ml <sup>-1</sup> ]	[U ml <sup>-1</sup> ]	[%]	[%]
N319C	0.0005	-0.0001	0.10	-0.01
N319G	0.0013	0.0001	0.23	0.01
N319Q	0.0003	-0.0001	0.06	-0.01
N319N	0.5386	1.13758	100.00	100.00

### Expression and purification of *AmPDH1* variants

*AmPDH1* N252Q, N75G/N252Q and N175Q/N252Q were expressed in methanol induced *Pichia pastoris* in 7 L stirred-tank bioreactors and purified (Fig. 1, Table 2), to a specific activity of 33-46 U mg<sup>-1</sup>. The other *AmPDH1* mutants investigated in this work (N75G, N175Q, N75G/N175Q and N75G/N175Q/N252Q) were expressed and purified previously [23]. Native *AmPDH1* wt was purified (Fig. 1, Table 2) from *Agaricus meleagris* supernatant (stored at -30°C) from Sygmund et al. [2]. Final specific activity was comparable to previously published data [2].

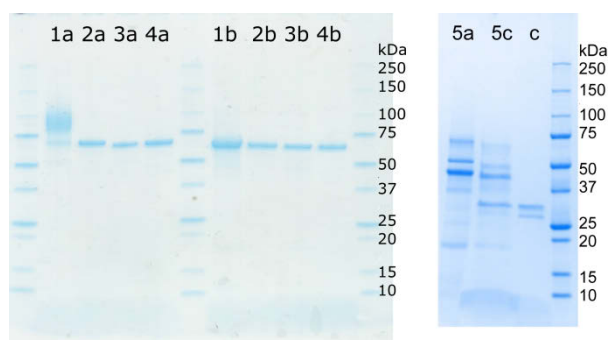


**Figure 1:** SDS-Page of purified *AmPDH1* wt from Graf et al. [20] (1), *AmPDH1* N252Q (2), N75G/252Q (3), N175Q/N252Q (4) and native *AmPDH1* wt (5). Glycosylated enzyme (1a-5a) is compared to enzyme deglycosylated with Endo Hf (1b-4b) and PNGase F (5c), respectively. PNGase F without enzyme is shown separately (c).

### HPLC-ESI-MS

N-glycosylated amino acids in recombinant *AmPDH1* wt and knock out mutants were identified by analysing Endo Hf digested enzymes after tryptic/chymotryptic digest by HPLC-ESI-MS. Endo Hf digest leaves one N-acetylglucosamine (GlcNAc) residue at a modified site. N<sup>75</sup>, N<sup>175</sup>, N<sup>252</sup> and N<sup>319</sup> were found to be modified in the wild type. The *AmPDH1* mutants (N75G, N175Q, N75G/N175Q and

N75G/N175Q/N252Q from [23]; N252Q, N75G/N252Q, N175Q/N252Q from this work) were confirmed to be not modified at the mutated sites while retaining N-glycosylation at the other sites (Fig. S1).

**Table 2: Purification of recombinant *AmPDH1* N252Q, N75G/252Q and N175Q/N252Q and native *AmPDH1* wt from culture supernatant**

Sample	Total activity	Total protein	Spec. activity	Purif. factor	Recovery
<b><i>AmPDH1</i> N252Q</b>	[U]	[mg]	[U mg <sup>-1</sup> ]	[x-fold]	[%]
Culture supernatant	2635.8	905.7	2.9		
Phenyl-Sepharose FF 600 ml	2546.8	182.7	13.9	4.8	97
DEAE-Sepharose FF 60 ml	1376.5	45.6	30.2	10.4	52
<b>Phenyl-Source 70 ml, after concentrating</b>	<b>883.6</b>	<b>19.4</b>	<b>45.6</b>	<b>15.7</b>	<b>34</b>
<b><i>AmPDH1</i> N75G/N252Q</b>	[U]	[mg]	[U mg <sup>-1</sup> ]	[x-fold]	[%]
Culture supernatant	2063.6	1167.1	1.8		
Phenyl-Sepharose FF 600 ml	1888.0	197.7	9.6	5.4	80
DEAE-Sepharose FF 60 ml	553.4	42.3	13.1	7.3	23
<b>Phenyl-Source 70 ml, after concentrating</b>	<b>562.1</b>	<b>16.0</b>	<b>35.2</b>	<b>19.7</b>	<b>24</b>
<b><i>AmPDH1</i> N175Q/N252Q</b>	[U]	[mg]	[U mg <sup>-1</sup> ]	[x-fold]	[%]
Culture supernatant	1114.7	748.8	1.5		
Phenyl-Sepharose FF 600 ml	1040.1	128.6	8.1	5.4	93
DEAE-Sepharose FF 60 ml	687.8	32.5	21.2	14.2	62
<b>Phenyl-Source 70 ml, after concentrating</b>	<b>312.2</b>	<b>9.4</b>	<b>33.2</b>	<b>22.3</b>	<b>28</b>
<b>Native <i>AmPDH1</i> wt</b>	[U]	[mg]	[U mg <sup>-1</sup> ]	[x-fold]	[%]
Culture supernatant	4426	241	18		
Phenyl-Sepharose FF 600 ml	5676	121	47	2.6	128
DEAE-Sepharose FF 60 ml	3822	54	71	4.0	86
<b>Superdex75 10/300 GL, after concentrating</b>	<b>1914</b>	<b>21</b>	<b>91</b>	<b>5.3</b>	<b>43</b>

The extent of N-glycosylation of native *AmPDH1* wt and *AmPDH1* wt expressed in *Pichia pastoris* (from [22]), was analysed and compared by HPLC-ESI-MS. The distribution of glycosyl chain lengths attached to the different N-glycosylation sites was quantified (Fig. 2; Table S2, Fig. S1). Interestingly native *AmPDH1* had only a single N-acetylhexosamine (HexNAc) at N<sup>175</sup> and N<sup>252</sup>. At the other positions (N<sup>75</sup>, N<sup>319</sup>) two HexNAcs with 5 to 11 hexose residues were found. The recombinant *AmPDH1* featured slightly longer glycosyl chains of 2 HexNAc with 5-13 hexose residues. The length

distribution differed not only between the two variants but also between different sites of the same variant. Only N<sup>319</sup> showed a high similarity of the glycosylation pattern between native and recombinant enzyme (predominantly 2 HexNAc, 7-9 hexoses). No N-glycosylation of N<sup>252</sup> could be found in fully glycosylated recombinant *AmpDH1* even though Endo Hf deglycosylated *AmpDH1* featured a modified N<sup>252</sup> with an attached GlcNAc residue, like the other examined sites.

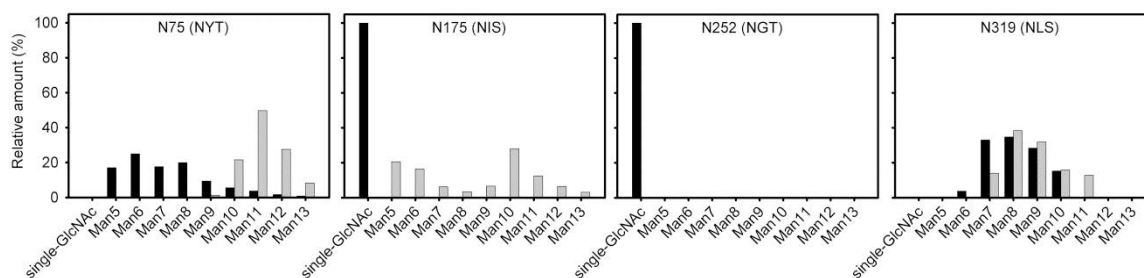


**Figure 2:** N-glycosylation pattern of *AmpDH1* wt expressed by the native producer *A. meleagris* [2] (black), and in the heterologous production system *Pichia pastoris* X33 [22] (grey). The glycopeptides from tryptic digest were identified by HPLC-ESI-MS and relative distributions were calculated based on peak areas.

### Thermo-FAD

Thermal stability constants of the glycosylation site variants and *AmpDH1* wt were determined by the ThermoFAD protocol and compared (Fig. 3). Thereby the fluorescent capability of the enzyme cofactor FAD is used to observe the unfolding of the active site by following the changes in the fluorescence signal [26]. Three different pH environments were chosen: pH 5.5, which was closest to the previously reported pH dependent thermostability maximum of *AmpDH1* wt [27], the storage pH 6.5, and the standard assay pH 7.5.  $T_m$  decreased for all variants towards the higher pH values. *AmpDH1* N75G/N175Q and N75G/N175Q/N252Q were the only enzyme variants with a significantly decreased  $T_m$  by 4-7°C on average.

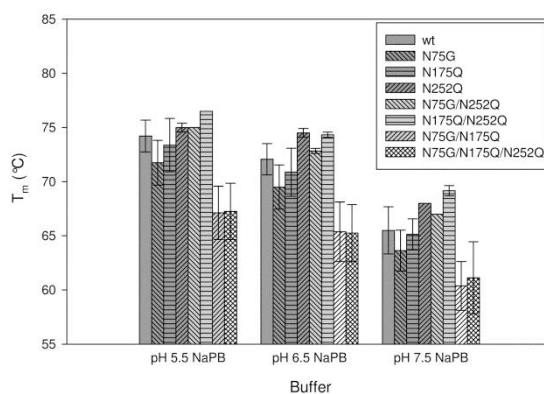


**Figure 3:**  $T_m$  of *AmpDH1* and N-glycosylation site variants (2 mg ml<sup>-1</sup>) in sodium phosphate buffer (app. 80 mM) of pH 5.5, 6.5 and 7.5, determined according to the Thermo-FAD protocol [26,27].

**Table 3: Apparent kinetic constants of N-glycosylation site variants.** Assays were conducted at 30°C and pH 7.5 (sodium phosphate buffer 50 mM). e<sup>-</sup>-donors were measured with 0.2 mM Fc<sup>+</sup> and the e<sup>-</sup>-acceptor in the presence of 25 mM D-glucose. \*AmPDH1 wt was supplied by [22]

	<i>AmPDH1</i> wt	N75G	N175Q	N252Q	N75G/ N252Q	N175Q/ N252Q	N75G/ N175Q	N75G/ N175Q/ N252Q
<b><i>k</i><sub>cat</sub></b>	[s <sup>-1</sup> ]	[s <sup>-1</sup> ]	[s <sup>-1</sup> ]	[s <sup>-1</sup> ]	[s <sup>-1</sup> ]	[s <sup>-1</sup> ]	[s <sup>-1</sup> ]	[s <sup>-1</sup> ]
<b>Substrate</b>								
D-Glucose	36.6 ± 0.5 *	45.3 ± 8.1	48.1 ± 0.9	50.8 ± 2.0	40.8 ± 0.6	45.4 ± 1.5	36.0 ± 0.8	49.7 ± 2.2
D-Galactose	31.8 ± 0.6 *	25.7 ± 3.3	40.3 ± 2.3	45.9 ± 1.7	37.9 ± 1.8	39.3 ± 0.5	34.2 ± 0.5	38.9 ± 0.2
D-Mannose	27.4 ± 0.6 *	22.1 ± 1.1	40.8 ± 2.1	41.9 ± 0.7	31.5 ± 0.3	33.5 ± 0.7	35.0 ± 2.7	27.0 ± 2.0
Cellobiose	30.9 ± 0.3 *	33.0 ± 1.4	55.1 ± 2.4	43.8 ± 1.0	31.3 ± 1.2	35.2 ± 2.0	29.1 ± 1.8	34.7 ± 4.8
<b>e<sup>-</sup>-acceptor</b>								
Ferrocenium (pH 7.5)	87.4 ± 6.1 *	65.8 ± 18.4	125 ± 56	66.3 ± 1.7	54.6 ± 3.9	50.7 ± 4.7	44.8 ± 6.5	54.2 ± 5.5
<b><i>K</i><sub>m</sub></b>								
	[mM]	[mM]	[mM]	[mM]	[mM]	[mM]	[mM]	[mM]
<b>Substrate</b>								
D-Glucose	0.87 ± 0.03 *	1.85 ± 0.28	0.97 ± 0.05	0.58 ± 0.00	0.88 ± 0.06	0.72 ± 0.03	1.50 ± 0.15	1.94 ± 0.14
D-Galactose	1.00 ± 0.02 *	2.19 ± 0.23	1.10 ± 0.19	0.80 ± 0.06	1.14 ± 0.04	0.86 ± 0.03	3.09 ± 0.00	3.55 ± 0.14
D-Mannose	74.2 ± 3.0 *	227 ± 19	142 ± 16	83.7 ± 3.0	116 ± 7	87.9 ± 4.3	355 ± 43	380 ± 36
Cellobiose	6.69 ± 7.10 *	7.10 ± 1.66	8.13 ± 0.35	5.52 ± 0.54	6.38 ± 0.76	5.70 ± 0.88	4.74 ± 0.32	5.72 ± 1.47
<b>e<sup>-</sup>-acceptor</b>								
Ferrocenium (pH 7.5)	0.27 ± 0.24 *	0.24 ± 0.11	0.39 ± 0.18	0.30 ± 0.02	0.29 ± 0.04	0.37 ± 0.03	0.11 ± 0.01	0.10 ± 0.02

### Steady-state kinetic constants

*AmPDH1* N75G, N175Q, N75G/N175Q (DM) and N75G/N175Q/252Q (TM) were from Yakovleva et al. [23] and kinetic characterization was conducted subsequently to their purification, during this time they were stored at 4°C. The *AmPDH1* mutants expressed and purified in this work were stored at -30°C. Storage of *in-vitro* deglycosylated *AmPDH1* at 4°C was previously observed to increase the enzymatic activity in the standard ferrocenium assay over time [10]. The mutants DM and TM showed a similar behaviour. To make the determined apparent  $k_{\text{cat}}$  values comparable, a correction factor, based on reference standard activity assays from the same day, was applied to enzymes stored at 4°C (Table S3).

Enzyme variants were tested with the standard substrate D-glucose, its C4-epimer D-galactose and its C2-epimer D-mannose, the disaccharide cellobiose, as well as with the standard assay  $e^-$ -donor ferrocenium (Table 3). Apparent  $k_{\text{cat}}$  values were similar for all variants with those sugars and ranged from 22-55  $\text{s}^{-1}$ . The apparent turnover numbers of ferrocenium with the variants were comparable to the 87  $\text{s}^{-1}$  of *AmPDH1* wt. The affinities to the tested monosaccharides decreased up to five-fold for DM and TM, and two- to three-fold for N75G. However, affinity towards cellobiose was not affected and affinity towards ferrocenium was even modestly improved (two-fold) for those mutants. The other variants showed no substantial changes in affinity.

**Table 4: Flow Injection Amperometry of graphite electrodes modified with Os-polymer and *AmPDH* variants.** *AmPDH1* wt (\*\*: supplied by [22]), *AmPDH1* N252Q, N75G/252Q and N175Q/N252Q were tested.  $E^{\text{app1}}=444$  mV vs. NHE,  $v=0.5$  ml min<sup>-1</sup>, pH 7.4 (sodium phosphate buffer 50 mM, 137 mM NaCl), sample injection: 50  $\mu\text{l}$  D-glucose at varying concentrations. For comparison previously published  $j_{\text{max}}$  and  $K_{\text{m}}^{\text{app}}$  from *AmPDH1* mutants [23] are included and marked by “\*\*”

	<i>AmPDH1</i> $W_j^{**}$	N75G* N175Q*	N75G/ N175Q/ N252Q	N75G/ N175Q/ N252Q	N75G/ N175Q/ N252Q	N75G/ N175Q/ N252Q		
$j_{\text{max}}$ [ $\mu\text{A cm}^{-2}$ ]	31.2 $\pm 8.6^{**}$	2.5 $\pm 0.1^*$	20.9 $\pm 0.7^*$	<b>26.3</b> $\pm 9.8$	<b>71.7</b> $\pm 8.3$	<b>13.2</b> $\pm 2.0$	290.1 $\pm 15.9^*$	51.7 $\pm 0.6^*$
$K_{\text{m}}^{\text{app}}$ [mM]	2.6 $\pm 0.7^{**}$	5.9 $\pm 0.2^*$	3.8 $\pm 0.4^*$	<b>0.6</b> $\pm 0.2$	<b>1.8</b> $\pm 0.3$	<b>1.3</b> $\pm 0.3$	2.1 $\pm 0.2^*$	4.4 $\pm 0.6^*$

### Flow Injection Amperometry

The *AmPDH1* variants created in this work (N252Q, N75G/N252Q, N175Q/N252Q) and wild type enzyme (from [22]), as reference, were also tested for catalytic current on graphite electrodes.  $[\text{Os}(\text{dmbpy})_2(\text{PVI})_{10}\text{Cl}]^{+2/+}$  was used as mediator and Flow Injection Amperometry was conducted under the same conditions as the previously published variants [23], with D-glucose as substrate. As

the previously chosen graphite electrodes were not produced anymore, equivalent electrodes from Alfa Aesar & Co KG were used. Table 4 shows determined  $j_{\max}$  and  $K_m^{\text{app}}$  of variants from this work and compares them to the other variants tested by Yakovleva et al. [23] and the wild type.

### Alignment of structurally related enzymes to *AmPDH1* and structural comparison

Polar interactions by  $N^{319}$ , the resolved sugar moieties and neighbouring amino acids in the *AmPDH1* crystal structure **4H7U** [18] were predicted using Pymol 1.3 and are shown in Fig. 4. The glycosylated  $N^{319}$  was at the C-terminal end of the FAD binding Rossmann-fold [18,19], surrounded by 3 segments of the other conserved domain (GMC\_oxred\_C): its N-terminal end (I), a loop leading to the central active site residue  $H^{512}$  (II) and a loop close to its C-terminal end (III). The C- and N-terminal segment of GMC\_oxred\_C and  $N^{319}$  were connected by polar interactions via  $R^{433}$ . The two resolved GlcNAc residues covalently linked to  $N^{319}$  interacted with the peripheral and exposed loop of GMC\_oxred\_C (II) via polar interaction with  $S^{525}$  and a planar/planar interaction with  $W^{526}$ , according to the MSDSite database [33].

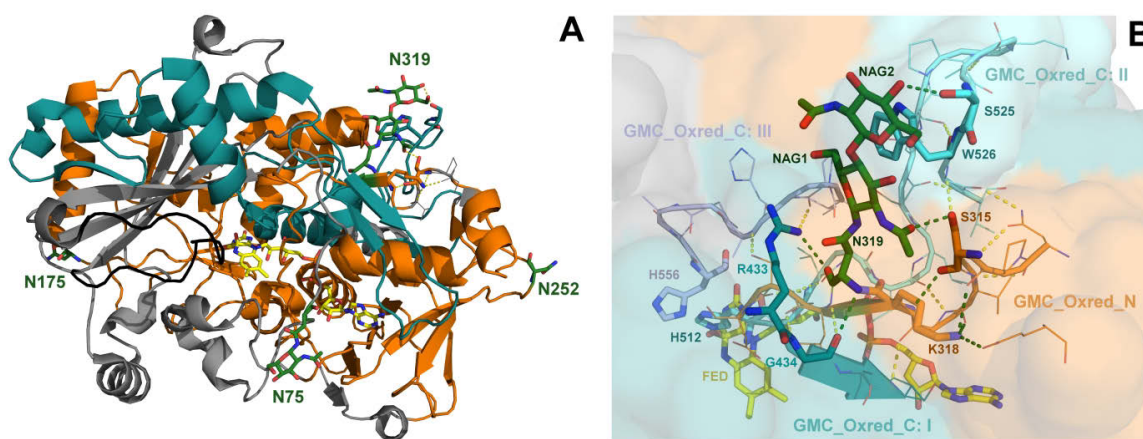


**Figure 4:** *AmPDH1* crystal structure **4H7U** from Tan et al. [18] (A) showing the 4 N-glycosylation sites ( $N^{75}$ ,  $N^{175}$ ,  $N^{252}$  and  $N^{319}$ ) whereas one GlcNAc could be resolved at  $N^{75}$  and 2 GlcNAc bound to  $N^{319}$ . (B) Detailed view of the surrounding of  $N^{319}$  and the interaction of the glycosyl moiety with the polypeptide chain.

Structural alignment of **4H7U** in the RCSB-pdb-database [34,35] listed 15 significant results. 8 of them were manually reviewed members of the GMC structural family (SwissProt database) and the other 6 annotated as such by TrEMBL. aryl-alcohol oxidase (PDB-ID: **3FIM**, UniProt-ID: **O94219**) had, as previously reported [18], the most similar protein structure. *AmPDH1* was aligned via the inbuilt sequence alignment tool with those other 15 enzymes (Fasta S1) and all 192 manually reviewed members of the GMC family of oxidoreductases from Uniprot database (Fasta S2) [36]. Among the aligned enzymes all pyranose dehydrogenases (Uniprot-ID: **Q3L245**, **Q3L1D1**, **Q3L243**, **Q0R4L2**, **V5NC32**, **V5NDL4**) and aryl-alcohol oxidase (**O94219**) had an N-glycosylation consensus sequence and a concomitant aromatic residue equivalent to *AmPDH1*  $N^{319}$ SL and  $W^{526}$ , respectively. There was

no aromatic amino acid counterpart to W<sup>526</sup> in any of the other enzymes except for the two alcohol oxidases of *Pichia pastoris* (AOX1, AOX2). However, an N-glycosylation consensus sequence in a homologous location to N<sup>319</sup> was only found in *Aspergillus nidulans* pyranose-2-oxidase among the other enzymes.

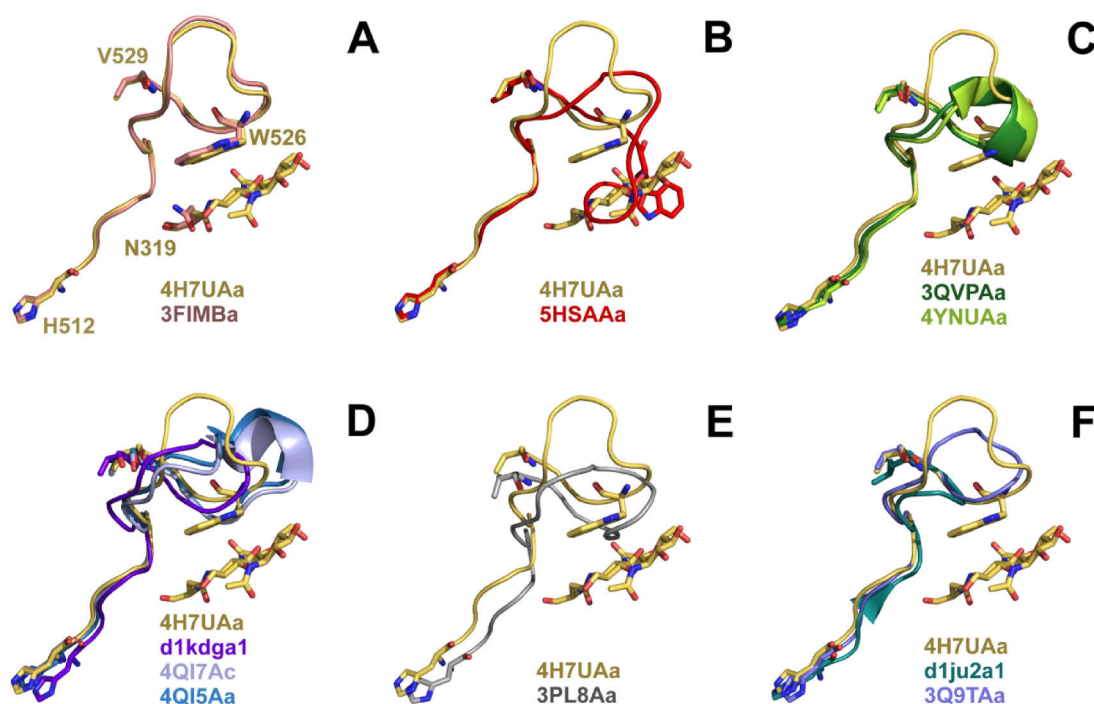


**Figure 5: Structural alignment of related proteins to *AmPDH1* (4H7UAa) by Pymol 1.3.** The amino acid backbone between *AmPDH1* H<sup>512</sup> and V<sup>529</sup> was compared to the equivalent peptide chain of *Pleurotus eryngii* aryl-alcohol oxidase (A; 3FIMBa), *Pichia pastoris* alcohol oxidase 1 (B; 5HSAAa), glucose oxidases (C; *Aspergillus niger*: 3QVPAa, *Aspergillus flavus*: 4YNUAa), cellobiose dehydrogenases (D; *Phanerochaete chrysosporium*: d1kdga1, *Neurospora crassa*: 4QI7Ac, *Myriococcum thermophilum*: 4QI5Aa), *Trametes ochracea* pyranose 2-oxidase (E; 3PL8Aa), and two other enzymes (F; *Prunus dulcis* hydroxynitrile lyase: d1ju2a1, *Aspergillus oryzae* formate oxidase: 3Q9TAa). W<sup>526</sup>/N-glycosylation site N<sup>319</sup> and potential homologs are shown, where present.

All eukaryotic crystal structures homologous to *AmPDH1* were aligned and visualized with Pymol 1.3. In Fig. 5 the GMC\_oxred\_C: II loop between the conserved active site H<sup>512</sup> and V<sup>529</sup> was compared to those of aryl-alcohol oxidase (*Pleurotus eryngii*, PDB-ID: **3FIM**) [37], alcohol oxidase 1 (*Pichia pastoris*, PDB-ID: **5HSA**) [17], glucose oxidases (*Aspergillus niger*, PDB-ID: **3QVP**; *Aspergillus flavus*, PDB-ID: **4YNU**) [38,39], cellobiose dehydrogenases (*Phanerochaete chrysosporium*, PDB-ID: **1KDG**; *Neurospora crassa*, PDB-ID: **4QI7**; *Myriococcum thermophilum*, PDB-ID: **4QI5**) [40-42], pyranose 2-oxidase (*Trametes ochracea*, PDB-ID: **3PL8**) [43], and two other enzymes (*Prunus dulcis* hydroxynitrile lyase, PDB-ID: **1JU2**, *Aspergillus oryzae* formate oxidase, PDB-ID: **3Q9T**) [44,45]. Aryl-alcohol oxidase has an almost identical loop backbone with the same tryptophan motive and

N<sup>319</sup>SL consensus sequence as *AmPDH1*. On the other side *Pichia pastoris* alcohol oxidase 1, which features a homologous tryptophan but no homologous N-glycosylation site in the sequence alignment, has the most deviating loop from all visualized structures. It takes up the space which is occupied by the GlycNAcs in the *AmPDH1* structure.

## **Discussion**

### **N-glycosylation of *AmPDH1* and heterologous expression**

*Pichia pastoris* is known to overglycosylate to a lesser extent than *Saccharomyces cerevisiae* but was nonetheless observed to do so [21]. The higher sugar content of recombinant *AmPDH1* (30%, m/m) compared to native *AmPDH1* (7%, m/m), was therefore not surprising. Improved current output for electrodes modified with deglycosylated *AmPDH1* or the N-glycosylation site variant *AmPDH1* N75G/N175Q [9,23] highlighted, however, that N-glycosylation can have a significant impact on the performance of enzymatic systems. This was confirmed by the recent biofuel cell prototype employing *AmPDH1* for the anode, where deglycosylated enzyme lead to approximately 10-fold increased  $j_{\max}$  over glycosylated one [15].

In this work, N-glycosylation of *AmPDH1*, recombinantly expressed in *Pichia pastoris*, was investigated in greater detail and a systematic set of functionally expressible N-glycosylation knock out mutants was characterized. Yakovleva et al., could already confirm the N-glycosylation of the *AmPDH1* consensus sequences N<sup>75</sup>, N<sup>175</sup> and N<sup>252</sup> [10]. N-glycosylation of N<sup>319</sup> was predicted with a low likelihood but in the *AmPDH1* crystal structure from Tan et al. (PDB-ID: **4H7U**) [18], modifications of N<sup>75</sup> and N<sup>319</sup> could be partially resolved, featuring two core GlcNAcs at N<sup>319</sup> and one at N<sup>75</sup> (Fig. 4). The modification of N<sup>319</sup> remained unverified by mass spectrometry however, as the respective peptide could not be identified with two different mass-spectrometry systems [10]. Therefore, Endo Hf digested *AmPDH1* was analysed again in this work, using a different system (Dionex UltiMate 300 LC). The peptide containing N<sup>319</sup> had a surprisingly long retention time on the HPLC column but could be identified and was shown to be N-glycosylated as well.

To clarify the differences in the N-glycosylation pattern of these 4 N-glycosylation sites of recombinant *AmPDH1* wt and native *AmPDH1*, the glycosylated enzymes were analysed by HPLC-ESI-MS as well. The length of the found glycosyl moieties and their prevalence was determined for each N-glycosylation site. Peculiar single HexNAcs at N<sup>175</sup> and N<sup>252</sup> of native *AmPDH1* were in line with previous reports of secreted fungal enzymes [46,47]. Cleavage by co-expressed fungal endoglycosidases was suggested, but the biological function of this phenomenon remains unknown. Interestingly only two out of the four sites were modified in this way in native *AmPDH1*. N-glycosylation of N<sup>75</sup> and N<sup>319</sup>, which appeared less exposed and could be partially resolved in the

crystal structure **4H7U** [18], was predominantly modified according to fungal type N-glycosylation as described by Archer and Peberdy [48]. The recombinantly expressed *AmPDH1* featured, as expected, no single HexNAcs and its N-glycosylation pattern was compatible to previous studies of heterologously expressed enzymes in *Pichia pastoris* [49,50]. However, even though N<sup>252</sup> was found to be modified in Endo Hf deglycosylated PDH, no modified peptide containing N<sup>252</sup> could be identified from glycosylated PDH. Hyperglycosylation of this site is a possible explanation for this behaviour as the glycosylated peptide could be too heavy and too heterogeneous for detection in HPLC-ESI-MS, while the peptide with the single remaining HexNAc was detectable. This hypothesis is supported by previous results with N-glycosylation knock out mutants *AmPDH1* N75G/N175Q and N75G/N175Q/N252Q [23]. While the former formed a broad smear on an SDS-PAGE, comparable to the recombinantly expressed wild type enzyme, the latter appeared as a well-defined band at ~65 kDa, indicating that hyperglycosylation specifically happens at N<sup>252</sup>. This was confirmed by the single site mutant *AmPDH1* N252Q described in this work, which also formed a sharp band at around 70 kDa.

The N-glycosylation site N<sup>319</sup> differed from the others. Its glycosylation pattern in homologous and heterologous expression was remarkably similar, and while knock out mutants of N<sup>75</sup>, N<sup>175</sup> and N<sup>252</sup> could be expressed efficiently in *Pichia pastoris* (this work and [23]), no N<sup>319</sup> knock out variant could be expressed at levels sufficient for purification and further study. N<sup>319</sup> may be remotely located in the *AmPDH1* crystal structure (PDB-ID: **4H7U**), seen from the active site access (Fig. 4), but it appears to be at a central point of polar inter-domain interactions. However, rather than N<sup>319</sup> directly, the covalently bound resolved core GlcNAcs interact with the exposed adjacent loop GMC\_oxred\_C: II via planar-planar interaction towards W<sup>526</sup> and polar interaction with S<sup>525</sup>. This is in line with the known carbohydrate binding capability of aromatic amino acids and especially tryptophan [51]. The N<sup>319</sup>SL consensus sequence/W<sup>526</sup> combination was conserved in all characterized PDHs but not found in any other protein except for the structurally closely related aryl-alcohol oxidase. The structure of *Pichia pastoris* alcohol oxidase 1 suggests that the presence of a homologous tryptophan could facilitate a dramatically different loop confirmation in the absence of the concomitant N-glycosylation. Exchange of N<sup>319</sup> and consequently missing glycosyl residues could therefore result in non-functional or unstable alternative folding patterns and prevent secretion of functional enzyme by the expression host *Pichia pastoris*. N<sup>319</sup> has thus to be considered an indispensable glycosylation site in eukaryotic expression hosts (and in the wild-type enzyme). In the non-N-glycosylating prokaryotic host *Escherichia coli* *AmPDH1* and aryl-alcohol oxidase were expressed as inactive inclusion bodies. An *in-vitro* refolding procedure for the activation of aryl-alcohol oxidase inclusion bodies has been described [22,52]. This strategy has not been attempted for *AmPDH1* to this date but could be promising. Functional expression of an N<sup>319</sup> *AmPDH1* knock out mutant could require more extensive site directed or site saturation mutagenesis, of among others W<sup>526</sup>, S<sup>525</sup> or a mimicking of the GMC\_oxred\_C II loop sequence from structurally related enzymes without the N<sup>319</sup>SL consensus

sequence. It has to be noted that for the purpose of a more efficient electron transfer to electrode surfaces, a glycosyl moiety consisting of two HexNAc residues attached to N<sup>319</sup> should not be a hindrance, as it is largely buried in a fold of the protein and oriented away from the active site access.

### ***Am*PDH1 variant stability and enzymatic activity**

T<sub>m</sub> values of the wild type enzyme were in line with previous experiments [20,27] and only variants devoid of both glycosylation sites near the active site entrance (N<sup>75</sup> and N<sup>175</sup>) deviated by a moderately reduced thermostability. Interestingly this effect could not be observed with only one missing N-glycosyl modification, and not with other double mutants (N75G/N252Q and N175Q/N252Q). This suggests a less stable active site entrance in the absence of both N-glycosyl groups in its vicinity.

Apparent kinetic constants in photometric redox assays were determined with the substrates D-glucose and cellobiose that had been shown to induce PDH expression in *A. meleagris* [16], and two epimers of D-glucose. Knocking out N-glycosylation sites caused no substantial change in catalytic turnover numbers but moderately reduced affinity towards most sugars, especially towards the D-glucose epimers. This is in line with the non-mutated active site but modified active site access environment.

Selected N-glycosylation knock out mutants involving mutations around the active site access (N75G, N175Q, N75G/N175Q and N75G/N175Q/N252Q) were already studied on Os-polymer modified graphite electrodes in Flow Injection Amperometry for electric current output by Yakovleva et al. [23]. The remaining functionally expressible mutants were tested in an equivalent setup in this work (N252Q, N75G/N252Q, N175Q/N252Q) and compared to *Am*PDH1 wt. Only the double mutant lacking the N-glycosylation around the active site access (N<sup>75</sup> and N<sup>175</sup>) achieved substantially higher electric current than the wild type enzyme. Knocking out N<sup>252</sup>, which is the apparent location of most of the recombinant enzyme's overglycosylation, did not improve the performance of the enzyme on the Os-modified electrode. It appears therefore that a better accessibility of the active site by the Os-complexes improves electrode performance but overglycosylation on the far side of the enzyme does not negatively affect performance.

### **Acknowledgments**

Professor Christina Divne helped in the interpretation of the *Am*PDH1 crystal structure and Dr. Christopher Schulz in setting up Flow Injection Amperometry measurements. This study was supported by FWF grant TRP 218-B20 to CKP, the Swedish Research Council grant 2014-5908 and The European Commission grant "Bioenergy" FP7-PEOPLE-2013-ITN-607793 to LG.CG is a student of the FWF doctoral program BioToP at BOKU (grant W 1224).

## References

- 1 Volc J, Kubátová E, Wood DA & Daniel G (1997) Pyranose 2-dehydrogenase, a novel sugar oxidoreductase from the basidiomycete fungus *Agaricus bisporus*. *Arch. Microbiol.* **167**, 119–125.
- 2 Sygmund C, Kittl R, Volc J, Halada P, Kubátová E, Haltrich D & Peterbauer CK (2008) Characterization of pyranose dehydrogenase from *Agaricus meleagris* and its application in the C-2 specific conversion of D-galactose. *J. Biotechnol.* **133**, 334–342.
- 3 Sedmera P, Halada P, Kubátová E, Haltrich D, Přikrylová V & Volc J (2006) New biotransformations of some reducing sugars to the corresponding (di)dehydro(glycosyl) aldoses or aldonic acids using fungal pyranose dehydrogenase. *J. Mol. Catal. B Enzym.* **41**, 32–42.
- 4 Peterbauer CK & Volc J (2009) Pyranose dehydrogenases: biochemical features and perspectives of technological applications. *Appl. Microbiol. Biotechnol.* **85**, 837–848.
- 5 Volc J, Sedmera P, Kujawa M, Halada P, Kubátová E & Haltrich D (2004) Conversion of lactose to  $\beta$ -D-galactopyranosyl-(1 $\rightarrow$ 4)-D-arabino-hexos-2-ulose-(2-dehydrolactose) and lactobiono-1, 5-lactone by fungal pyranose dehydrogenase. *J. Mol. Catal. B Enzym.* **30**, 177–184.
- 6 Sedmera P, Halada P, Peterbauer C & Volc J (2004) A new enzyme catalysis: 3,4-dioxidation of some aryl  $\beta$ -D-glycopyranosides by fungal pyranose dehydrogenase. *Tetrahedron Lett.* **45**, 8677–8680.
- 7 Zafar MN, Tasca F, Boland S, Kujawa M, Patel I, Peterbauer CK, Leech D & Gorton L (2010) Wiring of pyranose dehydrogenase with osmium polymers of different redox potentials. *Bioelectrochemistry* **80**, 38–42.
- 8 Tasca F, Gorton L, Kujawa M, Patel I, Harreither W, Peterbauer CK, Ludwig R & Nöll G (2010) Increasing the coulombic efficiency of glucose biofuel cell anodes by combination of redox enzymes. *Biosens. Bioelectron.* **25**, 1710–1716.
- 9 Yakovleva ME, Killyéni A, Ortiz R, Schulz C, MacAodha D, Conghaile PÓ, Leech D, Popescu IC, Gonaus C, Peterbauer CK & Gorton L (2012) Recombinant pyranose dehydrogenase—A versatile enzyme possessing both mediated and direct electron transfer. *Electrochem. Commun.* **24**, 120–122.
- 10 Yakovleva ME, Killyéni A, Seubert O, Ó Conghaile P, MacAodha D, Leech D, Gonaus C, Popescu IC, Peterbauer CK, Kjellström S & Gorton L (2013) Further insights into the catalytical properties of deglycosylated Pyranose Dehydrogenase from *Agaricus meleagris* recombinantly expressed in *Pichia pastoris*. *Anal. Chem.* **85**, 9852–9858.
- 11 Tasca F, Timur S, Ludwig R, Haltrich D, Volc J, Antiochia R & Gorton L (2007) Amperometric biosensors for detection of sugars based on the electrical wiring of different Pyranose Oxidases and Pyranose Dehydrogenases with Osmium redox polymer on graphite electrodes. *Electroanalysis* **19**, 294–302.
- 12 Cruys-Bagger N, Badino SF, Tokin R, Gontsarik M, Fathalinejad S, Jensen K, Toscano MD, Sørensen TH, Borch K, Tatsumi H, Våljamäe P & Westh P (2014) A pyranose dehydrogenase-based biosensor for kinetic analysis of enzymatic hydrolysis of cellulose by cellulases. *Enzyme Microb. Technol.* **58–59**, 68–74.

- 13 Shao M, Nadeem Zafar M, Sygmund C, Guschin DA, Ludwig R, Peterbauer CK, Schuhmann W & Gorton L (2012) Mutual enhancement of the current density and the coulombic efficiency for a bioanode by entrapping bi-enzymes with Os-complex modified electrodeposition paints. *Biosens. Bioelectron.*
- 14 Shao M, Zafar MN, Falk M, Ludwig R, Sygmund C, Peterbauer CK, Guschin DA, MacAodha D, Conghaile PÓ, Leech D, Toscano MD, Shleev S, Schuhmann W & Gorton L (2013) Optimization of a membraneless glucose/oxygen enzymatic fuel cell based on a bioanode with high coulombic efficiency and current density. *ChemPhysChem* **14**, 2260–2269.
- 15 Ó Conghaile P, Falk M, MacAodha D, Yakovleva ME, Gonaus C, Peterbauer CK, Gorton L, Shleev S & Leech D (2016) Fully enzymatic membraneless glucose|oxygen fuel cell that provides 0.275 mA cm<sup>-2</sup> in 5 mM glucose, operates in human physiological solutions, and powers transmission of sensing data. *Anal. Chem.* **88**, 2156–2163.
- 16 Kittl R, Sygmund C, Halada P, Volc J, Divne C, Haltrich D & Peterbauer CK (2008) Molecular cloning of three pyranose dehydrogenase-encoding genes from *Agaricus meleagris* and analysis of their expression by real-time RT-PCR. *Curr. Genet.* **53**, 117–127.
- 17 Koch C, Neumann P, Valerius O, Feussner I & Ficner R (2016) Crystal Structure of Alcohol Oxidase from *Pichia pastoris*. *PLOS ONE* **11**, e0149846.
- 18 Tan CT, Spadiut O, Wongnate T, Sucharitakul J, Krondorfer I, Sygmund C, Haltrich D, Chaiyen P, Peterbauer CK & Divne C (2013) The 1.6 Å crystal structure of Pyranose Dehydrogenase from *Agaricus meleagris* rationalizes substrate specificity and reveals a flavin intermediate. *PLoS ONE* **8**, art. no. e53567.
- 19 Marchler-Bauer A, Derbyshire MK, Gonzales NR, Lu S, Chitsaz F, Geer LY, Geer RC, He J, Gwadz M, Hurwitz DI, Lanczycki CJ, Lu F, Marchler GH, Song JS, Thanki N, Wang Z, Yamashita RA, Zhang D, Zheng C & Bryant SH (2015) CDD: NCBI's conserved domain database. *Nucleic Acids Res.* **43**, D222–D226.
- 20 Graf MMH, Sucharitakul J, Bren U, Chu DB, Koellensperger G, Hann S, Furtmüller PG, Obinger C, Peterbauer CK, Oostenbrink C, Chaiyen P & Haltrich D (2015) Reaction of pyranose dehydrogenase from *Agaricus meleagris* with its carbohydrate substrates. *FEBS J.* **282**, 4218–4241.
- 21 Ahmad M, Hirz M, Pichler H & Schwab H (2014) Protein expression in *Pichia pastoris*: recent achievements and perspectives for heterologous protein production. *Appl. Microbiol. Biotechnol.* **98**, 5301–5317.
- 22 Sygmund C, Gutmann A, Krondorfer I, Kujawa M, Glieder A, Pscheidt B, Haltrich D, Peterbauer C & Kittl R (2011) Simple and efficient expression of *Agaricus meleagris* pyranose dehydrogenase in *Pichia pastoris*. *Appl. Microbiol. Biotechnol.* **94**, 695–704.
- 23 Yakovleva ME, Gonaus C, Schropp K, ÓConghaile P, Leech D, Peterbauer CK & Gorton L (2015) Engineering of pyranose dehydrogenase for application to enzymatic anodes in biofuel cells. *Phys. Chem. Chem. Phys.* **17**, 9074–9081.
- 24 Weis R, Luiten R, Skranc W, Schwab H, Wubbolts M & Glieder A (2004) Reliable high-throughput screening with *Pichia pastoris* by limiting yeast cell death phenomena. *FEMS Yeast Res.* **5**, 179–189.

- 25 Gonaus C, Kittl R, Sygmund C, Haltrich D & Peterbauer C (2016) Transcription analysis of pyranose dehydrogenase from the basidiomycete *Agaricus bisporus* and characterization of the recombinantly expressed enzyme. *Protein Expr. Purif.* **119**, 36–44.
- 26 Forneris F, Orru R, Bonivento D, Chiarelli LR & Mattevi A (2009) ThermoFAD, a ThermoFluor®-adapted flavin ad hoc detection system for protein folding and ligand binding. *FEBS J.* **276**, 2833–2840.
- 27 Krondorfer I, Brugger D, Paukner R, Scheiblbrandner S, Pirker KF, Hofbauer S, Furtmüller PG, Obinger C, Haltrich D & Peterbauer CK (2014) *Agaricus meleagris* pyranose dehydrogenase: Influence of covalent FAD linkage on catalysis and stability. *Arch. Biochem. Biophys.* **558**, 111–119.
- 28 Pabst M, Chang M, Stadlmann J & Altmann F (2012) Glycan profiles of the 27 N-glycosylation sites of the HIV envelope protein CN54gp140. *Biol. Chem.* **393**.
- 29 Kujawa M, Volc J, Halada P, Sedmera P, Divne C, Sygmund C, Leitner C, Peterbauer C & Haltrich D (2007) Properties of pyranose dehydrogenase purified from the litter-degrading fungus *Agaricus xanthoderma*. *FEBS J.* **274**, 879–894.
- 30 Růžička J & Hansen EH (1975) Flow injection analyses. *Anal. Chim. Acta* **78**, 145–157.
- 31 Stulík K & Pacáková V (1987) *Elektroanalytik: Electroanalytical Measurements in Flowing Liquids* John Wiley and Sons, New York.
- 32 Appelqvist R, Marko-Varga G, Gorton L, Torstensson A & Johansson G (1985) Enzymatic determination of glucose in a flow system by catalytic oxidation of the nicotinamide coenzyme at a modified electrode. *Anal. Chim. Acta* **169**, 237–247.
- 33 Golovin A, Dimitropoulos D, Oldfield T, Rachedi A & Henrick K (2005) MSDsite: A database search and retrieval system for the analysis and viewing of bound ligands and active sites. *Proteins Struct. Funct. Bioinforma.* **58**, 190–199.
- 34 Prlić A, Bliven S, Rose PW, Bluhm WF, Bizon C, Godzik A & Bourne PE (2010) Pre-calculated protein structure alignments at the RCSB PDB website. *Bioinformatics* **26**, 2983–2985.
- 35 Ye Y & Godzik A (2003) Flexible structure alignment by chaining aligned fragment pairs allowing twists. *Bioinformatics* **19**, ii246–ii255.
- 36 Consortium TU (2015) UniProt: a hub for protein information. *Nucleic Acids Res.* **43**, D204–D212.
- 37 Fernandez IS, Ruiz-Duenas FJ, Santillana E, Ferreira P, Martinez MJ, Martinez AT & Romero A (2009) Novel structural features in the GMC family of oxidoreductases revealed by the crystal structure of fungal aryl-alcohol oxidase. *Acta Crystallogr. Sect. D* **65**, 1196–1205.
- 38 Kommoju P-R, Chen Z, Bruckner RC, Mathews FS & Jorns MS (2011) Probing oxygen activation sites in two flavoprotein oxidases using chloride as an oxygen surrogate. *Biochemistry (Mosc.)* **50**, 5521–5534.
- 39 Yoshida H, Sakai G, Mori K, Kojima K, Kamitori S & Sode K (2015) Structural analysis of fungus-derived FAD glucose dehydrogenase. *Sci. Rep.* **5**, 13498.
- 40 Martin Hallberg B, Henriksson G, Pettersson G & Divne C (2002) Crystal structure of the flavoprotein domain of the extracellular flavocytochrome cellobiose dehydrogenase1. *J. Mol. Biol.* **315**, 421–434.

- 41 Tan TC, Gandini R, Sygmund C, Kittl R, Haltrich D, Ludwig R, Hallberg BM, Divne C. (2015) Cellobiose dehydrogenase from *Neurospora crassa*, NcCDH. PDB ID: 4QI7. DOI: 10.2210/pdb4qi7/pdb
- 42 Tan TC, Gandini R, Sygmund C, Kittl R, Haltrich D, Ludwig R, Hallberg BM, Divne C. (2015) Dehydrogenase domain of *Myricoccum thermophilum* cellobiose dehydrogenase with bound cellobionolactam, MtDH. PDB ID: 4QI5. DOI: 10.2210/pdb4qi5/pdb
- 43 Tan T-C, Haltrich D & Divne C (2011) Regioselective control of  $\beta$ -d-glucose oxidation by Pyranose 2-Oxidase is intimately coupled to conformational degeneracy. *J. Mol. Biol.* **409**, 588–600.
- 44 Dreveny I, Gruber K, Glieder A, Thompson A & Kratky C (2001) The Hydroxynitrile Lyase from almond: A lyase that looks like an oxidoreductase. *Structure* **9**, 803–815.
- 45 Doubayashi D, Ootake T, Maeda Y, Oki M, Tokunaga Y, Sakurai A, Nagaosa Y, Mikami B & Uchida H (2011) Formate Oxidase, an enzyme of the Glucose-Methanol-Choline oxidoreductase family, has a His-Arg pair and 8-Formyl-FAD at the catalytic site. *Biosci. Biotechnol. Biochem.* **75**, 1662–1667.
- 46 Harrison MJ, Nouwens AS, Jardine DR, Zachara NE, Gooley AA, Nevalainen H & Packer NH (1998) Modified glycosylation of cellobiohydrolase I from a high cellulase-producing mutant strain of *Trichoderma reesei*. *Eur. J. Biochem.* **256**, 119–127.
- 47 Klarskov K, Piens K, Ståhlberg J, Høj PB, Van B & Claeysens M (1997) Cellobiohydrolase I from *Trichoderma reesei*: Identification of an active-site nucleophile and additional information on sequence including the glycosylation pattern of the core protein. *Carbohydr. Res.* **304**, 143–154.
- 48 Archer DB & Peberdy JF (1997) The molecular biology of secreted enzyme production by fungi. *Crit. Rev. Biotechnol.* **17**, 273–306.
- 49 Montesino R, García R, Quintero O & Cremata JA (1998) Variation in N-linked oligosaccharide structures on heterologous proteins secreted by the methylotrophic yeast *Pichia pastoris*. *Protein Expr. Purif.* **14**, 197–207.
- 50 Blanchard V, Gadkari RA, Gerwig GJ, Leeftang BR, Dighe RR & Kamerling JP (2006) Characterization of the N-linked oligosaccharides from human chorionic gonadotropin expressed in the methylotrophic yeast *Pichia pastoris*. *Glycoconj. J.* **24**, 33–47.
- 51 Malik A & Ahmad S (2007) Sequence and structural features of carbohydrate binding in proteins and assessment of predictability using a neural network. *BMC Struct. Biol.* **7**, 1.
- 52 Ruiz-Dueñas FJ, Ferreira P, Martínez MJ & Martínez AT (2006) In vitro activation, purification, and characterization of *Escherichia coli* expressed aryl-alcohol oxidase, a unique H<sub>2</sub>O<sub>2</sub>-producing enzyme. *Protein Expr. Purif.* **45**, 191–199.

## Discussion

As previously pointed out, pyranose dehydrogenase is a promising enzyme for enzymatic anodes due to the broad range of sugars it can oxidize, its ability of dioxidation of substrates, and because it does not utilize oxygen as electron acceptor. The primary aim of this work was to employ enzyme engineering of pyranose dehydrogenase to improve its performance on modified anodes.

### Choice of target pyranose dehydrogenase for rational engineering

As a starting point, the most promising pyranose dehydrogenase (PDH) variant was identified as basis for further engineering. Purification from native producers of pyranose dehydrogenase is laborious with low yields. Furthermore, rational enzyme engineering also relies on efficient methods of genetic engineering, which commended yeast or bacterial expression systems, rather than fungi. Even though the first pyranose dehydrogenase was published by Volc et al. already in 1997 [1], the first recombinant expression of *pdh* was not described before 2009 in another fungus, *Aspergillus niger* [2]. Subsequently, in 2011, Sygmund et al. reported the first expression of *pdh* in the yeast *Pichia pastoris* [3]. It was shown that *pdh* in combination with the commonly employed *Saccharomyces cerevisiae*  $\alpha$ -pre-pro-factor leader sequence, for production of secreted proteins in yeast, did not yield detectable functional enzyme in the supernatant. However, secretory expression of *pdh1* from *Agaricus meleagris* in yeast could be achieved with the native fungal leader sequence, instead. Based on this strategy, alternative variants of pyranose dehydrogenase, from *Agaricus xanthoderma* (AxPDH) and *Agaricus campestris* (AcPDH) were successfully produced by Staudigl et al. in *Pichia pastoris* [4]. In this work, pyranose dehydrogenase from *Agaricus bisporus* (AbPDH) was also recombinantly produced in the same recombinant production system and characterized with a focus on comparison of steady-state kinetics and enzyme stability to the other previously produced and characterized variants. The four compared variants are closely related with a sequence identity of >70% and could therefore be also structurally compared via homology modelling based on the single available PDH crystal structure 4H7U [5] from *Agaricus meleagris* pyranose dehydrogenase 1 (AmPDH1).

Enzyme stability of recombinant AbPDH was compared to native AmPDH1 [3] and AxPDH [6], as no information on the stability of the recombinant variants was reported. It was overall less stable than the other two at high temperatures and in basic pH, with AxPDH exhibiting the highest temperature optimum of the three, at 75°C. However, all three showed good stability at moderate conditions.

Under standard steady-state conditions (pH 7.5, 30°C) AmPDH1 [3,7] and AbPDH had the generally highest turnover numbers and oxidized a broad range of sugars. AbPDH showed a moderately higher affinity towards tested disaccharides, such as cellobiose and maltose, but lower affinity to

monosaccharides compared to *AmPDH1*. In both cases, however, *AmPDH1* exhibited similar or moderately higher catalytic turnover numbers than *AbPDH*. The two other variants, *AxPDH* and *AcPDH* [4], had a narrower substrate range. This was the most pronounced for *AcPDH*, where catalytic efficiency with all tested alternative sugars was substantially lower than with D-glucose. Unlike the other 3 variants it also showed low affinity to the tested metallo-complex e<sup>-</sup>-acceptor ferrocenium ion.

The structural analysis of the homology models revealed that the active site residues were highly conserved in all PDH variants. On the peripheral side of the substrate pocket, however, there were substantial differences. *AbPDH* was the only variant with a small non-polar amino acid in the equivalent position of *AmPDH1* Phe<sup>533</sup>, which could facilitate the accommodation of large substrates. Substrate promiscuity of the different variants appeared to correlate with the absence of certain charged residues in the active site pocket, as in *AxPDH* and *AcPDH* the equivalent residue to *AmPDH1* Phe<sup>533</sup> was charged. Additionally, the suggested gating segment in *AmPDH1* and *AbPDH* did not feature a charged amino acid, while it did in *AxPDH* and *AcPDH*.

As a broad substrate range is considered one of the defining advantages of pyranose dehydrogenase for use in enzymatic bio-fuel cells, *AmPDH1* and *AbPDH* were preferential targets for rational engineering. Whereby, *AmPDH1* exhibited higher enzyme stability and similar or moderately better catalytic efficiencies. Additionally, it is the best studied variant to date and its crystal structure has been resolved. Therefore it was chosen as the focus for subsequent work.

### **Rational enzyme engineering strategy**

As described in the introduction, N-glycosylation of secreted enzymes can be disadvantageous for performance of enzyme modified electrodes. Therefore, increased maximum current densities could be achieved when the applied oxidoreductases were expressed in non N-glycosylating recombinant production hosts, or when N-glycosylated proteins were *in-vitro* deglycosylated by endoglycosidases [8,9].

*AmPDH1* is a secreted N-glycosylated oxidoreductase but it could not be expressed in the non-N-glycosylating production system *Escherichia coli*, to date. Therefore, Yakovleva et al. *in-vitro* deglycosylated purified enzyme produced in *Pichia pastoris* with the endoglycosidase Endo Hf, which cleaves off high mannose type N-glycans, leaving single N-acetylglucosamine residues attached to N-glycosylation sites. Graphite electrodes modified with Os-polymer and deglycosylated *AmPDH1* (dg*AmPDH1*) had a two-fold increased maximum current density compared to equivalent electrodes with glycosylated *AmPDH1* [10]. This demonstrated that reduced N-glycosylation could be beneficial

for pyranose dehydrogenase as well. However, *in-vitro* deglycosylation relies on costly endoglycosidases, and adds further preparatory steps to enzyme production. An alternative to non-N-glycosylating expression hosts and *in-vitro* deglycosylation is the creation of knock-out mutants where the Asn of the N-glycosylation sequon is replaced by another residue. This enables production of enzymes with reduced N-glycosylation in *Pichia pastoris* without the need for additional modification steps. Furthermore, it allows the knock-out of specific N-glycosylation sites, instead of the indiscriminate removal of N-glycans from all sites by *in-vitro* deglycosylation.

To knock out the N-glycosylation sites they need to be identified first. In *AmPDH1* four of them were found. N<sup>75</sup>, N<sup>175</sup> and N<sup>252</sup> had been previously confirmed by MALDI-MS [10]. The crystal structure 4H7U however, indicated an additional site, N<sup>319</sup>, which could be finally verified in this work by HPLC-ESI-MS. Two of these sites, N<sup>75</sup> and N<sup>175</sup>, were located in the vicinity of the active site entrance. N<sup>252</sup> was remote and strongly exposed, while N<sup>319</sup> was much less accessible. The partially N-glycosylated variants were created by replacing the Asn of these N-glycosylation sites with Gln or Gly.

Of the four N-glycosylation sites, only N<sup>319</sup> appeared to be essential for functional expression in *Pichia pastoris*, as replacing this Asn with any other amino acid lead to production levels insufficient for further study. From the remaining 3 N-glycosylation sites a systematic set of possible combinations of knock-out mutants was created, expressed in *Pichia pastoris*, and the impact of partial N-glycosylation on enzyme stability and steady state kinetics in solution of the produced variants was investigated. Partially glycosylated *AmPDH1* / Os-polymer modified graphite electrodes were prepared with the different variants and tested for increased maximum current densities in a flow injection system.

### **N-glycosylation pattern of glycosylated and partially glycosylated *AmPDH1***

As described in the introduction, *AmPDH1* is overglycosylated by the recombinant production host *Pichia pastoris* compared to enzyme from the native producer *Agaricus meleagris* [3]. To clarify the differences in N-glycosylation between native and recombinant *AmPDH1*, both were investigated by HPLC-ESI-MS. The four sites of native *AmPDH1* were modified in line with previously described fungal type N-glycosylation [11–13], but modification varied heavily between individual sites. The two more exposed sites N<sup>175</sup> and N<sup>252</sup> were featuring only single N-acetylhexosamine residues. N<sup>75</sup> and N<sup>319</sup> on the other side were glycosylated with 2 N-acetylhexosamine and 5-11 hexose residues.

*Pichia pastoris* was, as expected, not found to form any of these peculiar single N-acetylhexosamine modifications. N<sup>75</sup> and N<sup>175</sup>, which are close to the active site entrance, were N-glycosylated to a larger

extend in recombinant enzyme than in native one, yet appeared to be still of the core-type N-glycosylation, with less than 15 hexose residues per N-glycan.

N<sup>319</sup>, the only apparently essential N-glycosylation site for recombinant production of *AmpDH1*, was interestingly also the only site which was N-glycosylated to a similar extent by *Pichia pastoris* and the native producer *Agaricus meleagris* alike. The crystal structure 4H7U [5] shows that N<sup>319</sup> is located at the back side of the enzyme, seen from the active site entrance, where the two conserved domains of PDH (GMC\_oxred\_C and GMC\_oxred\_N) form noncovalent bonds via polar interactions. Two N-acetylglucosamine residues could be resolved at the site N<sup>319</sup> and they were part of these non-covalent inter-domain contacts. W<sup>526</sup> and S<sup>525</sup>, from an adjacent exposed loop (GMC\_oxred\_C: II), were interacting with them via planar-planar and polar interaction, respectively. This *AmpDH1* N<sup>319</sup>SL / W<sup>526</sup> motif was conserved in all known pyranose dehydrogenase genes. However the only other manually annotated member of the GMC structural family with an equivalent motif was aryl-alcohol oxidase (AAO), which is especially closely structurally related to *AmpDH1* [5]. *Pichia pastoris* alcohol oxidase (AOX) on the other side had the only structurally related resolved crystal structure with an equivalent tryptophan residue but without a counterpart equivalent to the N-glycosylation site N<sup>319</sup>SL. Interestingly, it also had the most dramatically differing loop conformation. These findings suggest that the N<sup>319</sup>SL / W<sup>526</sup> motif is highly conserved in pyranose dehydrogenase but not in other members of the GMC structural family and that a lack of N-glycosylation of N<sup>319</sup> in *AmpDH1* could lead to an alternative conformation of the loop GMC\_oxred\_C: II, and as consequence to terminally misfolded proteins. Therefore, it has to be considered an essential N-glycosylation site for eukaryotic expression. Lack of modification of this site, and its equivalent in aryl-alcohol oxidase, could also be the reason why both enzymes are expressed as non-functional inclusion bodies in the non-N-glycosylating prokaryotic production host *Escherichia coli*. Production of a fully non-glycosylated *AmpDH1* may therefore not be easily possible. Successful *in-vitro* refolding has been reported for aryl-alcohol oxidase produced in *Escherichia coli*, however. This was not attempted with *AmpDH1* to date. An alternative approach for producing completely non-glycosylated *AmpDH1* could be replacing W<sup>526</sup> and S<sup>525</sup> with non-polar amino acids or a more extensive engineering of the GMC\_oxred\_C: II loop.

The fourth N-glycosylation site, N<sup>252</sup>, was not found to be modified at all in the glycosylated recombinant *AmpDH1* by HPLC-ESI-MS, in contrast to the other sites. This contradicted results from Endo Hf deglycosylated *AmpDH1*. The single N-acetylhexosamine, left in place by *in-vitro* deglycosylation with Endo Hf, could be identified at all 4 N-glycosylation sites, including N<sup>252</sup>, which were therefore found to be modified. Hyperglycosylation could explain these apparently contradictory results. N-glycans from hyperglycosylated sites could be too heterogenic and too heavy to be detectable by HPLC-ESI-MS. Analysis of the purified partially glycosylated *AmpDH1* variants by SDS-Page supported this hypothesis. Only variants with N<sup>252</sup> knocked out formed a well-defined band

around 70 kDa while all the other variants formed a broad smear comparable to the recombinantly produced wild type *AmPDH1*. Therefore, N<sup>252</sup> appears to be the only hyperglycosylated site of recombinant *AmPDH1*.

### **Stability and catalytic activity of partially N-glycosylated *AmPDH1* variants**

Only simultaneously knocking out the two N-glycosylation sites close to the active site entrance, N<sup>75</sup> and N<sup>175</sup>, caused a moderate decrease in  $T_m$ , as determined by ThermoFAD protocol. The thermal stability of all variants, other than *AmPDH1* N75G/N175Q and *AmPDH1* N75G/N175Q/N252Q differed therefore not significantly from the thermal stability of the recombinant wild type enzyme. This suggests that the presence of at least one of the two N-glycans close to the active site entrance stabilizes it and thereby increases the thermostability of the enzyme. However, even in the absence of both N-glycans,  $T_m$  remained above 60°C under the tested conditions.

Steady state kinetic measurements in solution did not show a substantial change of turnover numbers and moderate changes in substrate affinities of the partially glycosylated *AmPDH1* variants. This was expected as the active site remained unchanged, while its larger environment was modified by the removal of N-glycans.

### **Performance of partially N-glycosylated *AmPDH1* / Os-polymer electrodes**

All produced partially glycosylated *AmPDH1* variants were tested in flow injection systems on Os(dmbpy)-PVI modified graphite electrodes for improved current densities. *AmPDH1* N75G/N175Q based electrodes had a maximum current density of 290  $\mu\text{A cm}^{-2}$ , which is approximately 10-fold higher than that of equivalent electrodes based on recombinant wild type *AmPDH1* ( $J_{\text{max}} = 31 \mu\text{A cm}^{-2}$ ) and comparable to those based on *in-vitro* deglycosylated *AmPDH1* ( $J_{\text{max}} = 146 \mu\text{A cm}^{-2}$ ) [14]. Removal of the two N-glycans close to the active site entrance, simultaneously, and a thus improved accessibility of the active site could explain the moderately decreased thermal stability in solution as well as an improved electron transfer from the enzyme's active site to the Os-complexes. Surprisingly, the variant *AmPDH1* N75G/N175Q/N252Q did not replicate this improved current density. Also the other variants with missing N-glycan at N<sup>252</sup> did not yield substantial improvement of achievable current densities. This suggests that *in-vitro* deglycosylated recombinant *AmPDH1* is not performing better because of the removal of hyperglycosylation as such, and a thus reduced enzyme volume, but due to the removal of specific core type glycosylated sites hindering access to the active site pocket.

Graphite electrodes were also co-modified with *AmPDH1* N75G/N175Q and the alternative Os(bpy)PVI- based polymer. This Os-polymer had a higher  $E^{\circ}$  than polymers based on Os(dmbpy)PVI, which is disadvantageous for the application in enzymatic biofuel cell anodes, but also enabled an increase in maximum current density to  $802 \mu\text{A cm}^{-2}$ .

## Conclusion and outlook

Pyranose dehydrogenase was engineered for use in enzyme / Os-polymer modified electrodes. To this end, a systematic set of partially N-glycosylated variants was created. *AmPDH1* N75G/N175Q / [Os(dmbpy)<sub>2</sub>(PVI)<sub>10</sub>Cl]<sup>+2/+</sup> modified graphite electrodes yielded approximately 10-fold increased maximum current densities ( $290 \mu\text{A cm}^{-2}$ ) than equivalent electrodes with the wild type enzyme. This engineered *AmPDH1* variant has yet to be tested in a complete enzymatic bio-fuel cell prototype. However, a very recent glucose/O<sub>2</sub> fuel cell prototype was reported by Ó Conghaile et al., with a maximum power output  $275 \mu\text{W cm}^{-2}$  at a cell voltage of 0.3 V, which employed *in-vitro* deglycosylated *AmPDH1* [15]. This, in combination with the results presented in this thesis, recommend *AmPDH1* N75G/N175Q for application to enzymatic biofuel cells in future work.

## References

- 1 Volc J, Kubátová E, Wood DA & Daniel G (1997) Pyranose 2-dehydrogenase, a novel sugar oxidoreductase from the basidiomycete fungus *Agaricus bisporus*. *Arch. Microbiol.* **167**, 119–125.
- 2 Pisanelli I, Kujawa M, Gschnitzer D, Spadiut O, Seiboth B & Peterbauer C (2009) Heterologous expression of an *Agaricus meleagris* pyranose dehydrogenase-encoding gene in *Aspergillus* spp. and characterization of the recombinant enzyme. *Appl. Microbiol. Biotechnol.* **86**, 599–606.
- 3 Sygmund C, Gutmann A, Krondorfer I, Kujawa M, Glieder A, Pscheidt B, Haltrich D, Peterbauer C & Kittl R (2011) Simple and efficient expression of *Agaricus meleagris* pyranose dehydrogenase in *Pichia pastoris*. *Appl. Microbiol. Biotechnol.* **94**, 695–704.
- 4 Staudigl P, Krondorfer I, Haltrich D & Peterbauer CK (2013) Pyranose Dehydrogenase from *Agaricus campestris* and *Agaricus xanthoderma*: Characterization and Applications in Carbohydrate Conversions. *Biomolecules* **3**, 535–552.
- 5 Tan TC, Spadiut O, Wongnate T, Sucharitakul J, Krondorfer I, Sygmund C, Haltrich D, Chaiyen P, Peterbauer CK & Divne C (2013) The 1.6 Å Crystal Structure of Pyranose Dehydrogenase from *Agaricus meleagris* Rationalizes Substrate Specificity and Reveals a Flavin Intermediate. *PLoS ONE* **8**, e53567.
- 6 Kujawa M, Volc J, Halada P, Sedmera P, Divne C, Sygmund C, Leitner C, Peterbauer C & Haltrich D (2007) Properties of pyranose dehydrogenase purified from the litter-degrading fungus *Agaricus xanthoderma*. *FEBS J.* **274**, 879–894.

- 7 Sygmund C, Kittl R, Volc J, Halada P, Kubátová E, Haltrich D & Peterbauer CK (2008) Characterization of pyranose dehydrogenase from *Agaricus meleagris* and its application in the C-2 specific conversion of D-galactose. *J. Biotechnol.* **133**, 334–342.
- 8 Lindgren A, Tanaka M, Ruzgas T, Gorton L, Gazaryan I, Ishimori K & Morishima I (1999) Direct electron transfer catalysed by recombinant forms of horseradish peroxidase: insight into the mechanism. *Electrochem. Commun.* **1**, 171–175.
- 9 Courjean O, Gao F & Mano N (2009) Deglycosylation of Glucose Oxidase for Direct and Efficient Glucose Electrooxidation on a Glassy Carbon Electrode. *Angew. Chem. Int. Ed.* **48**, 5897–5899.
- 10 Yakovleva ME, Killyéni A, Seubert O, Ó Conghaile P, MacAodha D, Leech D, Gonaus C, Popescu IC, Peterbauer CK, Kjellstrom S & Gorton L (2013) Further Insights into the Catalytic Properties of Deglycosylated Pyranose Dehydrogenase from *Agaricus meleagris* Recombinantly Expressed in *Pichia pastoris*. *Anal. Chem.*, 130910071924000.
- 11 Harrison MJ, Nouwens AS, Jardine DR, Zachara NE, Gooley AA, Nevalainen H & Packer NH (1998) Modified glycosylation of cellobiohydrolase I from a high cellulase-producing mutant strain of *Trichoderma reesei*. *Eur. J. Biochem.* **256**, 119–127.
- 12 Klarskov K, Piens K, Ståhlberg J, Høj PB, Van B & Claeysens M (1997) Cellobiohydrolase I from *Trichoderma reesei*: Identification of an active-site nucleophile and additional information on sequence including the glycosylation pattern of the core protein. *Carbohydr. Res.* **304**, 143–154.
- 13 Archer DB & Peberdy JF (1997) The Molecular Biology of Secreted Enzyme Production by Fungi. *Crit. Rev. Biotechnol.* **17**, 273–306.
- 14 Killyéni A, Yakovleva ME, MacAodha D, Conghaile PÓ, Gonaus C, Ortiz R, Leech D, Popescu IC, Peterbauer CK & Gorton L (2013) Effect of deglycosylation on the mediated electrocatalytic activity of recombinantly expressed *Agaricus meleagris* pyranose dehydrogenase wired by osmium redox polymer. *Electrochimica Acta*.
- 15 Ó Conghaile P, Falk M, MacAodha D, Yakovleva ME, Gonaus C, Peterbauer CK, Gorton L, Shleev S & Leech D (2016) Fully Enzymatic Membraneless Glucose|Oxygen Fuel Cell That Provides 0.275 mA cm<sup>-2</sup> in 5 mM Glucose, Operates in Human Physiological Solutions, and Powers Transmission of Sensing Data. *Anal. Chem.* **88**, 2156–2163.

